BioMed Research International

Advances in Molecular Diagnostics

Guest Editors: Tavan Janvilisri, Arun K. Bhunia, and Joy Scaria

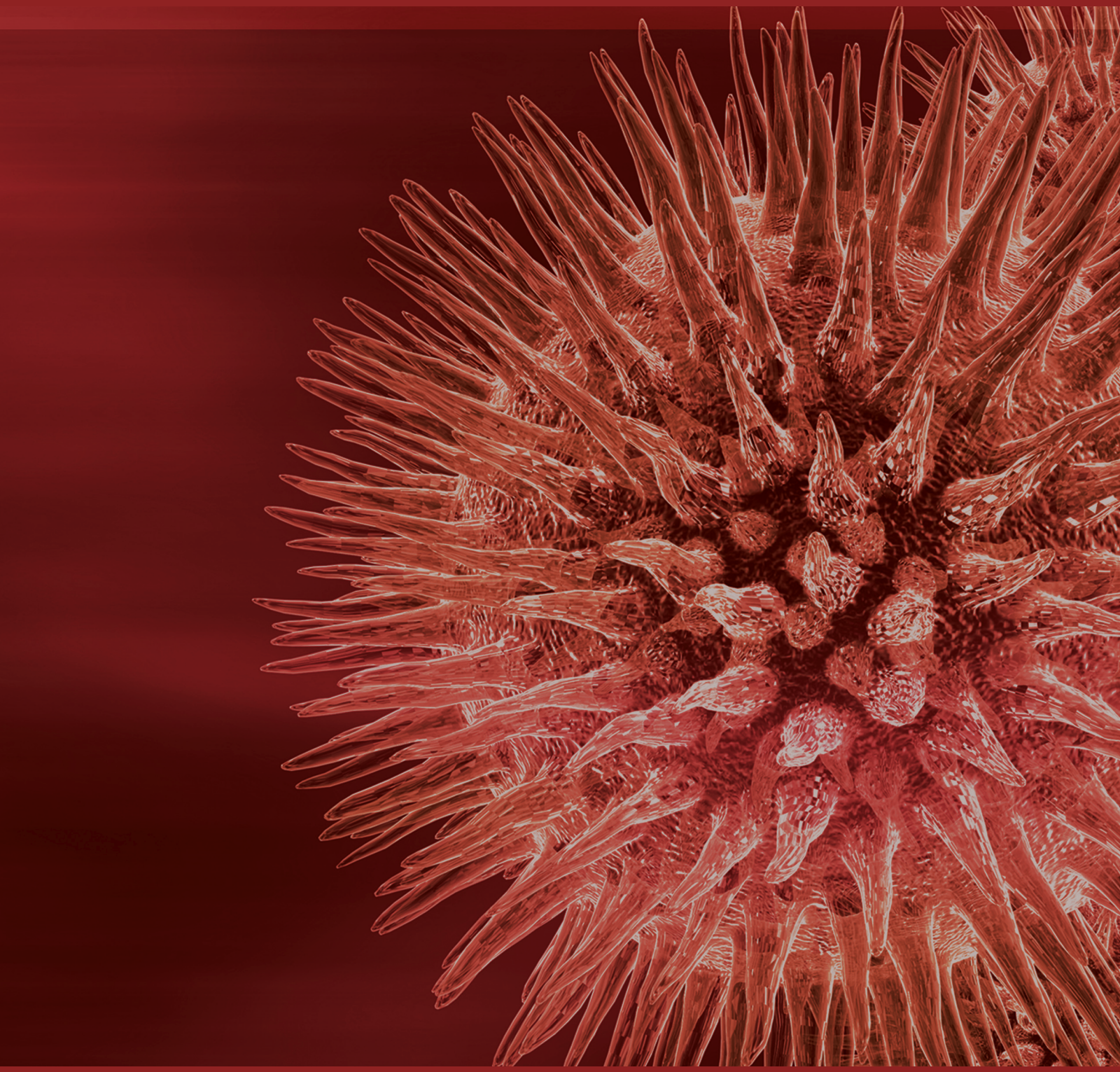

Advances in Molecular Diagnostics

BioMed Research International

Advances in Molecular Diagnostics

Guest Editors: Tavan Janvilisri, Arun K. Bhunia, and Joy Scaria

Contents

Hindawi Publishing Corporation
BioMed Research International
Volume 2013, Article ID 172521, 2 pages
http://dx.doi.org/10.1155/2013/172521

Editorial

Advances in Molecular Diagnostics

Tavan Janvilisri,[1] Arun K. Bhunia,[2] and Joy Scaria[3]

[1] *Department of Biochemistry, Faculty of Science, Mahidol University, Bangkok 10400, Thailand*
[2] *Department of Food Science and Department of Comparative Pathobiology, Purdue University, West Lafayette, IN 47907, USA*
[3] *Department of Population Medicine and Diagnostic Sciences, College of Veterinary Medicine, Cornell University, Ithaca, NY 14850, USA*

Correspondence should be addressed to Tavan Janvilisri; tavan.jan@mahidol.ac.th

Received 28 April 2013; Accepted 28 April 2013

People at present day are facing serious global challenges in healthcare from emerging and reemerging diseases. Research in molecular diagnostics has provided us with the better understanding of molecular processes affecting human health, and diseases and the tools derived thereof are becoming the standard of care for treatment of several diseases. The availability of new sequencing methods, microarrays, microfluidics, biosensors, and biomarker assays has made a shift toward developing diagnostic platforms, which stimulates growth in the field by providing answers to questions regarding diagnosis, prognosis, and best course of treatment, leading to improved outcomes and greater cost savings. It is equally important to identify and resolve existing challenges that impede the effective translation of validated diagnostic biomarkers from laboratory to clinical practice in order to see results from these efforts.

This special issue contains nine articles, where one review article focuses on microvesicles as a potential biomarker for ovarian cancer, three papers are related to nucleic-acid-based detection of pathogens. Two papers focus on the development of detecting methods while another paper aims to evaluate the types of samples for diagnosis. Finally, two papers address the relationship between biomarkers and cancer. Thus, the papers in this special issue, representing a broad spectrum of experimental approaches and areas of investigation, demonstrate a wide array of molecular diagnostic research. This unique and informative collection of papers in "Advances in Molecular Diagnostics" showcases the identification and characterization of molecular biomarkers and the development of practical applications or methodologies for diagnosis and prognosis including the evaluation of the efficacy of various diagnostic platforms in both laboratory and clinical settings. There are also papers dealing with criteria of optimal detection methods in clinical samples, leading to a guideline as a tool for clinical guidance.

In "*Microvesicles as potential ovarian cancer biomarkers*," I. Giusti et al. provided us a perspective review that summarizes the potential use of microvesicles released from tumor cells, especially regarding their microRNA profiles, as a novel molecular biomarker for ovarian cancer.

In "*Development of a broad-range 23S rDNA real-time PCR assay for the detection and quantification of pathogenic bacteria in human whole blood and plasma specimens*," P. Gaibani et al. developed a new broad-range real-time PCR assay targeting the 23S *rDNA* gene that could detect the targeted bacterial 23S *rDNA* gene as low as 10 plasmid copies per reaction. This assay could allow us to quantify total bacterial DNA in the whole blood and plasma samples without the need for a precise bacterial species identification.

In "*A pentaplex PCR assay for the detection and differentiation of Shigella species*," S. C. Ojha et al. developed a pentaplex PCR assay for the simultaneous detection and differentiation of the *Shigella* genus and the three *Shigella* species responsible for the majority of shigellosis cases. The average detection of this PCR assay was 5.4×10^4 CFU/mL, which is within the common detection limit for *Shigella*.

In "*Evaluation of multiplex PCR with enhanced spore germination for detection of Clostridium difficile from stool samples of the hospitalized patients,*" S. Chankhamhaengdecha et al. designed a new multiplex-PCR based assay for the

detection of *C. difficile* and evaluated the sample processing steps prior to the multiplex PCR diagnosis from clinical stool samples. This enrichment multiplex PCR could be an alternative approach to enzyme immuno assays for rapid and cost-effective detection of *C. difficile*.

In "*Microsphere suspension array assays for detection and differentiation of Hendra and Nipah viruses,*" A. J. Foord et al. presented microsphere suspension array assays to simultaneously identify multiple separate nucleotide targets in a single reaction. The main goal of this research was to incorporate the Hendra and Nipah viruses microsphere as modules in multiplexed microsphere arrays. Their results were comparable to qPCR, indicating high analytical and diagnostic specificity and sensitivity.

In "*Development of a generic microfluidic device for simultaneous detection of antibodies and nucleic acids in oral fluids*," Z. Chen et al. demonstrated a portable processing system for disposable microfluidic chips suitable for point-of-care settings in the diagnosis, detection, and confirmation of infectious disease pathogens. The HIV infection was used as a model to investigate the simultaneous detection of both human antibodies against the virus and viral RNA.

In "*Urine cell-free DNA integrity as a marker for early prostate cancer diagnosis: a pilot study,*" V. Casadio et al. evaluated the potential use of urine cell-free DNA as a promising noninvasive marker for the early diagnosis of prostate cancer. The overall diagnostic accuracy was approximately 80%. The preliminary data in this paper could pave the way for confirmatory studies on larger case series.

In "*Development of a novel system for mass spectrometric analysis of cancer-associated fucosylation in plasma α1-acid glycoprotein,*" T. Asao et al. evaluated the fucosylated glycans as novel tumor markers that could be of clinical relevance in the diagnosis and assessment of cancer progression as well as patient prognosis. They also developed a novel software system for use in combination with a mass spectrometer to determine N-linked glycans in α1-acid glycoprotein that could be valuable for screening plasma samples to identify biomarkers of cancer progression based on fucosylated glycans.

In "*The associated ion between the VDR gene polymorphisms and susceptibility to hepatocellular carcinoma and the clinicopathological features in subjects infected with HBV,*" X. Yao et al. evaluated the possible association between the vitamin D receptor (VDR), single-nucleotide polymorphisms (SNPs), and hepatocellular carcinoma (HCC) in patients with chronic hepatitis B virus (HBV) infection and found that the C > T polymorphisms at FokI position in the *VDR* gene served as a potential biomarker for the risk and the disease severity of HCC in those infected with HBV.

Finally, we would like to thank the authors for their contributions in this special issue and all reviewers for critical review of the manuscripts.

Tavan Janvilisri
Arun K. Bhunia
Joy Scaria

Hindawi Publishing Corporation
BioMed Research International
Volume 2013, Article ID 953974, 8 pages
http://dx.doi.org/10.1155/2013/953974

Research Article

The Associated Ion between the VDR Gene Polymorphisms and Susceptibility to Hepatocellular Carcinoma and the Clinicopathological Features in Subjects Infected with HBV

Xing Yao,[1] Huazong Zeng,[2] Guolei Zhang,[1] Weimin Zhou,[1] Qiang Yan,[1] Licheng Dai,[1] and Xiang Wang[1]

[1] *Huzhou Central Hospital, Huzhou, Zhejiang 313000, China*
[2] *School of Life Sciences and Technology, Tongji University, Shanghai 200092, China*

Correspondence should be addressed to Xiang Wang; drxiangwang@sina.cn

Received 18 November 2012; Revised 11 January 2013; Accepted 28 January 2013

Academic Editor: Tavan Janvilisri

Aim. To evaluate the possible association between the vitamin D receptor (VDR), single-nucleotide polymorphisms (SNPs), and hepatocellular carcinoma (HCC) in patients with chronic hepatitis B virus (HBV) infection. *Method*. 968 chronic HBV infection patients were enrolled, of which 436 patients were diagnosed HCC patients, and 532 were non-HCC patients. The clinicopathological characteristics of HCC were evaluated. The genotypes of VDR gene at FokI, BsmI, ApaI, and TaqI were determined. *Results*. The genotype frequencies of VDR FokI C>T polymorphism were significantly different between HCC and non-HCC groups. HCC patients had a higher prevalence of FokI TT genotype than non-HCC subjects. With FokI CC as reference, the TT carriage had a significantly higher risk for development of HCC after adjustments with age, sex, HBV infection time, α-fetoprotein, smoking status, and alcohol intake. In addition, we also found that the TT genotype carriage of FokI polymorphisms were associated with advanced tumor stage, presence of cirrhosis, and lymph node metastasis. The SNP at BsmI, ApaI, and TaqI did not show positive association with the risk and clinicopathological features of HCC. *Conclusion*. The FokI C>T polymorphisms may be used as a molecular marker to predict the risk and to evaluate the disease severity of HCC in those infected with HBV.

1. Introduction

Hepatocellular carcinoma (HCC) is one of the most common malignancies worldwide and the second leading cause of cancer-related death in China [1, 2]. The carcinogenesis of HCC is a multifactor, multistep, and complex process. It is known that multiple risk factors, including chronic hepatitis B virus (HBV) or hepatitis C virus (HCV) infection, cirrhosis, carcinogen exposure, and excessive alcohol consumption, contribute to hepatocarcinogenesis [3–5]. Epidemiological studies also showed that a variety of genetic factors mediate an individual's susceptibility to cancer [6–8]. The identification of genetic factors related to HCC susceptibility may help to elucidate the complex process of hepatocarcinogenesis and improve the scientific basis for preventative intervention.

The vitamin D receptor (VDR) is a member of the nuclear receptor superfamily of ligand-inducible transcription factors, which are involved in many physiological processes, including cell growth and differentiation, embryonic development, and metabolic homeostasis. The role of VDR in cancer has recently attracted much attention [9–11].

Several single nucleotide polymorphisms (SNP) have been described in the VDR gene, and some SNPs are associated with tumor development. For instance, VDR polymorphisms have been related to the risk and prognosis of breast, prostate, skin, colon rectum, bladder and renal cell carcinoma, and malignant melanoma [12–16]. VDR polymorphisms have been investigated in the context of some chronic liver diseases, such as primary biliary cirrhosis and autoimmune hepatitis [17–19]. In a very recent published study, VDR

Table 1: The primer sequences of VDR gene polymorphism at 4 loci.

SNP	Primer	Base change	T
FokI	5′AGCTGGCCCTGGCACTGACTCTGCTCT3′ (F) 5′ATGGAAACACCTTGCTTCTTCTCCCTC3′ (R)	C>T	61°C
BsmI	5′CAACCAAGACTACAAGTACCGCGTCAGTGA3′ (F) 5′AACCAGCGGGAAGAGGTCAAGGG3′ (R)	G>A	57°C
ApaI	5′CAGAGCATGGACAGGGAGCAA3′ (F) 5′GCAACTCCTCATGGCTGAGGTCTC3′ (R)	G>T	60°C
TaqI	5′CAGAGCATGGACAGGGAGCAA3′ (F) 5′GCAACTCCTCATGGCTGAGGTCTC3′ (R)	T>C	60°C

Table 2: The characteristics of the study population.

	HCC		Non-HCC		P
Age (years)	52.45 ± 4.6		51.95 ± 2.8		NS
Sex (male, %)	75.40%		74.84%		NS
HBV infection time (month)	15.4 ± 3.4		13.8 ± 4.6		0.053
BMI (kg/m^2)	20.4 ± 2.4		22.1 ± 1.9		0.03
Serum AFP (ng/mL)	3546 ± 224		—		
	n	%	n	%	
Heavy alcohol intake, n (%)					
Yes	152	34.86%	109	20.49%	0.034
No	284	65.14%	423	79.51%	
Smoking status, n (%)			532		
Smokers	122	27.98%	98	22.69%	
Nonsmokers	314	72.02%	334	77.31%	NS
Family cancer history					
Yes	72	16.51%	90	16.92%	NS
No	364	83.49%	442	83.08%	
Liver cirrhosis n (%)					
Yes	213	48.85%	195	36.65%	<0.001
No	223	51.15%	337	63.35%	

genetic polymorphisms are significantly associated with the occurrence of HCC in Caucasian patients with alcoholic liver cirrhosis [20]. In China, hepatitis virus infection is a highly endemic factor for HCC [21–24]. However, the association between the VDR gene polymorphisms and the risk and pathological development in Chinese subjects with chronic hepatitis virus infection remains unknown. This case-control study, therefore, aimed to evaluate the role of VDR gene SNPs in the susceptibility and clinicopathological status of HCC in Chinese subjects with chronic HBV infection.

2. Methods

2.1. Subjects and Specimen Collection. This is a hospital-based case-control study. A total of 968 chronic HBV infection patients were enrolled at our hospital between Jan 2006 and Mar 2010. Of 968 patients, 436 patients were recruited as a HCC group, and 532 were enrolled as non-HCC group according to the presence or absence of HCC. We also enrolled 132 patients with determined HCC, but without HBV infection as control. The patients were diagnosed with HCC based on the characteristic criteria of the national guidelines for HCC, such as liver injury diagnosed by either histology or cytology irrespective of α-fetoprotein (AFP) titer where imaging data showed any one of following three items: (1) one or more liver masses ≥2 cm in diameter via both computed tomography and magnetic resonance imaging; (2) imaging data with early enhancement and a high level of AFP ≥400 ng/mL; (3) imaging data with early arterial phase contrast enhancement plus early venous phase contrast washout regardless of AFP level. Liver cirrhosis was determined by histology, imaging, or clinical indications, such as esophageal varices or ascites. Age, gender, smoke status, and alcohol use were recorded. Relevant medical information including stage of HCC, liver cirrhosis history, lymph node metastasis, portal invasion, AFP, aspartate aminotransferase (AST), and alanine aminotransferase (ALT) was also collected from patients by medical chart review. Heavy alcohol intake was defined as ethanol intake ≥80 g/day for >10 years. Patients with other cancers and chronic diseases, especially kidney, bone metabolism diseases were strictly excluded. This study was approved by the Institutional Review Board of our Hospital, and written informed consent was obtained from all study subjects.

Table 3: The genotype frequencies of VDR gene in HCC and non-HCC among patients with chronic HBV infection.

	HCC		Non-HCC		Adjusted OR	95% CI		Adjusted *P* value
	N	%	*N*	%				
BsmI								
GG	112	25.69%	142	26.69%	1			
GA	217	49.77%	259	48.68%	1.062	0.782	1.443	0.699
AA	107	24.54%	131	24.62%	1.036	0.726	1.478	0.847
G	441	50.57%	543	51.03%	1			
A	431	49.43%	521	48.97%	1.019	0.852	1.218	0.84
FokI								
CC	107	24.54%	189	35.53%	1			
CT	198	45.41%	241	45.30%	1.451	1.072	1.964	0.016
TT	131	30.05%	102	19.17%	2.269	1.597	3.223	0.006
C	412	47.25%	619	58.18%	1			
T	460	52.75%	445	41.82%	1.553	1.297	1.86	<0.001
ApaI								
GG	108	24.77%	143	26.88%	1			
GT	216	49.54%	275	51.69%	1.04	0.765	1.414	0.802
TT	112	25.69%	114	21.43%	1.301	0.907	1.867	0.165
G	432	49.54%	561	52.73%	1			
T	440	50.46%	503	47.27%	1.136	0.95	1.359	0.163
TaqI								
TT	115	26.38%	137	25.75%	1			
TC	212	48.62%	252	47.37%	1	0.741	1.363	0.993
CC	109	25.00%	143	26.88%	0.915	0.644	1.279	0.592
T	442	50.69%	526	49.44%	1			
C	430	49.31%	538	50.56%	0.952	0.823	1.145	0.581

2.2. DNA Extraction and Genotyping. Genomic DNA was extracted using QIAamp DNA blood mini kits (Qiagen, Valencia, CA) following the manufacturer's instructions. For the detection of the VDR polymorphisms, the polymerase chain reaction (PCR) technique was applied and followed by restriction fragment length polymorphism assays. The primer sequences were shown in Table 1. The cycling conditions for all the VDR polymorphisms were set as 40 cycles at 95°C for 30 s, 61°C for 30 s, and 72°C for 1 min. In a total volume of 20 μL, amplified DNA (10 μL) was digested overnight with 2 U of restriction endonucleases using the buffers and temperatures recommended by the manufacturers. All the PCR products were sized by electrophoresis on a 2% agarose gel stained with ethidium bromide.

2.3. Statistical Analysis. The distributions of demographic characteristics and genotype frequencies between the cases and controls and the clinicopathological features in different genotypes were analyzed by Fisher's exact test, since the small sample size was present in some categories of variables. Hardy-Weinberg equilibrium was assessed using χ^2 test. The odds ratios (ORs) with their 95% confidence intervals (CIs) of the association between genotype frequencies and HCC were estimated by multiple logistic regression models, after controlling for other covariates, including age, gender, and genotypes for each estimated variable. A *P* value of less than 0.05 was considered significant. The data were analyzed on SAS statistical software (Version 9.1, 2005; SAS Institute Inc., Cary, NC).

3. Results

The characteristics of the study population are presented in Table 2. There were no significant differences of age, gender, HBV infection time, smoker status, and family cancer history between HCC and non-HCC. However, HCC group had a significantly higher rate of heavy alcohol intake compared with controls ($P = 0.034$). We observed a significant difference in BMI between HCC and non-HCC subjects. The mean serum AFP levels were significantly higher in HCC subjects than non-HCC subjects (all $P < 0.001$). HCC patients had a significantly higher rate of liver cirrhosis compared with non-HCC patients ($P < 0.001$).

The genotype frequencies of VDR gene in HCC and non-HCC subjects are presented in Table 3. The genotype frequencies of all SNPs in control patients were in Hardy-Weinberg equilibrium (all $P > 0.05$). The genotype frequencies of VDR FokI C>T polymorphism were

Table 4: The genotype frequencies of VDR gene in HCC patients with chronic HBV infection and HCC patient without HBV infection.

	HCC with HBV		HCC without HBV		Adjusted OR	95% CI		Adjusted P value
BsmI								
GG	112	25.69%	37	28.24%	1.000			
GA	217	49.77%	65	49.62%	1.103	0.694	1.753	0.679
AA	107	24.54%	29	22.14%	1.219	0.701	2.120	0.483
G	441	50.57%	139	53.05%	1.000			
A	431	49.43%	123	46.95%	1.104	0.838	1.456	0.481
FokI								
CC	107	24.54%	31	23.66%	1.000			
CT	198	45.41%	62	47.33%	0.925	0.566	1.512	0.756
TT	131	30.05%	38	29.01%	0.999	0.583	1.712	0.745
C	412	47.25%	124	47.33%	1.000			
T	460	52.75%	138	52.67%	1.003	0.761	1.323	0.982
ApaI								
GG	108	24.77%	22	16.79%	1.000			
GT	216	49.54%	75	57.25%	0.587	0.346	0.995	0.052
TT	112	25.69%	34	25.95%	0.671	0.369	1.220	0.571
G	432	49.54%	119	45.42%	1.000			
T	440	50.46%	143	54.58%	0.848	0.642	1.118	0.242
TaqI								
TT	115	26.38%	32	24.43%	1.000			
TC	212	48.62%	69	52.67%	0.855	0.531	1.377	0.519
CC	109	25.00%	30	22.90%	1.011	0.576	1.775	0.970
T	442	50.69%	133	50.76%	1.000			
C	430	49.31%	129	49.24%	1.003	0.761	1.322	0.983

significantly different between HCC and non-HCC groups. HCC patients had a higher prevalence of FokI TT genotype than non-HCC subjects (30.05% versus 19.17%, $P < 0.001$). For allele comparison, HCC subjects had higher T allele frequency than controls (52.75% versus 41.82%, $P < 0.001$). To identify the independent risk factor for the development of HCC, we performed the multivariate regression analyses. With FokI CC as reference, our data showed that the TT carriage had a significantly higher risk for development of HCC after adjustments with age, gender, HBV infection time, smoker status, family cancer history, alcohol intake, BMI, and serum AFP level (OR = 2.269, $P = 0.006$). With C allele as reference, the OR of T allele carriage for HCC was 1.553 ($P < 0.001$). For SNPs of BsmI, ApaI, and TaqI, their genotype and allele frequencies did not significantly differ between HCC and non-HCC group (all $P > 0.05$). Multivariate regression analyses showed no association between the above-mentioned SNPs of VDR gene and susceptibility of HCC in this study.

Table 4 showed the genotype frequencies of VDR gene in HCC patients with chronic HBV infection and HCC patient without HBV infection. We found that the VDR genotype frequencies were similar between HCC with HBV infection and HCC without HBV infection. None of the VDR SNPs showed significant difference between HCC with HBV infection and HCC without HBV infection (All $P > 0.05$).

We further analyzed the association between VDR polymorphisms and the clinicopathological features in HCC subjects (Table 5). We found that only the SNPs at FokI locus were significantly different when all HCC patients were stratified by tumor stage, presence of liver cirrhosis history, and lymph node metastasis (all $P < 0.05$), but not tumor size and portal invasion. We further performed the multivariate regression analyses to explore the role of SNPs at FokI locus in determining the clinicopathological features in HCC subjects. Taking the CC genotype as reference, we found that the TT genotype carriage of FokI polymorphisms was associated with advanced tumor stage (OR for III + IV stage = 2.335, $P = 0.001$), presence of cirrhosis (OR for presence = 2.714, $P < 0.001$), and lymph node metastasis (OR for presence of lymph node metastasis = 2.122, $P = 0.004$). No association between the FokI polymorphisms, tumor size, and portal invasion was observed (both adjusted $P > 0.05$). The SNP at other loci including BsmI, ApaI, and TaqI did not show positive association with the the clinicopathological features of HCC (data not shown).

AFP is the common clinical pathological markers of HCC. We compared the serum AFP levels among different VDR genotype carriers in HCC patients. We found HCC patients with FokI TT genotype had a much higher AFP level than CT and CC carriers (Figure 1(a), $P = 0.011$ versus CC; $P = 0.015$ versus CT, resp.). The AFP levels were similar

Table 5: Association between VDR polymorphisms and the clinicopathological features in HCC subjects.

FokI C>T	Tumor size				Adjusted OR	95% CI		Adjusted *P* value
	<30 mm	%	>30 mm	%				
CC	55	25.00%	57	26.39%	1			
CT	108	49.09%	109	50.46%	1.027	0.651	1.62	0.543
TT	57	25.91%	50	23.15%	1.181	0.695	2.008	0.068
	Cancer stage							
	III + IV		I + II					
CC	43	18.53%	64	29.91%	1			
CT	109	46.98%	99	46.26%	1.639	1.021	2.629	0.054
TT	70	34.48%	51	23.83%	2.335	1.385	3.936	0.001
	Liver cirrhosis history							
	Presence		Absence					
CC	40	18.78%	67	30.04%	1			
CT	92	43.19%	106	47.53%	1.454	0.899	2.352	0.127
TT	81	38.03%	50	22.42%	2.714	1.602	4.596	<0.001
	Lymph node metastasis							
	Presence		Absence					
CC	43	18.45%	64	29.77%	1			
CT	96	41.20%	102	47.44%	1.401	0.87	2.256	0.038
TT	77	33.05%	54	25.12%	2.122	1.262	3.57	0.004
	Portal invasion							
	Presence		Absence					
CC	53	25.48%	62	27.19%	1			
CT	110	52.88%	102	44.74%	1.260	0.843	1.991	0.326
TT	45	21.63%	64	28.07%	0.820	0.482	1.411	0.470
	Heavy alcohol intake, *n* (%)							
	Yes		No					
CC	43	28.29%	67	27.02%	1.000			
CT	75	49.34%	126	50.81%	0.927	0.575	1.496	0.757
TT	34	22.37%	55	22.18%	0.963	0.543	1.710	0.898

among BsmI, ApaI, and TaqI genotype carriers (data not shown). We also compared the liver function marker, namely, serum ALT and AST level according to the VDR genotypes. We found that only the FokI TT carriers had higher serum AST and ALT levels compared with TC and CC (all $P < 0.05$, Figures 1(b) and 1(c)) in HBV infection patient with HCC, but not in the HBV infection patients without HCC (data not shown).

4. Discussion

In the study, we investigated the possible association between the VDR gene polymorphisms and HCC in a Chinese population with HBV infection. We found that the FokI C>T polymorphisms was significantly associated with the susceptibility and clinical features of HCC, including advanced tumor stage, presence of liver cirrhosis history, and lymph node metastasis. Since the association between the VDR genetic polymorphism and HCC had not been previously reported, our data, for the first time, provide new information in this aspect. The results of this study suggest the FokI C>T polymorphisms may be used as a molecular marker to predict the risk and to evaluate the disease severity of HCC in those infected with HBV.

Hepatitis virus infection is associated with the increase of oxidative stress in liver cells and results in DNA changes and instability, thus increasing the risk of developing cirrhosis and/or HCC [21, 25]. Some previous studies provided evidence that genetic polymorphisms of certain genes may predict the HCC occurrence in hepatitis virus infection [26–29].

The VDR is an intracellular hormone receptor that specifically binds the biologically active form of vitamin D, 1,25-dihydroxyvitamin D or calcitriol and interacts with specific nucleotide sequences (response elements) of target

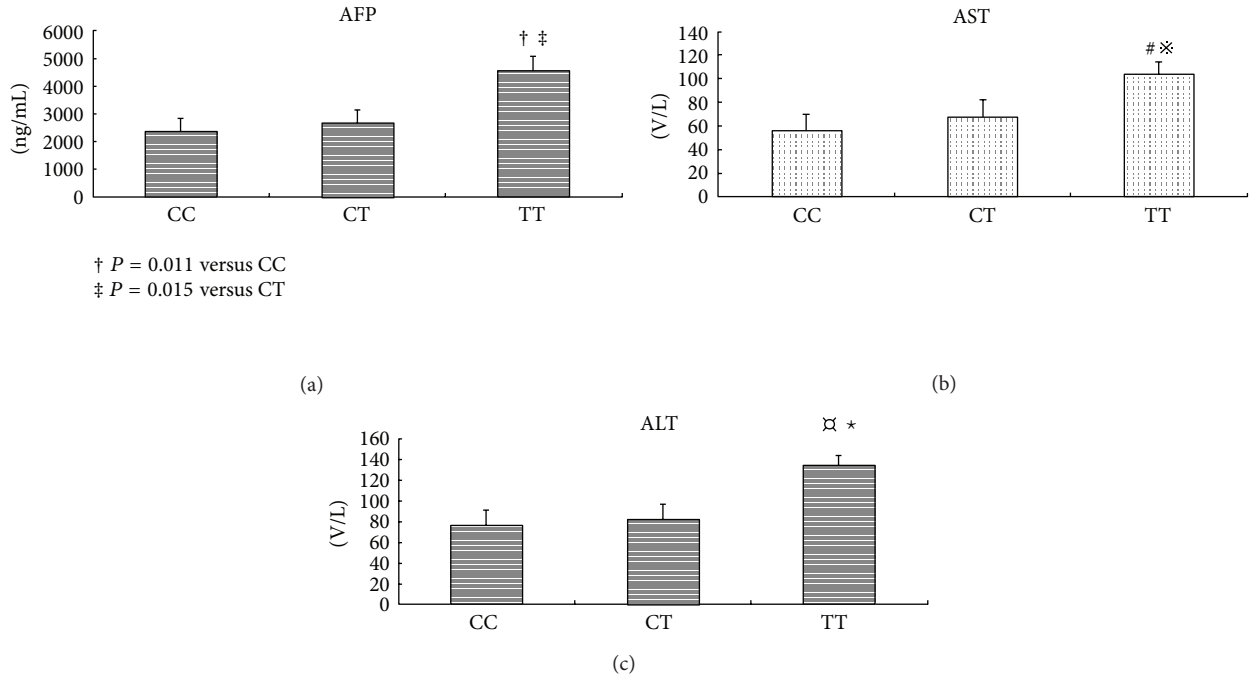

Figure 1: Serum AFP, AST, and ALT levels among different VDR FokI C>T genotype carriers in HCC patients.

genes to produce a variety of biologic effects [30]. The VDR gene is located on chromosome 12q12–q14, and several single-nucleotide polymorphisms have been identified that may influence cancer risk [31].

The FokI restriction fragment length polymorphism, located in the coding region of the VDR gene, results in the production of a VDR protein that is three amino acids longer and functionally less effective [32]. Arai et al. demonstrated that compared with the FokI T/T genotype, FokI C/C had 1.7-fold greater function of vitamin D-dependent transcriptional activation of a reporter construct under the control of a vitamin D response element in transfected HeLa cells [33]. It has been hypothesized that a less active VDR could be associated with either an increased susceptibility to cancer risk or to a more aggressive disease [31].

Vogel et al. detected a significant association between the F allele of the FokI C>T (F/f) polymorphism and autoimmune hepatitis patients, indicating a genetic link of VDR polymorphisms to autoimmune liver diseases such as primary biliary cirrhosis in German patients [19]. In Chinese population, Fan et al. reported a significant difference in FokI polymorphism between autoimmune hepatitis patients and controls, and a significant association in BsmI polymorphisms between primary biliary cirrhosis patients and controls [34]. In Italian population who underwent liver transplantation with the etiologies of liver disease as hepatitis C, hepatitis B, and alcoholic liver disease, carriage of the GG genotype of BsmI and the TT genotype of TaqI was significantly associated with occurrence of HCC. The authors concluded that VDR genetic polymorphisms are significantly associated with the occurrence of HCC in patients with liver cirrhosis, and this relationship is more specific for patients with an alcoholic etiology [20]. Our study showed that only the FokI C>T polymorphisms were associated with the HCC susceptibility in Chinese patient with chronic HBV infection; the other SNPs, including BsmI, were not related with the development of HCC. The HCC patients had a significantly higher cirrhosis rate than non-HCC patients ($P < 0001$), suggesting that the VDR polymorphisms at FokI locus may relate to HCC risk by enhancing the occurrence of liver cirrhosis. Although many factors may be account for the discrepancies among these studies, the ethnic difference should be predominately considered since Fan et al. found the distribution of FokI, BsmI, ApaI, and TaqI gene types significantly differed between Chinese healthy controls and Caucasian healthy controls [34].

The prognostic role of FokI C>T (F/f) polymorphism in cancer patients has been reported. Hama et al. reported the VDR FokI TT genotype was associated with a poor progression-free survival rate in patients with head and neck squamous cell carcinoma. In contrast, the other polymorphisms (BsmI, ApaI, and TaqI) showed no significant associations with progression-free survival [35]. In this study, we did not perform prognostic analyses; however, we found that the TT genotype carriage of TaqI polymorphisms was associated with advanced tumor stage, worse tumor differentiation, presence of cirrhosis, and lymph node metastasis. In addition, the TT carriers had higher serum AFP level than CC and CT carriers. The SNP at other loci including BsmI, ApaI, and TaqI did not show positive association with the clinicopathological features of HCC. Since tumor stage, tumor differentiation, presence of cirrhosis, and lymph node

metastasis are conventional factors associated with HCC prognosis, our data imply that the TT carriers had poorer prognosis than CC and CT carriers.

Some limitation in this study should be addressed. Firstly, this is a hospital-based case-control study, thus the enrollment bias was inevitable. Secondly, no information was available regarding vitamin D intake (dietary or supplemental) and circulating vitamin D levels of patients. Thirdly, we only enrolled subjects with HBV infection, and all the subjects were Chinese. As HCV infection is another major cause for HCC in China, future study with larger sample size including HCV subjects is warranted.

Conflict of interest

We do not have a conflict of interest with SAS.

Acknowledgment

The authors thank Dr. Xuwei Hou for his help in writing this paper and statistical analyses. This work was supported by The National Natural Science Foundation of China (no. 31171024) and huzhou Sci-tech program (2010YS17).

References

[1] P. Małkowski, M. Pacholczyk, B. Łagiewska et al., "Hepatocellular carcinoma—epidemiology and treatment," *Przeglad Epidemiologiczny*, vol. 60, no. 4, pp. 731–740, 2006.

[2] M. A. van den Bosch and L. Defreyne, "Hepatocellular carcinoma," *The Lancet*, vol. 380, no. 9840, pp. 469–470, 2012.

[3] P. A. Farazi and R. A. DePinho, "The genetic and environmental basis of hepatocellular carcinoma," *Discovery Medicine*, vol. 6, no. 35, pp. 182–186, 2006.

[4] R. Masuzaki, H. Yoshida, R. Tateishi, S. Shiina, and M. Omata, "Hepatocellular carcinoma in viral hepatitis: improving standard therapy," *Best Practice and Research: Clinical Gastroenterology*, vol. 22, no. 6, pp. 1137–1151, 2008.

[5] A. K. Singal, "Silent cirrhosis in hepatitis B virus related hepatocellular carcinoma," *Hepato-Gastroenterology*, vol. 55, no. 86-87, pp. 1734–1737, 2008.

[6] P. R. Wang, M. Xu, S. Toffanin, Y. Li, J. M. Llovet, and D. W. Russell, "Induction of hepatocellular carcinoma by in vivo gene targeting," *Proceedings of the National Academy of Sciences of the United States of America*, vol. 109, no. 28, pp. 11264–11269, 2012.

[7] N. F. Ma, S. H. Lau, L. Hu, S. S. Dong, and X. Y. Guan, "Hepatitis B virus X gene in the development of hepatocellular carcinoma," *Hong Kong Medical Journal*, vol. 17, supplement 6, pp. 44–47, 2011.

[8] C. Cillo, G. Schiavo, M. Cantile et al., "The HOX gene network in hepatocellular carcinoma," *International Journal of Cancer*, vol. 129, no. 11, pp. 2577–2587, 2011.

[9] Y. K. Yee, S. R. Chintalacharuvu, J. Lu, and S. Nagpal, "Vitamin D receptor modulators for inflammation and cancer," *Mini-Reviews in Medicinal Chemistry*, vol. 5, no. 8, pp. 761–778, 2005.

[10] M. Guy, L. C. Lowe, D. Bretherton-Watt et al., "Vitamin D receptor gene polymorphisms and breast cancer risk," *Clinical Cancer Research*, vol. 10, no. 16, pp. 5472–5481, 2004.

[11] M. L. Slattery, "Vitamin D receptor gene (VDR) associations with cancer," *Nutrition Reviews*, vol. 65, no. 8, part 2, pp. S102–S104, 2007.

[12] N. Denzer, T. Vogt, and J. Reichrath, "Vitamin D receptor (VDR) polymorphisms and skin cancer: a systematic review," *Dermato-Endocrinology*, vol. 3, no. 3, pp. 205–210, 2011.

[13] N. Buyru, A. Tezol, E. Yosunkaya-Fenerci, and N. Dalay, "Vitamin D receptor gene polymorphisms in breast cancer," *Experimental and Molecular Medicine*, vol. 35, no. 6, pp. 550–555, 2003.

[14] D. G. Blazer III, D. M. Umbach, R. M. Bostick, and J. A. Taylor, "Vitamin D receptor polymorphisms and prostate cancer," *Molecular Carcinogenesis*, vol. 27, no. 1, pp. 18–23, 2000.

[15] M. A. Murtaugh, C. Sweeney, K. N. Ma et al., "Vitamin D receptor gene polymorphisms, dietary promotion of insulin resistance, and colon and rectal cancer," *Nutrition and Cancer*, vol. 55, no. 1, pp. 35–43, 2006.

[16] W. Zhou, R. S. Heist, G. Liu et al., "Polymorphisms of vitamin D receptor and survival in early-stage non-small cell lung cancer patients," *Cancer Epidemiology Biomarkers and Prevention*, vol. 15, no. 11, pp. 2239–2245, 2006.

[17] A. Kempinska-Podhorecka, E. Wunsch, T. Jarowicz et al., "Vitamin D receptor polymorphisms predispose to primary biliary cirrhosis and severity of the disease in polish population," *Gastroenterology Research and Practice*, vol. 2012, Article ID 408723, 8 pages, 2012.

[18] A. Tanaka, S. Nezu, S. Uegaki et al., "Vitamin D receptor polymorphisms are associated with increased susceptibility to primary biliary cirrhosis in Japanese and Italian populations," *Journal of Hepatology*, vol. 50, no. 6, pp. 1202–1209, 2009.

[19] A. Vogel, C. P. Strassburg, and M. P. Manns, "Genetic association of vitamin D receptor polymorphisms with primary biliary cirrhosis and autoimmune hepatitis," *Hepatology*, vol. 35, no. 1, pp. 126–131, 2002.

[20] E. Falleti, D. Bitetto, C. Fabris et al., "Vitamin D receptor gene polymorphisms and hepatocellular carcinoma in alcoholic cirrhosis," *World Journal of Gastroenterology*, vol. 16, no. 24, pp. 3016–3024, 2010.

[21] Y. J. Tan, "Hepatitis B virus infection and the risk of hepatocellular carcinoma," *World Journal of Gastroenterology*, vol. 17, no. 44, pp. 4853–4857, 2011.

[22] J. Hou, Z. Liu, and F. Gu, "Epidemiology and prevention of hepatitis B virus infection," *International Journal of Medical Sciences*, vol. 2, no. 1, pp. 50–57, 2005.

[23] M. Moriyama, M. Mikuni, W. Longren et al., "Epidemiology of SEN virus infection among patients with hepatitis B and C in China," *Hepatology Research*, vol. 27, no. 3, pp. 174–180, 2003.

[24] I. Merican, R. Guan, D. Amarapuka et al., "Chronic hepatitis B virus infection in Asian countries," *Journal of Gastroenterology and Hepatology*, vol. 15, no. 12, pp. 1356–1361, 2000.

[25] Y. Jin, K. Abe, Y. Sato, K. Aita, H. Irie, and J. Shiga, "Hepatitis B and C virus infection and p53 mutations in human hepatocellular carcinoma in Harbin, Heilongjian Province, China," *Hepatology Research*, vol. 24, no. 4, pp. 379–384, 2002.

[26] K. Migita, Y. Maeda, S. Abiru et al., "Polymorphisms of interleukin-1β in Japanese patients with hepatitis B virus infection," *Journal of Hepatology*, vol. 46, no. 3, pp. 381–386, 2007.

[27] A. Al-Qahtani, M. Al-Ahdal, A. Abdo et al., "Toll-like receptor 3 polymorphism and its association with hepatitis B virus infection in Saudi Arabian patients," *Journal of Medical Virology*, vol. 84, no. 9, pp. 1353–1359, 2012.

[28] J. H. Kim, S. J. Yu, B. L. Park et al., "TGFBR3 polymorphisms and its haplotypes associated with chronic hepatitis B virus infection and age of hepatocellular carcinoma occurrence," *Digestive Diseases*, vol. 29, no. 3, pp. 278–283, 2011.

[29] K. Y. Chan, C. M. Wong, J. S. Kwan et al., "Genome-wide association study of hepatocellular carcinoma in Southern Chinese patients with chronic hepatitis B virus infection," *PLoS One*, vol. 6, no. 12, Article ID e28798, 2011.

[30] C. Gross, A. V. Krishnan, P. J. Malloy, T. R. Eccleshall, X. Y. Zhao, and D. Feldman, "The vitamin D receptor gene start codon polymorphism: a functional analysis of FokI variants," *Journal of Bone and Mineral Research*, vol. 13, no. 11, pp. 1691–1699, 1998.

[31] G. K. Whitfield, L. S. Remus, P. W. Jurutka et al., "Functionally relevant polymorphisms in the human nuclear vitamin D receptor gene," *Molecular and Cellular Endocrinology*, vol. 177, no. 1-2, pp. 145–159, 2001.

[32] A. G. Uitterlinden, Y. Fang, J. B. J. van Meurs, H. A. P. Pols, and J. P. T. M. van Leeuwen, "Genetics and biology of vitamin D receptor polymorphisms," *Gene*, vol. 338, no. 2, pp. 143–156, 2004.

[33] H. Arai, K. I. Miyamoto, Y. Taketani et al., "A vitamin D receptor gene polymorphism in the translation initiation codon: effect on protein activity and relation to bone mineral density in Japanese women," *Journal of Bone and Mineral Research*, vol. 12, no. 6, pp. 915–921, 1997.

[34] L. Fan, X. Tu, Y. Zhu et al., "Genetic association of vitamin D receptor polymorphisms with autoimmune hepatitis and primary biliary cirrhosis in the Chinese," *Journal of Gastroenterology and Hepatology*, vol. 20, no. 2, pp. 249–255, 2005.

[35] T. Hama, C. Norizoe, H. Suga et al., "Prognostic significance of vitamin D receptor polymorphisms in head and neck squamous cell carcinoma," *PLoS One*, vol. 6, no. 12, Article ID e29634, 2011.

Hindawi Publishing Corporation
BioMed Research International
Volume 2013, Article ID 875437, 6 pages
http://dx.doi.org/10.1155/2013/875437

Research Article

Evaluation of Multiplex PCR with Enhanced Spore Germination for Detection of *Clostridium difficile* from Stool Samples of the Hospitalized Patients

Surang Chankhamhaengdecha,[1] Piyapong Hadpanus,[1] Amornrat Aroonnual,[2] Puriya Ngamwongsatit,[3] Darunee Chotiprasitsakul,[4] Piriyaporn Chongtrakool,[5] and Tavan Janvilisri[6]

[1] *Department of Biology, Faculty of Science, Mahidol University, Bangkok 10400, Thailand*
[2] *Department of Tropical Nutrition and Food Science, Faculty of Tropical Medicine, Mahidol University, Bangkok 10400, Thailand*
[3] *Department of Clinical Sciences and Public Health, Faculty of Veterinary Science, Mahidol University, Nakhon Pathom 73170, Thailand*
[4] *Department of Medicine, Faculty of Medicine Ramathibodi Hospital, Mahidol University, Bangkok 10400, Thailand*
[5] *Department of Pathology, Faculty of Medicine Ramathibodi Hospital, Mahidol University, Bangkok 10400, Thailand*
[6] *Department of Biochemistry, Faculty of Science, Mahidol University, Bangkok 10400, Thailand*

Correspondence should be addressed to Tavan Janvilisri; tavan.jan@mahidol.ac.th

Received 23 November 2012; Revised 31 January 2013; Accepted 16 February 2013

Academic Editor: Joy Scaria

Clostridium difficile poses as the most common etiologic agent of nosocomial diarrhea. Although there are many diagnostic methods to detect *C. difficile* directly from stool samples, the nucleic acid-based approach has been largely performed in several laboratories due to its high sensitivity and specificity as well as rapid turnaround time. In this study, a multiplex PCR was newly designed with recent accumulated nucleotide sequences. The PCR testing with various *C. difficile* ribotypes, other *Clostridium* spp., and non-*Clostridium* strains revealed 100% specificity with the ability to detect as low as ~22 genomic copy number per PCR reaction. Different combinations of sample processing were evaluated prior to multiplex PCR for the detection of *C. difficile* in fecal samples from hospitalized patients. The most optimal condition was the non-selective enrichment at 37°C for 1 h in brain heart infusion broth supplemented with taurocholate, followed by the multiplex PCR. The detection limit after sample processing was shown as being 5 spores per gram of fecal sample. Two hundred and thirty-eight fecal samples collected from the University affiliated hospital were analyzed by the enrichment multiplex PCR procedure. The results suggested that the combination of sample processing with the high-performance detection method would be applicable for routine diagnostic use in clinical setting.

1. Introduction

Clostridium difficile is a motile, rod-shaped, Gram-positive bacterium, which is known to be a leading cause of antibiotic-associated diarrhea, especially nosocomial infections [1]. Though *C. difficile* is not a major component of natural gut flora, treatment with broad-spectrum antibiotics impedes the growth of other bacterial species and allows *C. difficile* to colonize. Following the colonization, an enterotoxin, TcdA, which is found in ~70% of *C. difficile* strains, and a cytotoxin, TcdB, which is found in all *C. difficile* strains, can be produced, thereby disrupting tight junctions of the intestinal epithelial cells resulting in inflammation and increased permeability of the intestine [2]. Approximately less than 10% of clinical *C. difficile* isolates possess binary toxins (cdt*A*/*B*), which have been associated with increased severity of the symptoms [3]. The pathogenic role of cdt*A*/*B* has been suggested to trigger microtubule protrusion, thereby increasing the adherence of *C. difficile* to the gut epithelium [4]. *C. difficile* infection (CDI) results in a wide range of

symptoms including fever, abdominal pains, mild diarrhea, and pseudomembranous colitis. Although CDI can be treated with certain antibiotics, the emergence of hypervirulent strains that are resistant to current chemotherapy and are able to produce high titers of toxins poses a challenge to the treatment of CDI worldwide [5].

To date, there are several diagnostic assays for the detection of *C. difficile*, each of which reveals the advantages and disadvantages and discrepancies in the performance existing in the literature [6, 7]. Conventional diagnostic methods, including toxigenic bacterial cell culture and tissue cell culture cytotoxicity neutralization assays, have been considered as the reference standard [8]. These assays require technical expertise and several days to obtain results: therefore, they are not appropriate for the clinical setting, where an accurate and rapid diagnosis is needed. An enzyme immunoassay (EIA) for TcdB alone or both TcdA and TcdB has been widely used in most laboratories because it is relatively simple, rapid, and commercially available [9]. However, it has been revealed that the sensitivity of EIA is as low as 23% and the specificity as low as 75% [10]. Therefore, in practice, a symptomatic patient with the EIA-negative result is usually tested by another assay with higher sensitivity. Many laboratories have reported the combination of assays to increase the sensitivity and specificity of the detection [11–13]. An example include a 2-step algorithm, in which the first step is to perform an EIA for glutamate dehydrogenase (GDH) and the second step is to test the GDH-positives with an EIA for toxins. The EIA for GDH step yields a highly sensitive result for *C. difficile*, but is not specific for toxigenic isolates; therefore, the GDH-positive results must be confirmed with a subsequent specific test such as EIA for toxins [13]. Although these algorithms improve the diagnostic performance, it has been shown that the levels of sensitivity of the EIA for GDH in this two-step algorithm vary depending on the *C. difficile* ribotypes [14]. Moreover, the two- or more step assays are cost-ineffective [15]. Recently, nucleic acid amplification tests (NAATs) have been developed as a single assay with the same day results for CDI. These assays aim to detect the toxin gene(s) and have been proven to be more superior than other methods, except the toxigenic bacterial cell culture, as they yield the high sensitivity and high negative predictive value [16]. Currently, there are a number of FDA-approved commercially available NAATs including (i) the Xpert *C. difficile*, (ii) Xpert *C. difficile*/Epi assays that detect *tcdB* by real-time PCR, and (iii) the Illumigene *C. difficile* assay that detects *tcdA* by loop-mediated isothermal amplification [17].

Although the NAATs have gained popularity for CDI diagnosis, the common drawbacks of this type of assays to detect pathogens directly from stool samples are the presence of PCR inhibitors, contamination of DNA from host and other microorganisms, and low quality and yield of bacterial DNA that is extracted from spores in stool samples from suspected patients. Thus, the objective of this study was to evaluate the multiplex PCR with enhanced spore germination for the detection of *C. difficile* directly from stool samples of hospitalized patients. The combination of sample processing with the high-performance detection method would be applicable for routine diagnostic use in clinical setting.

2. Materials and Methods

2.1. Specimen Collection and Acquisition. A total of 238 fecal specimens from inpatients that aged more than 15 years and developed diarrhea during hospitalization at Ramathibodi hospital, a 1,000-bed tertiary health care university Hospital, were collected from May 2010 to January 2011. The samples were subjected to the routine EIA test using VIDAS *C. difficile* Toxin A&B qualitative assay (BioMérieux, Marcy l'Etoile, France) according to the manufacturer's recommendations. The samples were also subjected to *C. difficile* selective culture by plating onto cycloserine cefoxitin fructose agar (CCFA) and incubated anaerobically at 37°C for up to 5 days. All samples were then subsequently stored at −80°C before use. The use of human materials has been approved by the research ethics committee of the Faculty of Medicine at Ramathibodi Hospital, Mahidol University, Thailand.

2.2. Bacterial Cell Culture. Clostridium strains were grown anaerobically in BHIS medium, brain heart infusion broth at 37°C (Oxoid, Basingstoke, UK), supplemented with 5% yeast extract, 0.1% sodium thioglycolate (TCI, Tokyo, Japan), and 0.1% L-cysteine (TCI). Before sterilization, anaerobic conditions were created by boiling the medium for 10 min and, during cooling, flushing the medium with nitrogen gas. All other bacteria were cultivated at 37°C in tryptone soy broth (Oxoid).

2.3. Multiplex PCR for the Detection of C. difficile Toxin Genes. A multiplex PCR was developed for the detection of toxin genes including *tcdA*, *tcdB*, *cdtA*, and *cdtB* as well as *16S rDNA* as a internal control. A total volume of 20 μL PCR reaction consisted of 1 × PCR buffer (10 mM Tris-HCl, 50 mM KCl, and pH 8.3), 5 mM $MgCl_2$, 250 μM dNTP, 1 × enhancer (0.5 M betaine, 1% DMSO), 1 U of Taq DNA polymerase (New England Biolabs, MA, USA), and 5 pairs of primers at indicated concentrations (Table 1). Thermal cycling parameters included (i) an initial denaturation at 92.5°C for 2 min; (ii) 30 cycles of denaturation at 92.5°C for 20 s, annealing at 60°C for 65 s, and extension at 68°C for 70 s; and (iii) a final extension at 68°C for 5 min. PCR products were resolved by electrophoresis on a 2% agarose gel stained with ethidium bromide.

2.4. Preparation of C. difficile Spores. Spores from *C. difficile* strain R20291 were produced in a sporulation medium as described previously [18]. Briefly, a culture of *C. difficile* was spread onto BHIS agar supplemented with 0.1% taurocholate (BHIS/TA). The plates were then incubated at 37°C under anaerobic conditions for 5 days. Spores were scraped off the plates and resuspended in deionized water. The samples were then washed ten times with water. The spores were checked for purity and enumerated using phase-contrast microscopy and light microscopy after staining with malachite green and

Table 1: Primers in the multiplex PCR for the detection of *C. difficile*.

Target	Primer	Sequence (5′-3′)	Primer concentration (μM)	Amplicon size (bp)
tcdA	tcdA-F	GTATGGATAGGTGGAGAAGTCAGTG	0.025	632
	tcdA-R	CGGTCTAGTCCAATAGAGCTAGGTC	0.025	
tcdB	tcdB-F	GAAGATTTAGGAAATGAAGAAGGTGA	0.01	441
	tcdB-R	AACCACTATATTCAACTGCTTGTCC	0.01	
cdtA	cdtA-F	ATGCACAAGACTTACAAAGCTATAGTG	0.2	260
	cdtA-R	CGAGAATTTGCTTCTATTTGATAATC	0.2	
cdtB	cdtB-F	ATTGGCAATAATCTATCTCCTGGA	0.5	179
	cdtB-R	CCAAAATTTCCACTTACTTGTGTTG	0.5	
16s rDNA	UFU-L	GCCTAACACATGCAAGTCGA	0.025	800
	UR802	TACCAGGGTATCTAATCC	0.025	

eosin Y. Spore samples were then stored at −20°C until further analysis.

2.5. Enrichment PCR Procedures. In order to evaluate the effects of enhanced spore germination and enrichment on the multiplex PCR detection of *C. difficile*, two consecutive methods were performed with spore-inoculated feces prior to the multiplex PCR. One hundred *C. difficile* spores were spiked into 1 gram of homogenized fecal samples. Bulk debris was avoided during sample withdrawal. The spiked samples were then subjected to the pretreatment conditions with or without alcohol shock for 20 min. Alcohol shock should eliminate vegetative bacterial cells from the samples, leaving viable spores to germinate. Following the alcohol shock, either nonselective spore germination medium BHIS/TA alone or selective BHIS/TA/CC medium (BHIS/TA in the presence of 250 mg/L cycloserine and 20 mg/L cefoxitin) was added to the samples, which were incubated anaerobically at 0, 1, 2, and 3 h. The samples were then divided to two halves, one of which was subjected to bacterial DNA extraction using EZNA stool DNA kit (Omega, GA, USA); the other was then cultured on either BHIS or CCFA plates. All experiments were performed in triplicate.

3. Results and Discussion

Toxigenic *C. difficile* strains are recognized as the main cause of nosocomial diarrhea [1–3]. Therefore, a rapid and cost-effective method to detect *C. difficile* directly from stool samples facilitates patient management to control CDI. The aim of this work was to design an optimized multiplex PCR for the detection of toxigenic *C. difficile* from stool samples of hospitalized patients and to evaluate the combination of various sample processing conditions and multiplex PCR on such detection.

3.1. Multiplex PCR for the Detection of Toxigenic C. difficile. In the past years, there have been an increasing number of *C. difficile* genome and toxin gene sequences deposited in the GenBank database, enabling us to design more specific primers. The 5-plex PCR primers were developed for the detection of the four *C. difficile* toxin genes including *tcdA*, *tcdB*, *cdtA*, and *cdtB*, together with *16S rDNA* as an internal PCR control (Figure 1). The primer set was chosen to amplify products with distinguishable sizes on agarose gel electrophoresis. The individual primer pairs for the amplification of the regions in the *tcdA*, *tcdB*, *cdtA* and *cdtB* genes were tested in single-plex PCRs (Figure 1; lanes 1–4, respectively). The multiplex PCR with a combination of all five primer pairs was optimized (Figure 1; lane 5) and was tested with different PCR *C. difficile* ribotypes (Figure 2). Our results are consistent with the previously reported data [19].

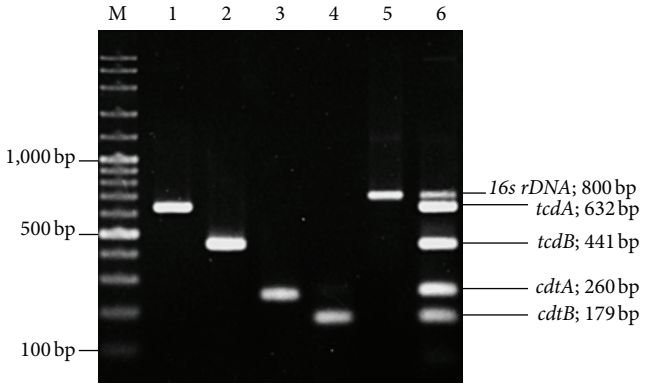

Figure 1: Agarose gel electrophoresis of the PCR products tested with five primer pairs using 20 ng of genomic DNA of *C. difficile* R20291 as template. Each primer pair was tested individually and in combination with all 5 primer pairs in the multiplex PCR. Lane M: 100-bp DNA ladder marker. Lanes 1–5, single-plex PCR reactions using primers specific to *tcdA*, *tcdB*, *cdtA*, *cdtB*, and *16s rDNA*, respectively. Lane 6: multiplex PCR with all four toxin-specific primers and 16S rDNA primers.

3.2. Sensitivity and Specificity Test. The sensitivity and specificity of the developed multiplex PCR for the detection of *C. difficile* were evaluated. The detection limit as measured with genomic DNA from toxigenic reference strain *C. difficile* R20291 was 0.1 pg or ~22 genomic copy number per reaction. To further evaluate the primer specificities for *C. difficile*,

Table 2: Evaluation of pretreatment and enrichment conditions prior to multiplex PCR and bacterial cell culture for the detection of *C. difficile* directly from stool samples.

Pretreatment condition	Enrichment condition	Incubation time (h)	Typical *C. difficile* colony		Multiplex PCR toxin genes detection
			CCFA agar plate	BHI agar plate	
Alcohol shock	BHIS/TA	0	−	−	−
		1	−	−	+
		2	−	ND	+
		3	+	ND	+
	BHIS/TA/CC	0	−	−	−
		1	−	−	+
		2	−	ND	+
		3	+	ND	+
No alcohol shock	BHIS/TA	0	−	ND	−
		1	−/+	ND	+
		2	+	ND	+
		3	+	ND	+
	BHIS/TA/CC	0	−	ND	−
		1	−/+	ND	+
		2	+	ND	+
		3	+	ND	+

ND stands for "not determined" because there were too many contaminated bacterial species, rendering it impossible to distinguish *C. difficile* colonies on the plates. −/+ indicates that typical *C. difficile* colonies could not be observed in at least one of the three replicates.

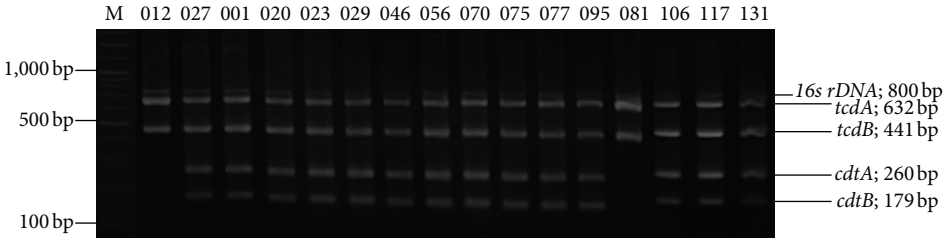

Figure 2: Multiplex PCR toxin gene amplification profiles of various *C. difficile* ribotypes. Lane M: 100 bp DNA ladder marker. The ribotypes and PCR products of detected genes are indicated.

7 other *Clostridium* spp. strains including *C. septicum*, *C. glycolicum*, *C. perfringens*, *C. tetani*, *C. sordellii*, *C. sporogenes*, and *C. botulinum*, as well as 7 of non-*Clostridium* strains including *Bacillus cereus*, *Salmonella* Typhi, *Shigella dysenteriae*, *Escherichia coli*, *Enterobacter faecalis*, *Klebsiella ozaenae*, and *Citrobacter fundi* were tested. None of the non-*C. difficile* strains gave rise to the PCR-positive results, thereby indicating the specificity of the multiplex PCR assay.

3.3. Enrichment Multiplex PCR for Detection of Toxigenic C. difficile. The multiplex PCR assays for detection of toxigenic *C. difficile* directly from fecal specimens have been previously reported [20–22]. However, the detection limit has been shown to be as low as 5×10^4 cfu per 1 g of feces [22]. The sensitivity of the PCR is usually affected by inhibitors found in stool samples including bile salts, complex polysaccharides, proteinases, a high concentration of background flora, and a low concentration and uneven distribution of target microorganism [23], rendering it not suitable for PCR detection of the pathogen from direct stool samples. In this study, different combinations of pretreatment conditions, enrichment conditions, and enrichment times prior to both multiplex PCR and conventional bacterial cell culture methods were evaluated to determine the possibility of detecting 100 *C. difficile* spores per 1 g of feces (Table 2). This low spore concentration was not detected by nonenrichment multiplex PCR and culture methods. Regarding the pretreatment step, the *C. difficile* colonies were observed on CCFA after 1 h of enrichment without alcohol shock, compared to 3 h with the alcohol shock. Under nonselective plating, most conditions yielded uninterpretable results due to the high levels of contamination of other microorganisms. Positive PCR results were obtained under the conditions of the 1 h enrichment time, regardless of pretreatment or enrichment broth. Therefore, the condition of no alcohol shock and enrichment with BHIS/TA for 1 h was identified as the optimal combination with practical working hours in laboratories and was appropriate for both bacterial cell culture and multiplex PCR diagnosis. Furthermore, the sensitivity of the developed multiplex PCR under the

Table 3: Comparison of different diagnostic assays including toxin EIA, multiplex PCR, and bacterial cell culture.

Toxin EIA	Multiplex PCR	Bacterial cell culture	Number of cases
+	+	+	16
+	+	−	4
+	−	−	18
−	+	+	10
−	+	−	24
−	−	−	166

described conditions was also tested with fecal samples spiked with different numbers of spores. We found that the multiplex PCR was able to detect as low as 5 spores/g feces. Therefore, the enrichment broth could enhance spore germination and transformation into vegetative cells, allowing them to grow to PCR-detectable levels.

3.4. Detection of Toxigenic C. difficile in Clinical Stool Samples. To examine the efficacy of the assay described in this study, 238 stool samples of patients suspected of CDI were subjected to multiple PCR with the enhanced spore germination as above. Routine EIA and bacterial cell culture assays were also performed. All samples were tested positive for the *16S rDNA* control gene. Comparison of different diagnostic assays is shown in Table 3. Sixteen cases were tested positive while 166 cases gave rise to negative results in all three assays. Eighteen samples were EIA positive, but both PCR and culture negative, and were, therefore, considered to be negative due to the low level of EIA specificity that requires the second assay to confirm the EIA results. Twenty-four cases were shown to be PCR positive with either EIA positive or culture positive. These results represented another two-step diagnostic process that increased the reliability of the PCR outcomes. Twenty-four samples were PCR positive, but both EIA and culture turned out negative. Although anaerobic culture was considered the most sensitive assay for the detection of *C. difficile*, it is also likely that the low spore counts in fecal samples and different rates of spore viability would account for such results. However, another confirmatory assay should be performed to support the PCR results. Of 54 PCR-positive samples, 7 were $tcdA^{+}\ tcdB^{+}\ cdtA/B^{+}$, 13 were $tcdA^{+}\ tcdB^{+}\ cdtA/B^{-}$, 30 were $tcdA^{-}\ tcdB^{+}\ cdtA/B^{-}$, and 4 were $tcdA^{-}\ tcdB^{+}\ cdtA/B^{-}$. Although, there are previous reports on *C. difficile* toxin types in Thailand [24, 25], this is the first time that the $tcdA^{+}\ tcdB^{+}\ cdtA/B^{+}$ isolates were detected. It is also noteworthy that PCR detection of *C. difficile* toxin genes might only detect DNA without the presence of toxin production; therefore, the PCR-positive cases should be carefully interpreted.

Although the enrichment multiplex PCR in this study showed superiority over the other two diagnostic methods, the limitations of our experimental setting include the lack of another confirmatory diagnostic test such as cell cytotoxicity; so the false positives or negatives in cases of discordant test results could not be identified. However, analytical sensitivity with the reference *C. difficile* strain and spore-inoculated fecal samples and specificity of the multiplex PCR assay with various *C. difficile* ribotypes, other *Clostridium* spp., and other bacteria species revealed high sensitivity with no false positive or false negative.

4. Conclusions

This work revealed the comprehensive evaluation of sample processing prior to the multiplex PCR diagnosis of *C. difficile* directly from clinical stool samples. The results demonstrated that the enrichment of nonselective medium for 1 h prior to both PCR or bacterial cell culture assays yielded the most optimal condition. The performance of the enrichment multiplex PCR was proven to be more superior to that of the routine EIA. This rapid and cost-effective diagnostic assay provides an alternative approach for the detection of *C. difficile*, thereby improving the CDI management. However, a large-scale clinical testing is warranted to further validate this assay.

Acknowledgments

The authors thank Professor Nigel Minton, University of Nottingham for providing us with *C. difficile* reference strains. They also thank Nattamon Malaisree for technical assistance. This work is supported by a Joint Grant from the Faculty of Science and Faculty of Medicine Ramathibodi Hospital, Mahidol University and a Supplementary Grant from the Faculty of Science, Mahidol University, Thailand.

References

[1] K. C. Carroll and J. G. Bartlett, "Biology of *Clostridium difficile*: implications for epidemiology and diagnosis," in *Annual Review of Microbiology*, vol. 65, pp. 501–521, 2011.

[2] N. Oezguen, T. D. Power, P. Urvil et al., "Clostridial toxins: sensing a target in a hostile gut environment," *Gut Microbes*, vol. 3, no. 1, pp. 35–41, 2012.

[3] S. Bacci, K. Mølbak, M. K. Kjeldsen, and K. E. P. Olsen, "Binary toxin and death after *Clostridium difficile* infection," *Emerging Infectious Diseases*, vol. 17, no. 6, pp. 976–982, 2011.

[4] C. Schwan, B. Stecher, T. Tzivelekidis et al., "*Clostridium difficile* toxin CDT induces formation of microtubule-based protrusions and increases adherence of bacteria," *PLoS Pathogens*, vol. 5, no. 10, article e1000626, 2009.

[5] S. T. Cartman, J. T. Heap, S. A. Kuehne, A. Cockayne, and N. P. Minton, "The emergence of 'hypervirulence' in *Clostridium difficile*," *International Journal of Medical Microbiology*, vol. 300, no. 6, pp. 387–395, 2010.

[6] E. J. Kuijper, R. J. van den Berg, and J. S. Brazier, "Comparison of molecular typing methods applied to *Clostridium difficile*," *Methods in Molecular Biology*, vol. 551, pp. 159–171, 2009.

[7] M. Delmée, J. Van Broeck, A. Simon, M. Janssens, and V. Avesani, "Laboratory diagnosis of *Clostridium difficile*-associated diarrhoea: a plea for culture," *Journal of Medical Microbiology*, vol. 54, part 2, pp. 187–191, 2005.

[8] L. R. Peterson, P. J. Kelly, and H. A. Nordbrock, "Role of culture and toxin detection in laboratory testing for diagnosis

of *Clostridium difficile*-associated diarrhea," *European Journal of Clinical Microbiology and Infectious Diseases*, vol. 15, no. 4, pp. 330–336, 1996.

[9] H. Snell, M. Ramos, S. Longo, M. John, and Z. Hussain, "Performance of the TechLab C. DIFF CHEK-60 enzyme immunoassay (EIA) in combination with the *C. difficile* tox A/B II EIA kit, the triage *C. difficile* panel immunoassay, and a cytotoxin assay for diagnosis of *Clostridium difficile*-associated diarrhea," *Journal of Clinical Microbiology*, vol. 42, no. 10, pp. 4863–4865, 2004.

[10] H. Vanpoucke, T. De Baere, G. Claeys, M. Vaneechoutte, and G. Verschraegen, "Evaluation of six commercial assays for the rapid detection of *Clostridium difficile* toxin and/or antigen in stool specimens," *Clinical Microbiology and Infection*, vol. 7, no. 2, pp. 55–64, 2001.

[11] B. M. Shin, Y. K. Eun, J. L. Eun, and J. G. Songer, "Algorithm combining toxin immunoassay and stool culture for diagnosis of *Clostridium difficile* infection," *Journal of Clinical Microbiology*, vol. 47, no. 9, pp. 2952–2956, 2009.

[12] E. J. Kvach, D. Ferguson, P. F. Riska, and M. L. Landry, "Comparison of BD GeneOhm Cdiff real-time PCR assay with a two-step algorithm and a toxin A/B enzyme-linked immunosorbent assay for diagnosis of toxigenic *Clostridium difficile* infection," *Journal of Clinical Microbiology*, vol. 48, no. 1, pp. 109–114, 2010.

[13] M. E. Reller, C. A. Lema, T. M. Perl et al., "Yield of stool culture with isolate toxin testing versus a two-step algorithm including stool toxin testing for detection of toxigenic *Clostridium difficile*," *Journal of Clinical Microbiology*, vol. 45, no. 11, pp. 3601–3605, 2007.

[14] F. C. Tenover, S. Novak-Weekley, C. W. Woods et al., "Impact of strain type on detection of toxigenic *Clostridium difficile*: comparison of molecular diagnostic and enzyme immunoassay approaches," *Journal of Clinical Microbiology*, vol. 48, no. 10, pp. 3719–3724, 2010.

[15] S. M. Novak-Weekley, E. M. Marlowe, J. M. Miller et al., "*Clostridium difficile* testing in the clinical laboratory by use of multiple testing algorithms," *Journal of Clinical Microbiology*, vol. 48, no. 3, pp. 889–893, 2010.

[16] J. A. Barkin, N. Nandi, N. Miller, A. Grace, J. S. Barkin, and D. A. Sussman, "Superiority of the DNA amplification assay for the diagnosis of *C. difficile* infection: a clinical comparison of fecal tests," *Digestive Diseases and Sciences*, vol. 57, no. 10, pp. 2592–2599, 2012.

[17] K. C. Carroll, "Tests for the diagnosis of *Clostridium difficile* infection: the next generation," *Anaerobe*, vol. 17, no. 4, pp. 170–174, 2011.

[18] D. Heeg, D. A. Burns, S. T. Cartman, and N. P. Minton, "Spores of *Clostridium difficile* clinical isolates display a diverse germination response to bile salts," *PLoS One*, vol. 7, no. 2, article e32381, 2012.

[19] M. Rupnik, "Heterogeneity of large clostridial toxins: importance of *Clostridium difficile* toxinotypes," *FEMS Microbiology Reviews*, vol. 32, no. 3, pp. 541–555, 2008.

[20] F. Barbut, M. Monot, A. Rousseau et al., "Rapid diagnosis of *Clostridium difficile* infection by multiplex real-time PCR," *European Journal of Clinical Microbiology & Infectious Diseases*, vol. 30, no. 10, pp. 1279–1285, 2011.

[21] R. A. Luna, B. L. Boyanton Jr., S. Mehta et al., "Rapid stool-based diagnosis of *Clostridium difficile* infection by real-time PCR in a children's hospital," *Journal of Clinical Microbiology*, vol. 49, no. 3, pp. 851–857, 2011.

[22] S. D. Bélanger, M. Boissinot, N. Clairoux, F. J. Picard, and M. G. Bergeron, "Rapid detection of *Clostridium difficile* in feces by real-time PCR," *Journal of Clinical Microbiology*, vol. 41, no. 2, pp. 730–734, 2003.

[23] P. Lantz, W. Abu Al-Soud, R. Knutsson, B. Hahn-Hagerdal, and P. Rådstrom, "Biotechnical use of polymerase chain reaction for microbiological analysis of biological samples," *Biotechnology Annual Review*, vol. 5, pp. 87–130, 2000.

[24] S. Wongwanich, S. Rugdeekha, P. Pongpech, and C. Dhiraputra, "Detection of *Clostridium difficile* toxin A and B genes from stool samples of Thai diarrheal patients by polymerase chain reaction technique," *Journal of the Medical Association of Thailand*, vol. 86, no. 10, pp. 970–975, 2003.

[25] D. Chotiprasitsakul, T. Janvilisri, S. Kiertiburanakul et al., "A superior test for diagnosis of *Clostridium difficile*-associated diarrhea in resource-limited settings," *Japanese Journal of Infectious Diseases*, vol. 65, pp. 326–329, 2012.

Hindawi Publishing Corporation
BioMed Research International
Volume 2013, Article ID 264651, 8 pages
http://dx.doi.org/10.1155/2013/264651

Research Article

Development of a Broad-Range 23S rDNA Real-Time PCR Assay for the Detection and Quantification of Pathogenic Bacteria in Human Whole Blood and Plasma Specimens

Paolo Gaibani,[1,2] Mara Mariconti,[3,4] Gloria Bua,[1] Sonia Bonora,[1] Davide Sassera,[3] Maria Paola Landini,[1] Patrizia Mulatto,[4] Stefano Novati,[4] Claudio Bandi,[3] and Vittorio Sambri[1]

[1] *Operative Unit of Clinical Microbiology, St. Orsola-Malpighi University Hospital, 40138 Bologna, Italy*
[2] *Department of Haematology and Oncology "L. and A. Seragnoli", Unit of Clinical Microbiology, Regional Reference Centre for Microbiological Emergencies (CRREM), St. Orsola-Malpighi Hospital, University of Bologna, 9 Via G. Massarenti, 40138 Bologna, Italy*
[3] *DIVET, University of Milan, 20100 Milan, Italy*
[4] *Fondazione IRCCS Policlinico San Matteo, 27100 Pavia, Italy*

Correspondence should be addressed to Paolo Gaibani; paolo.gaibani@unibo.it

Received 17 October 2012; Revised 15 January 2013; Accepted 29 January 2013

Academic Editor: Arun K. Bhunia

Molecular methods are important tools in the diagnosis of bloodstream bacterial infections, in particular in patients treated with antimicrobial therapy, due to their quick turn-around time. Here we describe a new broad-range real-time PCR targeting the 23S rDNA gene and capable to detect as low as 10 plasmid copies per reaction of targeted bacterial 23S rDNA gene. Two commercially available DNA extraction kits were evaluated to assess their efficiency for the extraction of plasma and whole blood samples spiked with different amount of either *Staphylococcus aureus* or *Escherichia coli*, in order to find the optimal extraction method to be used. Manual QIAmp extraction method with enzyme pre-treatment resulted the most sensitive for detection of bacterial load. Sensitivity of this novel assay ranged between 10 and 10^3 CFU per PCR reaction for *E. coli* and *S. aureus* in human whole blood samples depending on the extraction methods used. Analysis of plasma samples showed a 10- to 100-fold reduction of bacterial 23S rDNA in comparison to the corresponding whole blood specimens, thus indicating that whole blood is the preferential sample type to be used in this real-time PCR protocol. Our results thus show that the 23S rDNA gene represents an optimal target for bacteria quantification in human whole blood.

1. Introduction

Blood culture (BC) is the most widely used method for the diagnosis of bloodstream bacterial infections (BSIs) [1]. Major limitations of culture techniques are the intrinsic poor cultivability (or noncultivability) of some bacteria and the inhibitory effects of concurrent antibiotic therapy. In addition, the turn-around time of BC ranges from 24 to 72 hours, which implies that results might become available too late to be of clinical utility [2]. In recent years, molecular methods have been proposed as additional diagnostic tools for BSIs [2, 3]. Several studies reported the development and clinical assessment of broad-range real-time PCR protocols, capable of rapid detection and identification of a vast proportion of cultivable and uncultivable bacteria, from different types of biological samples [4–12]. The majority of the broad-range real-time PCRs use a single pair of universal primers to identify bacteria through the amplification of the 16S ribosomal DNA (16S 0072DNA), given the high level of homology of this gene throughout the bacterial species diversity [12]. The amplification of the 16S rDNA has been described as a specific and sensitive tool to identify and quantify different microorganisms depending on the specific protocol used [7, 13–17]. A major pitfall of 16S-based

panbacterial primers is their cross-reactivity with human ribosomal RNA genes; to overcome the problem, Kommedal and coworkers proposed a 16S rDNA-based dual-priming protocol [18]. In addition to 16S rDNA, the gene coding for the large subunit ribosomal RNA (23S rDNA) has also been targeted for the development of PCR methods for bacterial detection, but only a limited number of studies evaluated the utility of 23S-based panbacterial primers [4, 19], and no studies have so far exploited this target for BSI monitoring. The aim of our study was to develop a novel 23S rDNA-targeted real-time pan-bacterial PCR method, suitable for the detection of a wide range of bacterial species, for the monitoring of BSIs. In addition, since the amount of bacterial DNA detected in blood from healthy subjects is reported to be highly variable and profoundly influenced by the use of whole blood or plasma [4, 7, 20], we tested the suitability of different extraction procedures for the isolation of bacterial DNA from blood-derived specimens.

2. Materials and Methods

2.1. Design of the 23S rDNA Universal Primers. Complete 23S rDNA sequences from 50 bacterial species, spanning the eubacterial diversity, were retrieved from the NCBI database (http://www.ncbi.nlm.nih.gov/). Alignment of the sequences was performed using the MUSCLE software [21] and manually checked. 28S rDNA sequences from *Caenorhabditis elegans*, *Candida albicans*, *Drosophila melanogaster,* and *Homo sapiens* were also included in the alignment, in order to evaluate the specificity for the bacterial rDNA of the designed primers. Primers were manually designed on the obtained alignment, and then evaluated using mfold (http://mfold.rna.albany.edu/?q=mfold) and the Operon oligo analysis tool (http://www.operon.com/tools/oligo-analysis-tool.aspx). The sequences of the 23S rDNA-targeted pan-bacterial primers are PAN23S-F, 5′-TCGCTC-AACGGATAAAAG-3′ and PAN23S-R, 5′-GATGAnCCG-ACATCGAGGTGC-3′; the amplified fragment size is 97 base pairs in *Escherichia coli*. The designed primers were then compared to the nonredundant nucleotide eukaryotic database using the Blast software (http://blast.ncbi.nlm.nih.gov/Blast.cgi), to highlight possible unwanted matches.

2.2. 23S rDNA Real-Time PCR. PCR reactions were effected in a final volume of 25 μL, containing 12.5 μL of SYBR Green PCR Master Mix Reagent (Biorad-Hercules, CA, USA), 250 nM of each primer, and 5 μL of the extracted DNA solution. PCR was performed in an IQ5 thermocycler (Biorad-Hercules, CA, USA) with an initial step of 5 min at 95°C, followed by 40 cycles of 15 s at 95°C and 30 s at 58°C. After PCR amplification, the melting curve was established by increasing the temperature from 55°C to 95°C.

2.3. Bacterial Isolates. A panel of 47 different bacterial isolates, 20 Gram-positive, and 27 Gram-negative was included in the study (Table 1). These strains were either obtained from routine cultures, identified at the Unit of Clinical Microbiology, St. Orsola Malpighi Hospital, or obtained from the bacterial collection at the same Institution (BACSO). A cell suspension containing 10^8 CFU/mL was obtained from each bacterial isolate, and the DNA was extracted using described protocols [22]. PCR products obtained from bacterial cultures were then sequenced to verify whether just bacterial DNA had been amplified and cloned. In addition,

Table 1: Bacterial strains utilized in this study. The strains were either obtained from the bacterial collection of the St. Orsola Hospital (BACSO) or derived from routine workflow. In this last case the procedure for identification are reported in the Qualty Assurance files of the Laboratory.

Microorganisms species	Origin of the isolate
Acinetobacter baumannii	Urine
Acinetobacter lwoffii	Urine
Alcaligenes xylosoxidans	Urine
Bacteroides fragilis	Cerebrospinal fluid
Campylobacter jejuni	Feces
Citrobacter braakii	Abdominal drainage
Citrobacter freundii	Blood
Citrobacter koseri	Urine
Corynebacterium jeikeium	Blood
Corynebacterium minutissimum	Blood
Corynebacterium striatum	Blood
Corynebacterium urealyticum	Blood
Enterobacter cloacae	Urine
Enterobacter aerogene	Urine
Enterococcus casseliflavus	Blood
Enterococcus faecalis	Bacso/atcc 29212
Enterococcus faecium	Blood
Enterococcus gallina rum	Blood
Escherichia coli	Bacso/atcc 25922
Haemophilus influenzae	Bacso/atcc 49247
Haemophilus influenzae	Bacso/atcc 49766
Hafnia alvei	Bile
Klebsiella oxytoca	Blood
Klebsiella pneumoniae	Urine
Morganella morganii	Urine
Nocardia sp.	Bronchial aspirate
Proteus mirabilis	Urine
Proteus vulgaris	Bronchial aspirate
Providencia stuartii	Urine
Pseudomonas aeruginosa	Bacso/atcc 27853
Pseudomonas luteola	Bronchial aspirate
Salmonella sp. Group B	Feces
Salmonella sp. Group C	Feces
Salmonella sp. Group D	Feces
Serratia marcescens	Urine
Staphylococcus aureus	Bacsoatcc 29213
Staphylococcus epidermidis	Blood
Staphylococcus haemolyticus	Blood
Staphylococcus hominis	Blood
Staphylococcus warneri	Blood
Stenotrophomonas maltophilia	Faringeal swab
Streptococcus agalactiae	Uretral swab
Streptococcus anginosus	Blood
Streptococcus mitis	Blood
Streptococcus parasanguinis	Blood
Streptococcus pyogene	Faringeal swab
Streptococcus pneumoniae	Bacso/atcc 49619

five eukaryotic species from the genus *Candida* (*Candida albicans, Candida glabrata, Candida tropicalis, Candida parapsilosis,* and *Candida guilliermondii*) were included in the study.

2.4. PCR Sensitivity Test. An external standard for absolute quantification (i.e., the target 23S rDNA gene fragment, cloned into a plasmid vector) was prepared. PCR was effected on *Staphylococcus aureus* DNA using the above described primers PAN23S-F and PAN23S-R according to standard PCR conditions. The band resolved on a 2% agarose gel was excised and the PCR product was then purified, quantified, and cloned using the pGEM T-easy vector (Qiagen, Basel, Switzerland) according to manufacturers' instructions. Ten randomly selected clones were sequenced with ABI technology. A plasmid containing the 23S rDNA insert was purified from one of the clones, using the QIAprep Spin Miniprep Kit (Qiagen, Basel, Switzerland). After quantification, a serial dilution of the plasmid was used to assess the sensitivity of the above PCR assay, with plasmid at concentrations ranging from 10^8 to 10^1 copies per reaction, to generate the standard curve.

2.5. DNA Extraction from Whole Blood Spiked with Gram-Positive and Gram-Negative Bacteria. Tenfold serial dilution of bacteria in blood was prepared, by spiking fresh K_3EDTA blood samples with *S. aureus* ATCC 25923 or *E. coli* ATCC 25922 (as representative strains for Gram-positive and Gram-negative bacteria), to obtain final concentrations of bacteria ranging from 10^7 CFU per mL to 10 CFU per mL of blood. A written informed consent was obtained from each blood donor following the ethical rules of the St. Orsola Hospital Blood Bank in Bologna. As a control, identical series were prepared in phosphate buffer saline (PBS). Standard 100 μL volumes from each sample of these spiked series (blood or PBS) were subjected to DNA extraction, using the different protocols reported below. Two different commercially available methods were used following the manufacturers' instructions: the automated nucleic acid extractor NucliSens EasyMag (BioMerieux, Marcy l'Etoile, France) and the manual QIAmp DNA blood mini kit (Qiagen, Basel, Switzerland). As a third option, the following modification of the QIAmp DNA blood mini kit was also used: 100 μL of fresh whole blood or PBS spiked series were preincubated with 90 μL of the enzyme solution buffer (20 mg/mL lysozyme, 20 mM Tris HCl, 2 mM EDTA, 1% Triton). After 2 h of incubation at 37°C, the mixture was incubated at 56°C for 2 h with addition of 10 μL of proteinase K, at a concentration of 20 mg/mL (Sigma-Aldrich, St. Louis, MO, USA) and 100 μL of AL Buffer. Then, the mixture (of 300 μL) was subjected to DNA extraction with the QIAmp DNA blood mini kit. The DNA obtained using the three different procedures was eluted to a final volume of 50 μL. In summary, these 50 μL of eluted DNA derived from 1/10 of the blood spiked with the above number of CFUs (i.e., 10^6–10^0 CFU in each 50 μL elution). This implies that the five microliters used as template DNA for real-time PCR contained bacterial DNAs derived from $10^5 - 10^{-1}$ CFU. A series of blood samples spiked as above with *E. coli* or *S. aureus* were processed for plasma preparation: the spiked series of blood samples were incubated for 2 hours at room temperature (RT) and then centrifuged at 400 g for 15 minutes at RT. DNA was then extracted as above, using the three different procedures. Each extracted DNA was tested by real-time PCR, and the *CT* values were applied to the standard curve generated in the same experiment to obtain the corresponding copy number of bacterial 23S rDNA gene targets in each reaction. Additionally, real-time PCR was performed on DNA extracted from blood from healthy donors, used as negative control.

Klebsiella pneumoniae	5′	----------	3′
Enterococcus faecalis	5′	----------	3′
Streptococcus pneumoniae	5′	----------	3′
Staphylococcus aureus	5′	----------	3′
Escherichia coli	5′	----------	3′
Pseudomonas aeruginosa	5′	----------	3′
Acinetobacter baumanii	5′	----------	3′
Candida sp.	5′	CTAGAGGTGCC-G------	3′
Homo sapiens	5′	CA-GAGGTGTC-G------	3′
Drosophila melanogaster	5′	CAAGAGGTGTC-G------	3′
Caenorhabditis elegans	5′	CA-GAGGTGT-GG-----T	3′
PANB-forward	5′	-TCGCTCAACGGATAAA G	3′

Klebsiella pneumoniae	5′	----------	3′
Enterococcus faecalis	5′	----------	3′
Streptococcus pneumoniae	5′	----------	3′
Staphylococcus aureus	5′	----------	3′
Escherichia coli	5′	----------	3′
Pseudomonas aeruginosa	5′	----------	3′
Acinetobacter baumanii	5′	----------	3′
Candida sp.	5′	--A----------A-AAT	3′
Homo sapiens	5′	--A----------A-AAT	3′
Drosophila melanogaster	5′	--A----------A-AAT	3′
Caenorhabditis elegans	5′	--A----------A-AAT	3′
PANB-reverse	5′	GATGANCCGACATCGAGGTGC	3′

Figure 1: Analysis of PANB-forward and PANB-reverse primers homology sequences against the 23S rDNA of the most common pathogenic bacteria species, *Homo sapiens, Caenorhabditis elegans*, *Candida albicans* and *Drosophila melanogaster* in their binding areas.

3. Results

3.1. Specificity and Sensitivity of the 23S Real-Time PCR Assay. The comparison of the designed primers with the sequences from the 50 bacterial species included in the alignment shows an almost complete identity, with no mismatches at the 3′ end, while a high number of mismatches are present in the alignment with the eukaryotic organisms included, that is, *H. sapiens*, *C. elegans*, *C. albicans,* and *D. melanogaster*, as shown in Figure 1.

In order to validate our *in silico* findings, the specificity of the novel 23S rDNA-targeted primers was also evaluated on a total of 20 Gram-positive and 27 Gram-negative bacterial strains (see Table 1 for details) and on five eukaryotic species, from the genus *Candida* (see Section 2). PCR amplification was obtained from the 47 bacterial DNAs,

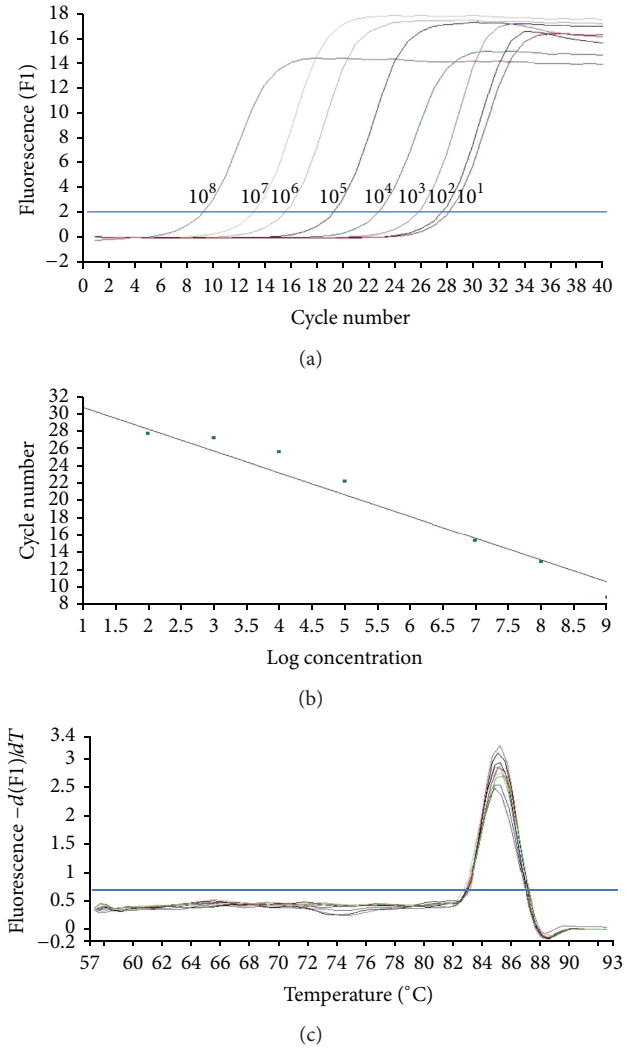

Figure 2: Standard curve amplification of cloned bacterial 23S rDNA plasmid real-time PCR ranging from 10^8 to 10^1 copies per reaction. Panel (a) shows the amplification curve constructed by PCR assay. The fluorescence and the corresponding cycle numbers are shown in the vertical and horizontal axes, respectively. Panel (b) shows the relative standard curve ranging from 10^1 to 10^8 copies per reaction. Panel (c) shows the corresponding melting curve.

with all the melting curves displaying a sharp peak at the expected Tm; no amplification was obtained from any of the *Candida*-derived DNA (results not shown). Additionally, PCR products obtained from each bacterial amplification were cloned and sequenced as previously described. Sequence of all PCR products obtained was identified as derived from the expected 23S rDNA fragment; these results demonstrate that the developed PCR method specifically detects all the bacterial species tested.

PCR sensitivity was evaluated on a serial dilution of the plasmid containing the 23S rDNA fragment (with each dilution tested in triplicate), at concentrations ranging from 10^8 to 10^1 plasmid copies per reaction, to generate a standard curve (R value: 0.97; slope value: −2,527; Figure 2). The detection limit of this PCR assay (standard curve method) was 10 copies of 23S rDNA copies/reaction. The melting curve analysis of the 23S rDNA gene product is shown in Figure 2(c). The electrophoresis run for the PCR products showed a unique specific band of 97 pb corresponding to the 23S rDNA gene, thus indicating high specificity. These results demonstrate that the developed PCR method can detect up to 10 copies per reaction, as shown in Figure 2.

3.2. DNA Extraction from Whole Blood and PBS Spiked with Gram-Positive and Gram-Negative Bacteria. We evaluated the efficiency of the two commercially DNA extraction methods in PBS and whole blood spiked with *E. coli* and *S. aureus*. Each experiment included a nonspiked whole blood sample as a negative control. In these negative specimens we never observed a completely negative amplification, given the presence of traces of environmental bacterial DNA. Therefore, in order to set up and define the exact number of 23S rDNA copies detected for each sample, the cycle threshold value of the corresponding negative control was used as the edge limit of detection for each run.

The examination of sensitivity for detection of *E. coli* in PBS after EasyMag extraction showed a positive signal for concentrations in each PCR reaction in the 10 to 10^2 CFU range; when blood samples were examined, a 10-fold decrease in the detection sensitivity was observed (Figure 3(a)). When *S. aureus* was tested, the detection sensitivity decreased to 10^3 CFU per PCR in the case of PBS suspension and to above 10^3 CFU per PCR when whole blood specimens were evaluated, as shown in Figure 3(d).

The QIAmp DNA blood mini kit extraction method showed a detection limit for *E. coli* of 1 CFU per PCR in PBS and of 10 CFU per PCR in whole blood samples (Figure 3(b)). The lowest detectable concentrations of *S. aureus* in PBS and whole blood specimens were 10^2 and 10^3 CFU per PCR, respectively (Figure 3(e)).

When the pre-treatment step with lysozime and proteinase K was introduced in the QIAmp extraction protocol the PCR sensitivity rose 10-fold for *S. aureus* (Figure 3(f)) whereas no increase was demonstrated for *E. coli* (Figure 3(d)). In particular, the detection limit for *E. coli* was 1 and 10 CFU per PCR in PBS and in whole blood, respectively. The detection limit for *S. aureus* 23S rDNA ranged from 1 to 10 CFU per PCR and 10 to 10^2 CFU per PCR, respectively, for the bacterial suspension in PBS and whole blood. Similar results were shown for whole blood samples by Zucol and coworkers by using a set of primers and a specific probe targeted on the 16S RNA gene with an extraction protocol based on enzymatic [6].

3.3. Comparison of the Bacterial 23S rDNA Copy Number in Whole Blood and in Plasma. Given the potential application of the novel broad-spectrum PCR assay either in plasma or whole blood specimens, we quantified and compared the detection limit of the novel PCR protocol in whole blood specimens spiked with different bacteria and in the derived corresponding plasma samples, as described above. Our results showed that the EasyMag extraction protocol presented a 100-fold reduction of detection sensitivity in

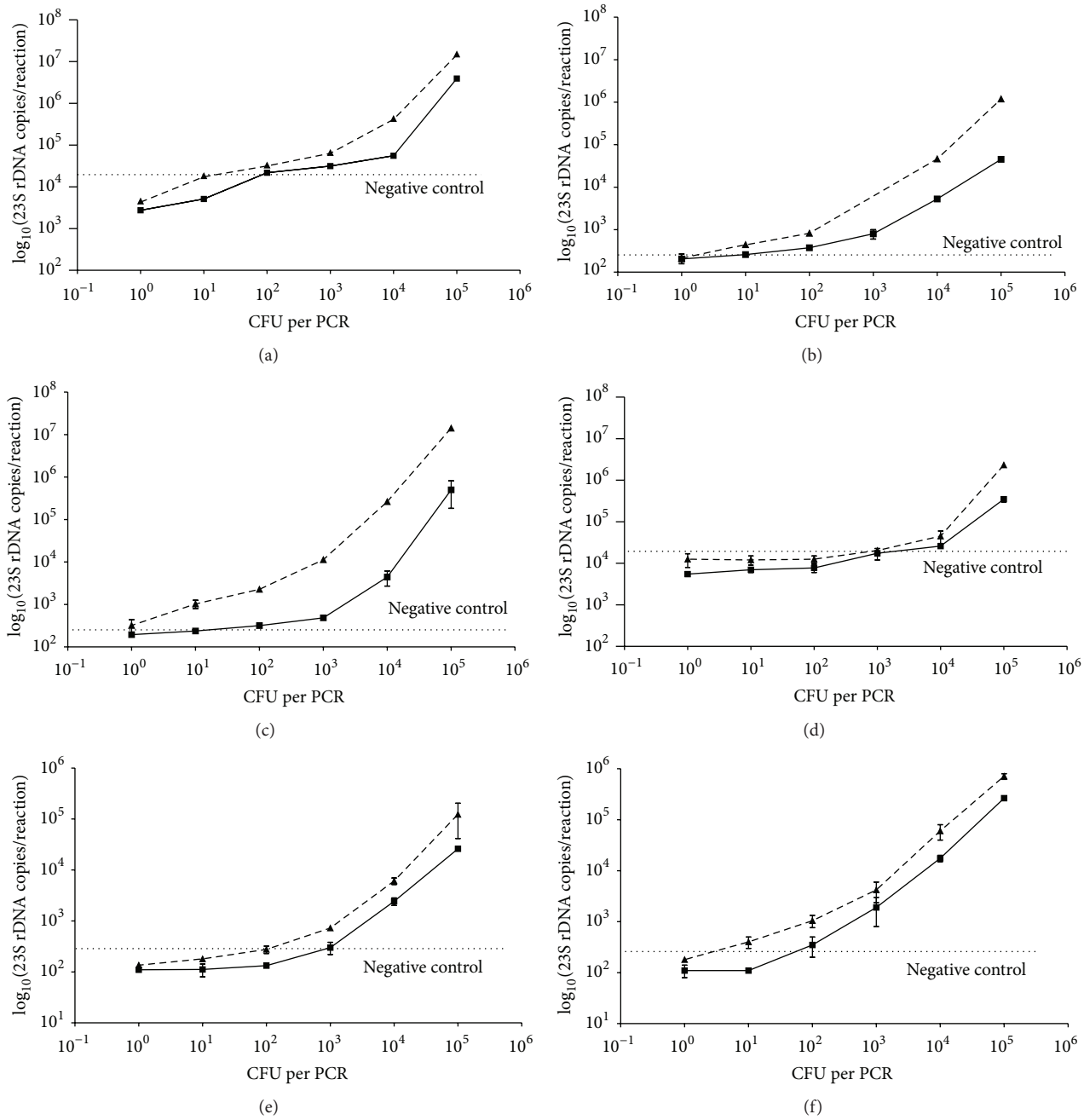

Figure 3: Analytical sensitivities of three different extraction protocols following quantification by the novel 23S rDNA real-time PCR from whole blood (continuous line) and PBS (dotted line) spiked with different Gram-negative (*Escherichia coli*) or Gram-positive (*Staphylococcus aureus*) bacteria ranging from 1 to 10^5 bacteria per reaction. EasyMag automated extraction protocols with *E. coli* (a) or with *S. aureus* (d) spiked in PBS and in whole blood. QIAmp DNA blood mini kit extraction methods with *E. coli* (b) or with *S. aureus* (e) spiked in PBS and in whole blood; QIAmp DNA blood mini kit extraction with pretreatment with lysozyme and proteinase K with *E. coli* (c) or with *S. aureus* (f), spiked in PBS and in whole blood. Results are representative of three independent experiments, effected on three independent DNA extractions and expressed as mean ± standard deviations.

the plasma in comparison to the corresponding WB samples (Figures 4(a) and 4(d)). Similarly, the QIAmp DNA blood mini kit with or without the enzymatic pre-treatment showed a similar behavior (Figures 4(b), 4(c), 4(e), and 4(f)). In particular, the QIAmp DNA blood mini kit with pre-treatment showed a positive signal for *E. coli* for as low as 10^1 and 10^3 CFU per PCR from whole blood and plasma, respectively (Figure 4(c)), and the minimum detection limit for *S. aureus* ranged from 10^1 to 10^2 CFU per PCR and 10^2 to 10^3CFU per PCR from whole blood and plasma (Figure 4(f)). Our results showed that the PCR sensitivity was lower in plasma samples than in the corresponding whole blood samples for both *S. aureus* and *E. coli*, independently from the extraction method used.

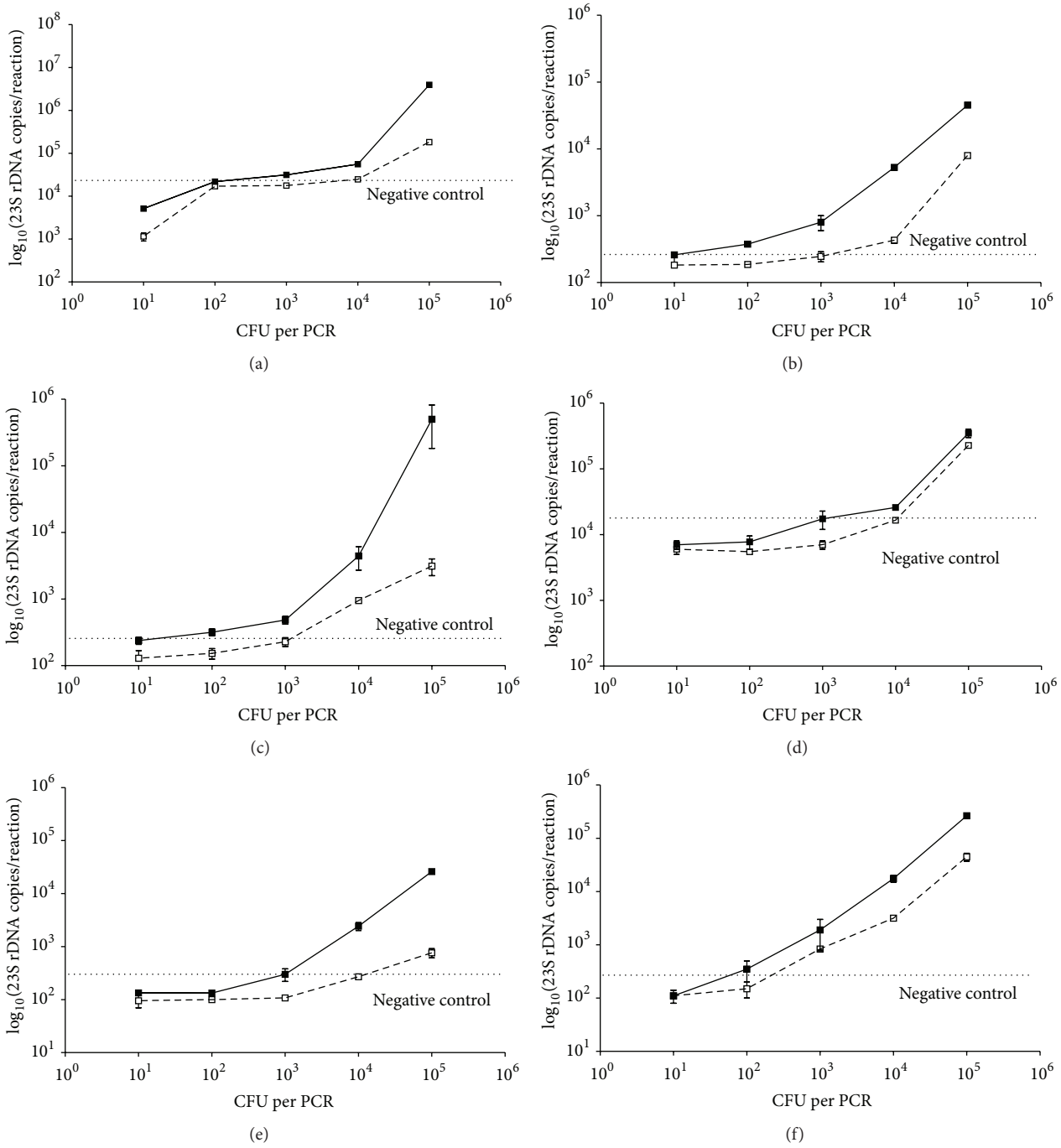

Figure 4: Analytical detection range and sensitivities of different extraction protocols from whole blood (continuous line) spiked with Gram-negative (*E. coli*) or Gram-positive (*S. aureus*) bacteria and their corresponding plasma (dotted line). EasyMag protocols with *E. coli* (a) or with *S. aureus* (d), spiked in plasma and in whole blood. QIAmp DNA blood mini kit extraction with *E. coli* (b) or with *S. aureus* (e), spiked in plasma and in whole blood; QIAmp DNA blood mini kit extraction with pre-treatment with lysozime and proteinase K with *E. coli* (c) or with *S. aureus* (f), in plasma and in whole blood.

4. Discussion

In this study, we developed and assessed the analytical performance of a novel real-time PCR method targeted on a conserved region of the 23S ribosomal DNA gene, for the detection and quantification of a wide range of human pathogenic bacteria in human blood and plasma samples. PCR assays capable of detecting a wide range of human pathogens are nowadays important tools in microbiology laboratories, useful for the detection and identification of infecting bacteria, in particular in the case of blood stream infections. This approach demonstrated its utility in cases of patients receiving ongoing antimicrobial therapy or infected by fastidious/not cultivable bacteria [1, 9]. So far, 16S rDNA

has been the most widely used target for these applications. As detailed in the introduction, one concern that was raised against 16S rDNA-based approaches was its possible lack of specificity, for example, the cross-reactivity with human DNA, but this issue was not largely investigated [18, 23–25]. As target for a pan-bacterial PCR, the 23S rDNA region offers some advantages compared to 16S rDNA: (i) a higher content of variable sequence stretches, (ii) the presence of unique insertions/deletions, and (iii) possibility of a better phylogenetic resolution because of a higher sequence variation [19, 26, 27].

The novel 23S rDNA-targeted PCR assay described here was able to specifically detect all of the 47 bacterial isolates included in the study that represent an estimated 90% of the reported causes of blood stream infections [6]; no false positive reactions were observed when eukaryotic DNAs of diverse origin were tested. A previous study conducted by Zucol and co-workers showed a sensitivity lower than that reported here, when combined nucleic acids extraction methods were applied to water bacterial suspensions and then followed by a 16SrDNA-targeted broad-spectrum real-time PCR assay [6]. As expected, the performance of that method was lower when applied to detect Gram-positive in respect to Gram-negative bacteria, likely due to the thicker cell wall of the former [6].

The minimal detection limits determined for the novel real-time PCR described here were in the range of 1 to 10^3 CFU per reaction in whole blood spiked with *E. coli* or *S. aureus*, depending on DNA extraction methods; as expected, this indicates that the DNA purification step can have a profound effect on the final results. The modified QIAmp DNA blood mini kit, with pre-treatment of the samples with proteinase K and lysozyme that contribute to the disruption of the bacterial cell envelopes, led to a sensitivity of the overall procedure that appears superior compared to methods without preenzymatic treatments (see Figure 3).

Some previously published studies showed controversial results for the detection of the bacterial 16S rDNA in blood. In particular, differences were found when whole blood or plasma specimens were evaluated [7, 15, 20, 28]. The effective difference in the amount of bacterial rDNAs detectable in whole blood or plasma samples remains up to today not fully investigated, so that the discussion about the optimal type of samples to be used for the detection of bacterial rDNAs from blood stream specimens is still ongoing [2]. In this study, we tested whole blood samples spiked with either *E. coli* or *S. aureus* and the derived plasma specimens, demonstrating that the detection of 23S rDNA was more effective when whole blood was used.

These results suggest that for an appropriate and effective detection of bacterial 23S rDNA the most promising type of sample is whole blood, while plasma must be considered a second choice, given the lower detection limit. A major weakness of the novel test described in this paper is the short sequence, 97 base pair, used as target for the assay, that makes quite unlikely the possibility to use the amplicons for a successive species identification, based on sequence analysis. On the other hand, it should be considered that in most cases of invasive bacterial disease and in particular in blood stream infections, the bacterial load in biological samples, such as cerebrospinal fluid and blood, is usually quite low and the use of a very sensitive diagnostic method, like the novel PCR assay described in this paper, is highly desirable in order to prove the microbial etiology. A similar approach was recently described by Banada and co-workers, who showed that an increase in the sensitivity of the PCR protocol can be obtained by a decrease in amplicon size [28]. Additional methods, capable of identifying the infective germs could be applied later on in the diagnostic workflow, eventually with additional steps capable of increasing the bacterial load, such as enrichment broth culture or testing on specimens obtained after withdrawal or suspension of the antimicrobial therapy. The presence of bacterial products, including nucleic acids, in the blood is nowadays a well-recognized phenomenon that frequently occurs when pathological conditions allow translocation from highly colonized sites, such as the bowel [29, 30]. One major application of the method in this study could be the quantification of total bacterial DNA in the bloodstream in all the cases in which a sensitive detection of DNA is desired without the need for a precise bacterial species identification.

Authors' Contribution

P. Gaibani and M. Mariconti equally contributed to this paper.

Acknowledgments

The authors thank M. Cordovana for the selection of the BACSO isolates utilized in this study. They thank Chiara Bazzocchi for useful discussion. This study was supported by funds RFO 2010 and 2011 from University of Bologna to V. Sambri and by funds IRCCS Policlinico S. Matteo Pavia to S. Novati.

References

[1] J. M. Mylotte and A. Tayara, "Blood cultures: clinical aspects and controversies," *European Journal of Clinical Microbiology and Infectious Diseases*, vol. 19, no. 3, pp. 157–163, 2000.

[2] M. Paolucci, M. P. Landini, and V. Sambri, "Conventional and molecular techniques for the early diagnosis of bacteraemia," *International Journal of Antimicrobial Agents*, vol. 36, no. 2, pp. S6–S16, 2010.

[3] P. Gaibani, G. Rossini, S. Ambretti et al., "Blood culture systems: rapid detection: how and why?" *International journal of antimicrobial agents*, vol. 34, pp. S13–S15, 2009.

[4] R. M. Anthony, T. J. Brown, and G. L. French, "Rapid diagnosis of bacteremia by universal amplification of 23S ribosomal DNA followed by hybridization to an oligonucleotide array," *Journal of Clinical Microbiology*, vol. 38, no. 2, pp. 781–788, 2000.

[5] A. L. Rosey, E. Abachin, G. Quesnes et al., "Development of a broad-range 16S rDNA real-time PCR for the diagnosis of septic arthritis in children," *Journal of Microbiological Methods*, vol. 68, no. 1, pp. 88–93, 2007.

[6] F. Zucol, R. A. Ammann, C. Berger et al., "Real-time quantitative broad-range PCR assay for detection of the 16S rRNA gene followed by sequencing for species identification," *Journal of Clinical Microbiology*, vol. 44, no. 8, pp. 2750–2759, 2006.

[7] W. Jiang, M. M. Lederman, and P. Hunt, "Plasma levels of bacterial DNA correlate with immune activation and the magnitude of immune restoration in persons with antiretroviral-treated HIV infection," *Journal of Infectious Diseases*, vol. 199, no. 1177, p. 1185, 2009.

[8] K. Matsuda, H. Tsuji, T. Asahara, Y. Kado, and K. Nomoto, "sensitive quantitative detection of commensal bacteria by rRNA-targeted reverse transcription-PCR," *Applied and Environmental Microbiology*, vol. 73, no. 1, pp. 32–39, 2007.

[9] S. K. Rampini, G. V. Bloemberg, P. M. Keller et al., "Broad-range 16S rRNA gene polymerase chain reaction for diagnosis of culture-negative bacterial infections," *Clinical Infectious Diseases*, vol. 53, no. 12, pp. 1245–1251, 2011.

[10] S. Yang, S. Lin, G. D. Kelen et al., "Quantitative multiprobe PCR assay for simultaneous detection and identification to species level of bacterial pathogens," *Journal of Clinical Microbiology*, vol. 40, no. 9, pp. 3449–3454, 2002.

[11] P. Zapater, R. Francés, J. M. González-Navajas et al., "Serum and ascitic fluid bacterial DNA: a new independent prognostic factor in noninfected patients with cirrhosis," *Hepatology*, vol. 48, no. 6, pp. 1924–1931, 2008.

[12] J. E. Clarridge, "Impact of 16S rRNA gene sequence analysis for identification of bacteria on clinical microbiology and infectious diseases," *Clinical Microbiology Reviews*, vol. 17, no. 4, pp. 840–862, 2004.

[13] T. Bacchetti De Gregoris, N. Aldred, A. S. Clare, and J. G. Burgess, "Improvement of phylum- and class-specific primers for real-time PCR quantification of bacterial taxa," *Journal of Microbiological Methods*, vol. 86, no. 3, pp. 351–356, 2011.

[14] A. Cherkaoui, S. Emonet, D. Ceroni et al., "Development and validation of a modified broad-range 16S rDNA PCR for diagnostic purposes in clinical microbiology," *Journal of Microbiological Methods*, vol. 79, no. 2, pp. 227–231, 2009.

[15] E. Ferri, S. Novati, M. Casiraghi et al., "Plasma levels of bacterial DNA in HIV infection: the limits of quantitative polymerase chain reaction," *Journal of Infectious Diseases*, vol. 202, no. 1, pp. 176–177, 2010.

[16] V. Gentili, P. G. Balboni, E. Menegatti et al., "Panbacterial real-time PCR to evaluate bacterial burden in chronic wounds treated with Cutimed Sorbact," *European Journal of Clinical Microbiology and Infectious Diseases*, vol. 31, no. 7, pp. 1523–1529, 2011.

[17] E. T. Zemanick, B. D. Wagner, S. D. Sagel, M. J. Stevens, F. J. Accurso, and J. Kirk Harris, "Reliability of quantitative real-time PCR for bacterial detection in cystic fibrosis airway specimens," *PLoS ONE*, vol. 5, no. 11, Article ID e15101, 2010.

[18] Ø. Kommedal, K. Simmon, D. Karaca, N. Langeland, and H. G. Wikera, "Dual priming oligonucleotides for broad-range amplification of the bacterial 16S rRNA gene directly from human clinical specimens," *Journal of Clinical Microbiology*, vol. 50, no. 4, pp. 1289–1294, 2012.

[19] D. E. Hunt, V. Klepac-Ceraj, S. G. Acinas, C. Gautier, S. Bertilsson, and M. F. Polz, "Evaluation of 23S rRNA PCR primers for use in phylogenetic studies of bacterial diversity," *Applied and Environmental Microbiology*, vol. 72, no. 3, pp. 2221–2225, 2006.

[20] S. Nikkari, I. J. McLaughlin, W. Bi, D. E. Dodge, and D. A. Relman, "Does blood of healthy subjects contain bacterial ribosomal DNA?" *Journal of Clinical Microbiology*, vol. 39, no. 5, pp. 1956–1959, 2001.

[21] R. C. Edgar, "MUSCLE: multiple sequence alignment with high accuracy and high throughput," *Nucleic Acids Research*, vol. 32, no. 5, pp. 1792–1797, 2004.

[22] S. Epis, P. Gaibani, U. Ulissi, B. Chouaia, I. Ricci et al., "Do mosquito-associated bacteria of the genus Asaia circulate in humans?" *European Journal of Clinical Microbiology & Infectious Diseases*, vol. 31, pp. 1137–1140, 2012.

[23] K. A. Harris and J. C. Hartley, "Development of broad-range 16S rDNA PCR for use in the routine diagnostic clinical microbiology service," *Journal of Medical Microbiology*, vol. 52, no. 8, pp. 685–691, 2003.

[24] K. Rantakokko-Jalava, S. Nikkari, J. Jalava et al., "Direct amplification of rRNA genes in diagnosis of bacterial infections," *Journal of Clinical Microbiology*, vol. 38, no. 1, pp. 32–39, 2000.

[25] B. Vandercam, S. Jeumont, O. Cornu et al., "Amplification-based DNA analysis in the diagnosis of prosthetic joint infection," *Journal of Molecular Diagnostics*, vol. 10, no. 6, pp. 537–543, 2008.

[26] W. Ludwig and K. H. Schleifer, "Bacterial phylogeny based on 16S and 23S rRNA sequence analysis," *FEMS Microbiology Reviews*, vol. 15, no. 2-3, pp. 155–173, 1994.

[27] A. Pei, C. W. Nossa, P. Chokshi et al., "Diversity of 23S rRNA genes within individual prokaryotic genomes," *PloS One*, vol. 4, no. 5, Article ID e5437, 2009.

[28] P. P. Banada, S. Chakravorty, D. Shah, M. Burday, F. M. Mazzella, and D. Alland, "Highly sensitive detection of *staphylococcus aureus* directly from patient blood," *PLoS ONE*, vol. 7, no. 2, Article ID e31126, 2012.

[29] I. Gómez-Hurtado, A. Santacruz, G. Peiró et al., "Gut microbiota dysbiosis is associated with inflammation and bacterial translocation in mice with CCl4-Induced fibrosis," *PLoS ONE*, vol. 6, no. 7, Article ID e23037, 2011.

[30] M. Kramski, A. J. Gaeguta, R. Rajasuriar et al., "Novel sensitive real-time PCR for quantification of bacterial 16S rRNA genes in plasma of HIV-infected patients as a marker for microbial translocation," *Journal of Clinical Microbiology*, vol. 49, no. 10, pp. 3691–3693, 2011.

Hindawi Publishing Corporation
BioMed Research International
Volume 2013, Article ID 543294, 12 pages
http://dx.doi.org/10.1155/2013/543294

Research Article

Development of a Generic Microfluidic Device for Simultaneous Detection of Antibodies and Nucleic Acids in Oral Fluids

Zongyuan Chen,[1] William R. Abrams,[2] Eran Geva,[2] Claudia J. de Dood,[3] Jesús M. González,[4] Hans J. Tanke,[3] R. Sam Niedbala,[4] Peng Zhou,[1] Daniel Malamud,[2,5] and Paul L. A. M. Corstjens[3]

[1] *Rheonix, Inc., Ithaca, NY 14850, USA*
[2] *Department of Basic Science and Craniofacial Biology, New York University College of Dentistry, New York, NY 10010, USA*
[3] *Department of Molecular Cell Biology, Leiden University Medical Center, Building 2, S-01-030, P.O. Box 9600, 2300 RC Leiden, The Netherlands*
[4] *Department of Chemistry, Lehigh University, Bethlehem, PA 18015, USA*
[5] *Department of Medicine, NYU School of Medicine, New York, NY, USA*

Correspondence should be addressed to Paul L. A. M. Corstjens; p.corstjens@lumc.nl

Received 19 October 2012; Accepted 30 December 2012

Academic Editor: Joy Scaria

A prototype dual-path microfluidic device (Rheonix CARD) capable of performing simultaneously screening (antigen or antibody) and confirmatory (nucleic acid) detection of pathogens is described. The device fully integrates sample processing, antigen or antibody detection, and nucleic acid amplification and detection, demonstrating rapid and inexpensive "sample-to-result" diagnosis with performance comparable to benchtop analysis. For the chip design, a modular approach was followed allowing the optimization of individual steps in the sample processing process. This modular design provides great versatility accommodating different disease targets independently of the production method. In the detection module, a lateral flow (LF) protocol utilizing upconverting phosphor (UCP) reporters was employed. The nucleic acid (NA) module incorporates a generic microtube containing dry reagents. Lateral flow strips and PCR primers determine the target or disease that is diagnosed. Diagnosis of HIV infection was used as a model to investigate the simultaneous detection of both human antibodies against the virus and viral RNA. The serological result is available in less than 30 min, and the confirmation by RNA amplification takes another 60 min. This approach combines a core serological portable diagnostic with a nucleic acid-based confirmatory test.

1. Introduction

Infectious diseases including malaria, pulmonary tuberculosis, and viral infections (e.g., human immunodeficiency virus (HIV)) remain major public health problems particularly in the developing world. As individuals unaware of their infection status represent a high risk of transmission, rapid and accurate diagnostics are crucial to decrease incidence and allow for immediate therapeutic intervention. Rapid test devices (RTDs) are available for many infectious diseases allowing appropriate initial screenings. However, these RTDs typically require confirmation by a second test. Currently, confirmatory diagnostics are conducted in well-equipped clinics staffed with trained personnel. Moreover, confirmatory tests generally require a second visit to the clinic, and patients often do not return to collect confirmatory test; this reduces effectiveness in respect to prompt treatment of the infectious disease [1, 2].

Many of the available RTDs used in point-of-care (POC) settings use lateral flow in combination with a visual interpretation of the test result, and these devices do not always exhibit the expected sensitivity and specificity [3]. Often, this performance is a consequence of the testing conditions including how the clinical sample is collected and the level

of operator's experience with the test. In resource-limited settings, confirmation of the infection is often carried out with a different RTD. Although algorithms for serial and parallel testing are effective [4], confirmation of an infection by targeting a different analyte with a more sensitive assay is preferable.

Microfluidic lab-on-a-chip (LOC) devices performing high complexity assays may bring confirmatory testing from the specialized laboratories to the POC setting [5]. Several bench-top technologies have been translated to microfluidic platforms, sometimes by straightforward miniaturization of benchtop assays [6, 7]. In general, miniaturization effectively reduces the overall assay time, which is an important parameter for POC applications. Besides speed and appropriate specificity and sensitivity, successful integration of LOC diagnostics in the POC setting requires dedicated low cost operating devices.

To demonstrate active/acute infection, on-chip NA amplification methods have been developed based on their versatility, speed, and high sensitivity and specificity [9–11]. Microfluidic devices allowing detection of a single nucleic acid molecule have been developed [12]. However, amplification of submicroliter starting volumes of a target [13, 14] limits the actual sensitivity achievable because existing devices have not been integrated with an NA concentration step. When evaluating the theoretical lower limit of detection (LOD) of the pathogen in a clinical sample, the target concentration required to get the minimum amount of DNA molecules in the amplification compartment must be considered. Although extreme miniaturization of the amplification compartment will reduce the amounts of reagents and consequently the cost of the amplification reaction, it may negatively impact the LOD. In addition, when analyzing clinical samples such as saliva, plasma, urine, or stool, sample preparation steps are generally required in order to achieve maximum sensitivity. Full integration of sample collection, metering, cell lysis, nucleic acid purification, and concentration in a single POC device remains a challenge [9, 15–17].

LOC devices with highly functional modules are particularly useful when they include the capability for multiplexing, allowing for rapid screening and, if necessary, a confirmatory test. Here we describe the development of a device for simultaneous detection of antibody and nucleic acid using a test platform from Rheonix with their previously described CARD technology [18, 19]. The device is a microfluidic CARD designed to receive sample and perform dilution, lysis, NA purification and amplification, and LF-based detection using target-specific LF strips. It can complete the screening and confirmation of an HIV infection within 1 to 2 hours and is easily adapted to detect different targets by changing the NA amplification reagents with the appropriate set of primers and the LF strips with matching capture zones. The device described here can utilize a clinical sample and proceed through the entire "sample-to-result" process automatically. The Rheonix platform employs a portable controller to guide the fluid movement on the microfluidic CARD (Figure 1(A)). The CARD consists of a 3-layer polystyrene (PS) structure with a reagent reservoir layer attached on top (Figure 1(B)). The 3-layer PS structure housing channels and diaphragm valves and pumps represent the core technology of the CARD [18]. The circular chambers beneath valve/pump diaphragms are pneumatically connected to the manifold on the bottom of the CARD. A valve/pump diaphragm is deflected into a chamber when negative pressure is applied which results in the open status of valve/pump. In contrast, when positive pressure is applied to the chamber a valve/pump diaphragm is pushed against the valve seat and forms the closed status of valve/pump. Sequentially actuating multiple diaphragms in series creates a peristaltic pumping action. The capability to fabricate multiple pumps and valves in a single microfluidic chip provides a high degree of flexibility in the manipulation of multiple reagents and specimens, that is, transport of reagents from a reservoir to a reaction chamber, transport of water to a vessel to dissolve dry reagents, active mixing of two or more fluids, discharging of a product to downstream processes, and so forth. To use it, the CARD is first securely mounted with vacuum on the manifold. Microfluidic valves and pumps are pneumatically actuated by 32 individually addressable solenoids controlled by a user-interface program written using script language running on a Java-based software program. The script language program also controls the thermal (cycling) function for nucleic acid amplification, in this case RT-PCR.

2. Materials and Methods

2.1. Saliva Samples. Saliva was collected from a healthy volunteer according to protocols described earlier [20]. The UP*link* collector (previously available from OraSure Technologies) and the newly developed collector with solid Porex matrix were tested for potential application in the dual-path CARD. The dual-path CARD was eventually designed for use with the solid Porex matrix collector. Whole mouth saliva samples (WMSSs) clarified using either the collectors or centrifugation (or a combination) were spiked with plasma-based control samples as provided with the OraQuick ADVANCE Rapid HIV-1/2 Antibody Test (OraSure Technologies): a borderline positive and a negative control sample. Samples were furthermore spiked with Armored RNA particles (Asuragen Inc.) as noninfectious replacement for HIV.

2.2. RNA Isolation. RNA was isolated using either the High Pure Viral RNA kit (Roche) or the ZR Viral RNA kit (Zymo Research). In the procedures provided with both kits, the lysis/binding buffer could be replaced with Pluronic Lysis Buffer which contained 15% (w/v) of the nonionic detergent heteropolymer Pluronic F-68 (Sigma-Aldrich) in 50 mM Tris-Cl pH 6.6 and 4.5 M Guanidine Hydrochloride. Pluronic lysis buffer can be lyophilized to dryness, stored as a dry reagent, and readily dissolved in H_2O as required. Proprietary wash buffers from Rheonix with reduced EtOH concentrations were also successfully used to replace the wash buffers provided with the High Pure Viral RNA kit. RNA isolated using the Rheonix wash buffers (either by the benchtop or by on-chip protocols) improved downstream RT-PCR amplification yields. The Roche and Zymo kits utilize spin columns in the RNA isolation; the microfluidic chips

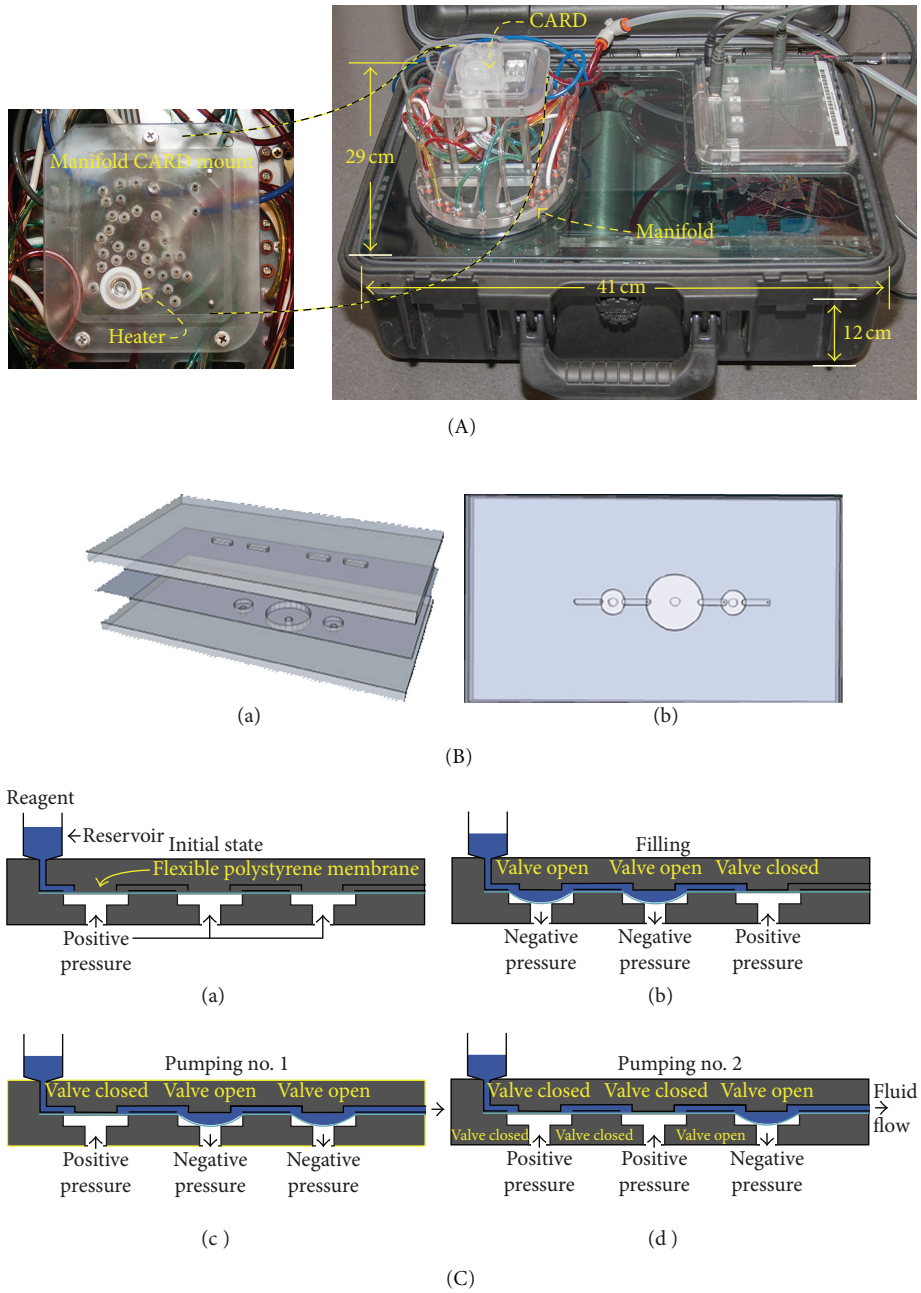

Figure 1: Rheonix processor platform (controller) and CARD technologies. (A) Controller box with integrated vacuum and pressure pump system. A manifold forms the interface between the controller box and the CARD; in the magnified top view the heating module and the solenoid connections (ports) are indicated. Vacuum and pressure ballast tanks are integrated within the controller box. (B (a)) panel showing a minimal schematic of the basic 3-layer PS CARD structure with 2 small and one larger diaphragm (valves/pumps); (B (b)) a top down view of the 3-layer laminated structure shown in panel (B (a)) (without any reservoirs mounted). (C) Diagram showing the valve operations required for peristaltic fluid movement in the CARD.

were provided with a Rheonix proprietary silica membrane suitable for filtration by vacuum.

2.3. Nucleic Acid Amplification. RT-PCR kits were obtained from Roche, Qiagen, GE Healthcare, and Zymo. In most experiments the QIAGEN OneStep RT-PCR Kit (QIAGEN) was used as its hot-start capability allowed convenient on-chip addition of the assay reagents to the microfluidic chip before initiation of the assay. Also, the kit materials could be lyophylized for storage in 0.2 mL microfuge tubes by the proprietary technology of Tetracore Inc., which is a format compatible with the dual CARD NA amplification compartment. The Transcriptor One-Step RT-PCR Kit (Roche) allowed the largest reduction in RT-PCR assay time. The illustra Ready-To-Go RT-PCR Beads (GE Healthcare) were the only commercially readily available dry reagents

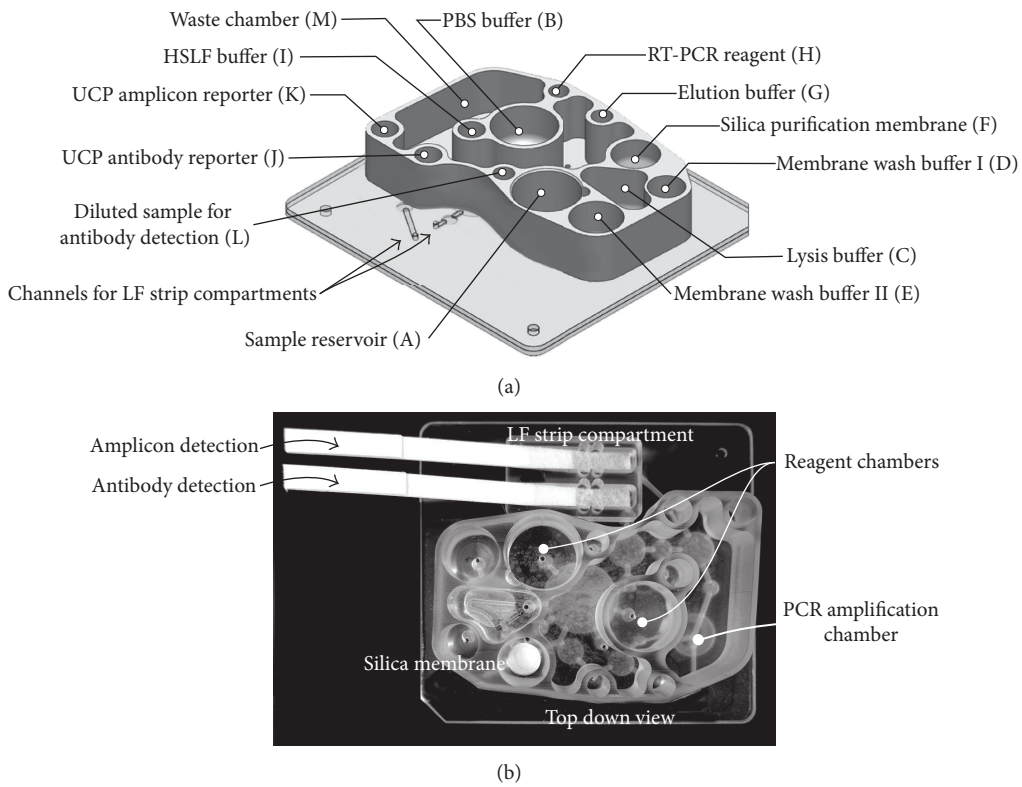

Figure 2: The dual-path antibody RNA CARD. Design (a) and top down image (b) of the dual path microfluidic device with the reagent reservoirs and other compartments used in the detection of anti-HIV antibody and HIV RNA.

successfully applied in on-chip RT-PCR amplification. All kits were used to amplify a 155 bp HIV *gag* fragment from RNA isolated from noninfectious Armored RNA particles (Asuragen Inc.). Amplification was performed using primers developed for the COBAS Amplicor HIV-1 Monitor Test v1.5 [21]; the forward (sense) primer was synthesized with a $5'$-end Digoxigenin (Dig) hapten and the reverse (antisense) primer with a $5'$-end Biotin (Bio) hapten (EuroGenTec).

2.4. UCP-LF Detection. Upconverting phosphor (UCP) particles are a highly sensitive reporter suitable for LF format analysis [22], were obtained from OraSure Technologies Inc. (Bethlehem, PA), and were conjugated with 25 μg mouse anti-digoxigenin antibodies or 25 μg protein-A as described [8, 23, 24]. Lateral flow strips for detection of anti-HIV antibodies and Dig-Bio labeled DNA amplicons were also produced as described [8, 23–25] with a 22 mm sample pad. The composition of the high salt lateral flow (HSLF) assay buffer was 270 mM NaCl, 1% w/v BSA (Sigma, A-2153) 0.5% v/v Tween-20 in 100 mM Hepes pH 7.4).

2.5. Microfluidic Chip/CARD Technology. Microfluidic chips were provided by Rheonix, Inc. Before designing the entire and comprehensive dual path CARD, various types of simpler intermediate devices were developed to allow the analysis of specific modules and assay steps. Required design changes were indicated by the users and implemented by Rheonix according to methods protocols described in Zhou et al. [18] and Spizz et al. [19].

2.6. Operation of the Dual Path Chip. Saliva from an uninfected individual was used to evaluate the dual path chip. Clarified saliva was spiked with 5% (v/v) of the OraQuick antibody control and 10% (v/v) dilution of Armored RNA (Asuragen Inc.). After buffer and reagents were loaded and 100 μL of saliva added to the sample reservoir, the automated protocol was initiated. Individual on-chip compartments referred to in different steps are indicated in Figure 2 with a few distinctive chip features shown in greater detail in Figure 3. A brief description of the different steps distinguished in the dual path assay protocol is listed in the following.

Step 1 (loading and dilution of saliva sample). 200 μL PBS (PBS—Compartment B) is used to release and dilute 100 μL of sample from the oral collector (Sample—Compartment A) by pumping. Note that the use of oral collector with the Porex matrix is shown in Figure 3(A).

Step 2 (detection of antibody). Initiated by transferring a 100 μL aliquot of the PBS diluted saliva sample to Compartment L. Part of the aliquot is further mixed/diluted with HSLF assay buffer from Compartment I while flowing to the antibody detection LF strip (Figure 2(b)). HSLF (50 μL) containing 100 ng UCP-protA conjugate is applied to the strip from Compartment J.

Step 3 (RNA isolation). The remainder (200 μL) of the PBS-diluted saliva sample is mixed with 400 μL of 15% (w/v)

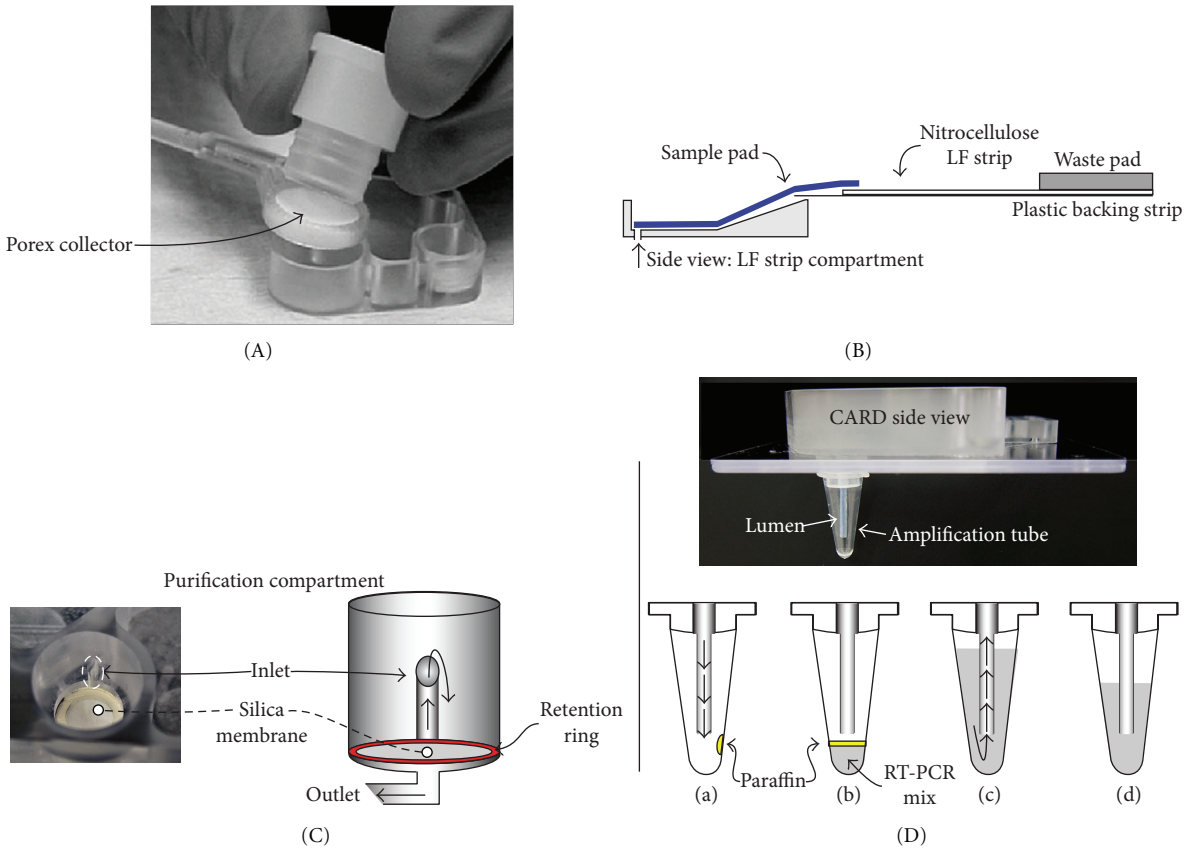

Figure 3: Unique modular components of the CARD. (A) Saliva collector with removable solid Porex matrix. (B) Illustration of the LF strip compartment and the LF strip schematic: the LF strip contains an extended sample pad that is positioned in a trough that prevents overflow of the LF sample pad and strip. (C) Schematic of the compartment with the NA-binding silica membrane; the inlet/outlet of the connected channels are indicated. (D) Schematic of the amplification microtube indicates how the lumen functions as both inlet and outlet. During amplification the opening of the lumen is well above the liquid surface. After amplification, HSLF buffer is added to tube through the lumen, and as a result the opening of the lumen will be below the liquid surface allowing it to function as an outlet.

Pluronic Lysis Buffer in the Lysis Buffer Compartment (C). The lysate is then drawn through the NA binding silica membrane in Compartment (F). The membrane is washed with 200 μL of Rheonix WB-I (containing EtOH) and twice with 200 μL EtOH free Rheonix WB-II and then air-dried for 5 min. Elution water is pumped (Compartment G) onto the top of the silica membrane and incubated for 1 min. RNA is subsequently eluted and directed through the silica back into Compartment G.

Step 4 (RT-PCR amplification). 15 μL RT-PCR reagent is added to RT-PCR reagent Compartment H and pumped to the microtube together with 1 μL of the eluted RNA from Compartment G. A drop of low melting paraffin (melt point <50°C) on the inner wall of the tube (Figure 3(D)) liquefies, covers the reaction mixture, and prevents evaporation during amplification.

Step 5 (detection of the DIG-BIO labeled amplicons using UCP-CF). Immediately after completion of the RT-PCR, 100 μL HSLF assay buffer from Compartment I is transferred to the amplification tube to dilute the RT-PCR reaction mixture. A 10 μL aliquot flows from the amplification tube to the LF strip for NA detection, directly followed by 10 μL HSLF. The DIG-BIO labeled amplicons bound to the Avidin Test line of the DNA detection LF strip are detected with 50 μL of UCP-MαDIG conjugate (containing 100 ng UCP particles) from Compartment K.

Step 6 (scanning of the LF strips and result analysis). A dedicated reader is used to read the UCP signal. Results are presented as the ratio of the Test line signal divided by the flow control signal.

3. Results

The design of the dual path CARD allowed convenient iterations of the various modules. In our evaluation we distinguish three units: (i) the sample application unit, (ii) the antibody detection unit, and (iii) the nucleic acid unit. Each unit has a modular design with variable complexity.

3.1. Sample Application. In a previous study [26] several commercially available oral collectors were assessed for their use in UCP-based assays. The UP*link* collector (OraSure

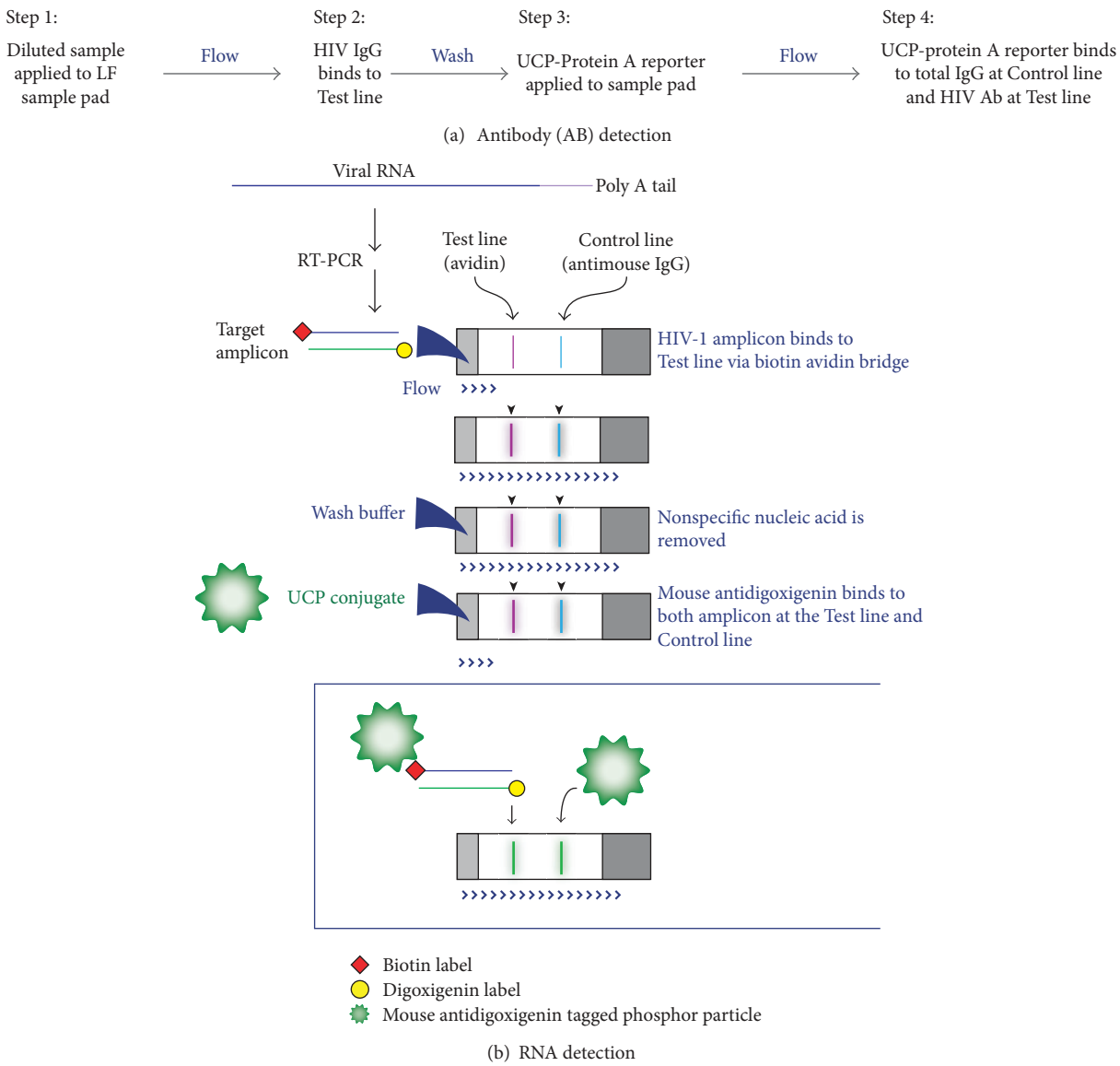

Figure 4: The consecutive flow protocol. (a) Schematic for the analysis of the antibody path, the Test Line was a proprietary peptide mix (OraSure Technologies), and the Flow Line anti-human IgG. (b) Schematic showing consecutive flow applied to detect RT-PCR amplicons provided with a digoxigenin and biotin hapten as described by Corstjens et al. [8], which was developed to detect antibodies against infectious disease pathogens. For analysis of amplicons, the Test line was antidigoxigenin and the Flow Line digoxigenin.

Technologies) designed to deliver a metered fluid sample directly into a cassette with a LF strip was identified as the most suitable collector. The UP*link* collector was successfully applied in this study, but as this collector is not easily available anymore, an alternative collector was designed. The new collector consists of a circular, solid, porous, and removable Porex disk (Porex Porous Corp., Fairburn, GA; 12.5 mm diameter by 3 mm deep) in a lever and a plastic handlebar. The disk can be conveniently forced out of the lever into a specially designed reagent vessel on the CARD (Figure 3(A)). The current dimension of the Porex collector allows for collection of ~100 μL of oral fluid. After application of the Porex disk to the CARD, the disk was rinsed with two volumes (200 μL) of PBS by pumping fluid reversibly through the disk. The porosity of the disk contributes to the efficient mixing of the saliva sample with PBS, which renders the sample less viscous for subsequent operations. Viscosity issues when analyzing untreated saliva in different types of antibody-only devices are part of a separate study (manuscript in preparation). The diluted sample was split between the antibody and NA analysis pathways.

3.2. Antibody Detection. The antibody detection path is directly modeled on the sequential flow assay format (referred to as consecutive flow (CF)) described previously for the detection of antibodies against infectious disease pathogens [8]. The applicability of this assay format for miniaturization was demonstrated earlier with a different

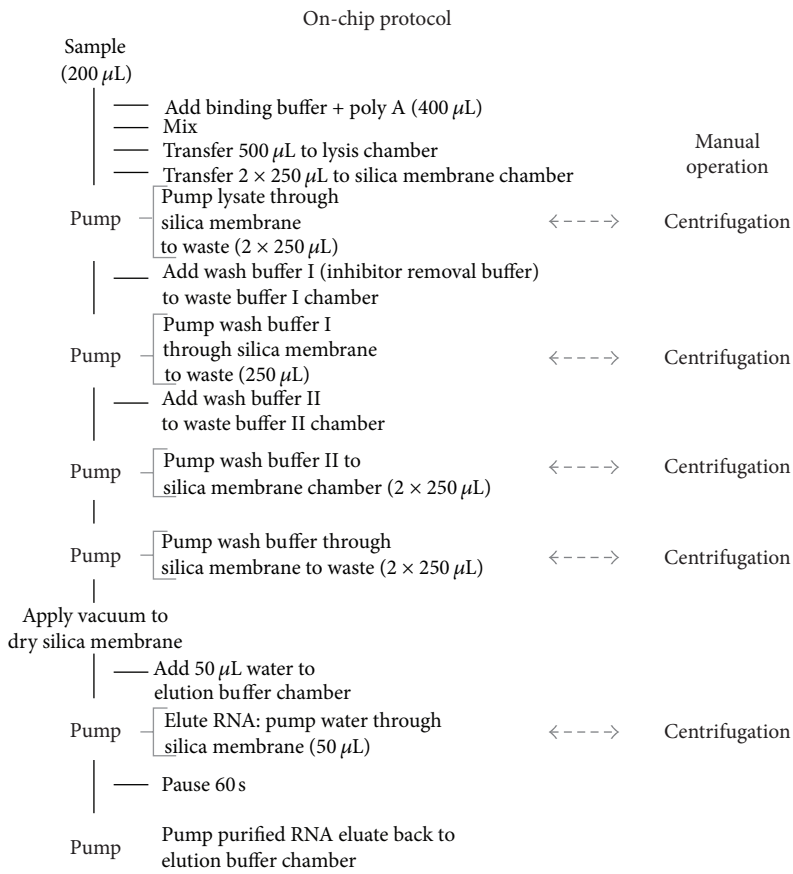

Figure 5: On-chip RNA isolation protocol compared to a typical manual benchtop operation. The bench top RNA isolation protocol involves several centrifugation steps using spin columns provided with a silica purification membrane. For the chip protocol, these steps were replaced by on-chip vacuum filtration.

type of chip [27]. A schematic of the CF protocol is shown in Figure 4. CF involves three sequential flow steps: the first flow on the LF strip is the clinical sample with the targeted antibody; the second flow is a wash step with HSLF buffer; and the third flow contains UCP reporter particles coated with protein A. The UCP reporter binds to human IgG from the clinical sample at the Test line (T) and Flow Control line (FC); to test samples for HIV infection, T contains HIV-specific peptides and FC contains anti-human IgG. In this study, CF was also used in the NA detection path for the detection of RT-PCR amplicons (Figure 4(b)). It should be noted that in contrast to the approximately vertical placement of the LF strips in tubes (or microtiter plate wells) when performing the benchtop assay, on the CARD they are placed horizontally. Therefore careful regulation of the liquid flow is important to assure a constant fluid stream and to prevent flooding of the nitrocellulose strip. The LF strip holders were designed with a "trough" to allow initiating liquid flow through the extended flexible sample pad of the LF strips without flooding (Figure 3(B)).

3.3. Nucleic Acid Unit: RNA Isolation. The NA analysis pathway is the most complex part of the dual path chip. It consists of several modules related to the various procedural steps in the benchtop protocols. The first step is the RNA isolation, by itself consisting of several subprocedures. The conventional protocol to isolate HIV RNA employed the High Pure Viral RNA Isolation Kit (Roche) including spin columns with a silica matrix. Centrifugation steps were replaced with chip-based vacuum filtration (Figure 5). Chips were provided with an RNA isolation compartment fitted with Rheonix proprietary silica membrane. During development the diameter of the matrix was varied between 3 and 5 mm with a constant ~1 mm thickness, and the optimal size was determined to be 4 mm. The larger diameter silica matrices required proportionately greater elution volumes that often resulted in higher concentrations of residual EtOH (or other contaminants) in the eluted RNA and resulted in poor target amplification. Conversely, the smaller sized matrices decreased binding capacity and were easily clogged resulting in slow or blocked flow. Besides the different silica membranes, all other steps in the isolation protocol were carried out identically on both the benchtop and the chip. When required, mixing of fluids was achieved by pumping fluids reciprocally between two reagent compartments. The viscosity of the lysis buffer was of particular concern with respect to efficient mixing and fluid movement and the efficiency of the wash buffers in removing amplification inhibitors.

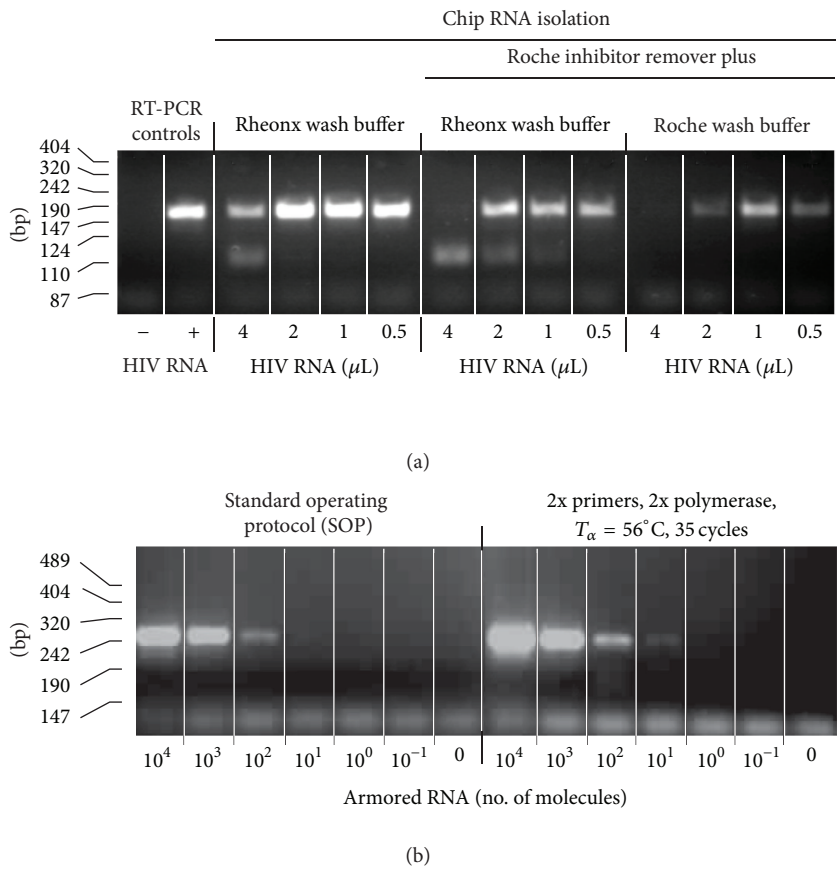

Figure 6: Optimization of the RT-PCR amplicon yield. (a) The effect of different wash buffers on the quality of on-chip RNA isolation was assessed by amplifying increasing amounts of CARD isolated RNA elute by RT-PCR. The volumes represent the amount of eluted RNA used in the amplification reaction using a 10 μL final assay volume. Note the decrease in amplicon yield with increased volume possibly due to the presence of residual EtOH. (b) Doubling of the primers and enzyme concentration and a 2°C lower annealing temperature increased the amplicon yield.

3.3.1. Viscosity of the Lysis Buffers. High viscosity buffers represent a problem for fluid transport through narrow channels on a microfluidic chip, and it is especially true for the lysis step. The first action in the on-chip RNA isolation protocol is the transport of diluted sample from the sample reservoir into the prefilled lysis buffer reservoir, which is then reciprocally pumped between compartments until the two fluids are homogenous. The porous matrix used to collect the oral clinical sample (e.g., a Porex disk from the oral collection device (Figure 3) may also facilitate mixing. The concave shape of the bottom of the lysis buffer reservoir assists in the mixing process where sample enters from the bottom into the prefilled lysis buffer reservoir (Figure 3(C)). Lysis buffer from the ZR Viral RNA Kit (Zymo Research) was also successfully used in combination with Rheonix wash buffers. An alternative lysis buffer was developed based on the nonionic detergent heteropolymer Pluronic F-68 and the chaotropic reagent guanidine hydrochloride. Pluronic-based buffers can be lyophilized, stored in dry form, and easily hydrated. The concentration (w/v) of Pluronic reagent in the lysis buffer was optimized and 15% (w/v), was found to be ideal for lysis of viral particles, with high RT-PCR yield and low viscosity.

3.3.2. Efficiency of the Wash Buffers. RNA isolated by benchtop and on-chip methods, using reagents from the High Pure Viral RNA Isolation Kit, were both analyzed by benchtop RT-PCR. To prevent variation caused by the on-chip mixing of lysis buffer and sample, mixing of lysis buffer and sample was performed manually before performing chip-based RNA isolation. Nevertheless, a lower yield of RT-PCR product was observed for the on-chip isolated RNA compared to benchtop isolated RNA. Other wash buffers were evaluated for on-chip application, including a proprietary EtOH-free wash buffers from Rheonix (Figure 6(a)). Use of Rheonix wash buffers as an alternative to the EtOH containing High Pure Viral RNA Isolation Kit buffers improved the quality of RNA isolation, which allowed an increase in the amount of eluted RNA in the RT-PCR reaction.

3.4. Nucleic Acid Unit: RNA Amplification (RT-PCR). The second step in the NA pathway is the amplification procedure. Initially PCR-only dedicated chips were used to investigate on-chip RT-PCR conditions for the amplification of a 155 bp *gag* HIV sequence. The amplified region and primers are identical to the Roche Amplicor HIV-1 Monitor test (Roche) version 1.5 [23]. As the various prototype chips used in this

research still have an open architecture, Armored RNA (Asuragen Inc.) was used in most cases as a surrogate for infectious HIV for safety reasons. Purified RNA and RT-PCR reagent mix were combined and mixed utilizing the action of the diaphragm valves. Doubling of the enzyme concentration and decreasing the annealing temperature by 2°C improved the amplification (Figure 6(b)). Also, priming (coating) of the channels with mineral oil led to better reproducibility. The optimized method allowed detectable amplification when initiating the RT-PCR with as little as 10 copies of Armored RNA. The potential of using different RT-PCR kits indicates that amplification within a POC functional assay time is feasible. The shortest protocol, using a 5 min RT step, 1 min hot start, and 5 sec each for denaturing, annealing, and extension *per* PCR cycle, was achieved with the Transcriptor One-Step RT-PCR Kit (Roche). For most of the on-chip experiments, the Qiagen OneStep RT-PCR Kit was used since the HotStarTaq DNA Polymerase permitted retaining mixtures of RT-PCR reagents and primers at ambient temperature allowing preloading of the RT-PCR reagents. The use of hot start conditions and polymerases is necessary to limit the formation of primer-dimers and other PCR artifacts when primers and RT-PCR reagents are mixed and preloaded in advance. In the final version of the CARD, dry target-specific amplification reagents will be provided to the amplification compartment, a replaceable 0.2 mL microtube affixed to the bottom of the microfluidic chip. One currently available dry reagent kit that was tested was the Ready-To-Go RT-PCR Beads (illustra, GE Healthcare), This kit performed well on chip using the original protocol and control target (a 425 bp *D. melanogaster* fragment), but it did not accommodate drastic shortening of the cycle time. A complete, ready-to-go reagent cocktail made from reagents supplied with the Qiagen kit and *gag*-specific primers (supplied with a Dig and Bio hapten) was successfully transformed to a dry format by Tetracore Inc., using their proprietary technology [28]; other technologies allowing storage/stabilization of biological at room temperature are available, for example, Biomatrica Inc. (San Diego, CA, USA). The Dig-Bio labeled amplicons were detected using a flow format similar to the one described for the antibody detection (Figure 4(b)), the saliva sample being replaced by a diluted RT-PCR mixture. Lateral flow strips provided with an Avidin capture line and an anti-mouse Flow Control line were used to detect the Dig-Bio amplicons utilizing a UCP reporter coated with mouse anti-DIG antibodies [23].

3.5. Performance of the Dual Path CARD to Detect Both Antibody and RNA. A typical experiment with the dual path CARD involves the simultaneous detection of antibody and RNA utilizing saliva containing HIV Armored RNA samples and antibody standards from the OraQuick ADVANCE Rapid HIV1/2 Antibody Test. The open structure allowed convenient manual addition of wet reagents and permitted visual observation of the on-chip fluid transport. In the on-chip protocol, the antibody detection path and the NA detection path proceed sequentially. Buffers and other reagents are loaded into their reservoirs prior to initiating computer control. Once initiated, the fully automated chip-based protocol dilutes the saliva sample with PBS and then transfers an aliquot to the antibody detection path for analysis. This aliquot is further diluted with HSLF assay buffer and transferred to the antibody LF strip containing a test zone to bind HIV-specific antibodies. The sample flow is followed by a wash and a flow of the IgG generic UCP-protA reporter conjugated to detect bound antibody. The strip is dried while the NA analysis path proceeds. NA is extracted from the remainder of the PBS diluted saliva sample by first mixing with Pluronic lysis buffer and then running the lysed sample over the NA-binding silica membrane. The membrane is flushed with the proprietary Rheonix wash buffers and air-dried to help remove residual EtOH prior to elution with nuclease-free water. RT-PCR reagents and eluted RNA are then added to the microtube through a plastic lumen (Figure 3(D)), and the amplification cycle is initiated. The targeted disease/pathogen-specific NA sequence is amplified, and resulting NA amplicons are provided with Dig-Bio tagged primers. Upon completion, HSLF assay buffer flows into the PCR tube through the lumen to mix and dilute the DIG-BIO tagged amplicon; subsequently, an aliquot is transferred to the NA LF strip. The NA LF strip contains an avidin capture line that binds the BIO tagged amplicon. Bound amplicons are then detected by UCP-MαDIG reporter particles that are bound to the DIG tag. When LF is completed, both the antibody and NA strips are removed from the CARD and scanned for the presence of UCP label. In future versions the controller box may contain a built-in IR scanner.

The dual path chip was tested with saliva samples spiked with the OraQuick positive control and Armored RNA or with the OraQuick negative control. Chips were loaded with 100 μL of the spiked saliva and run without operator interference. Figure 7 shows the result obtained after reading the LF strips and indicates a clear distinction between the seropositive and seronegative samples. Analysis of the LF strips gave Test line signals of 2818 relative fluorescent units (RFUs) versus 643 RFU for the low positive and the negative controls, respectively. If required, the assay components/conditions can be adapted in such a way that the negative control does not generate a signal. Above a certain threshold the ratio values are indicative of infection. The threshold is assay and device-specific, and the actual value is determined from a statistically relevant large set of negative controls. When testing patients in a POC setting, the serological results will already be available while the NA path is still in process. In cases where the antibody result indicates infection based on seroconversion, the NA result is required to confirm infection based on the presence of viral RNA. The presence of Armored RNA was also clearly demonstrated; the saliva sample spiked with Armored RNA demonstrated a clear signal (33735 RFU) whereas the control does not result in a signal at the Test line. Ratio values calculated by dividing T and FC signals indicate the same result. RT-PCR results were validated through various RT-PCR benchtop controls using the eluted RNA remaining in Compartment G.

Sample	Test line response	Control line response	Ratio (Test/Control)
Antibody positive	2818	2719	1.01
Antibody negative	643	4879	0.13
Nucleic acid positive	33735	26823	1.26
Nucleic acid negative	0	7974	0

(a) Test/control values

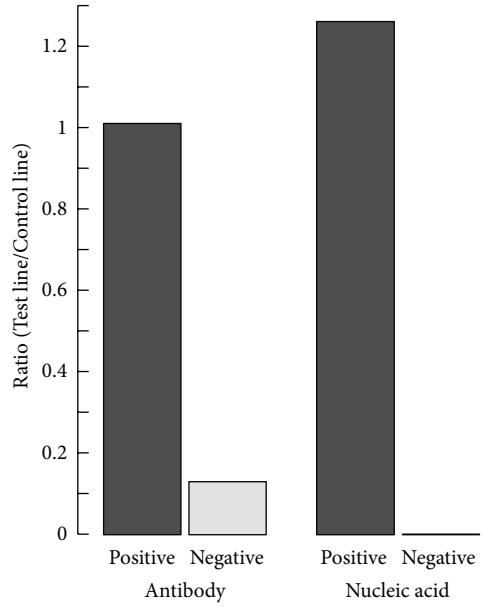

(b)

Figure 7: Analysis of saliva samples spiked with HIV RNA as Armored RNA and HIV antibodies on the dual path CARD. (a) Signals representing peak areas (emission in RFU after excitation with 980 nm IR light) of the Test and Flow Control lines. (b) Results are presented as Ratio Values calculated by dividing Test and Control line signals. Ratio values improve the interassay comparison obtained with different LF strips.

4. Conclusion

This study describes a portable processing system (Rheonix, Inc.) for disposable microfluidic chips suitable for POC applications in the diagnosis, detection, and confirmation of infectious disease pathogens. Prototype devices were developed and assessed for their potential to analyze saliva samples. Each step of the process was evaluated independently, from collection to detection of targets specific to pathogen infection. We note here that besides oral-based fluids, the system was successfully tested with blood-derived samples (mainly plasma and serum) spiked with cultures of HIV (instead of the noncontagious Armored RNA alternative) and can be adapted for use of other body fluids as well. For the oral-based sample analysis the use of a dedicated saliva collector was implemented. The device includes oral fluid-based sample preparation steps required for NA purification and allows the integration of essentially any NA amplification method. The device is suitable for simultaneous detection of multiple types of biomolecules. Here, the detection of antibody and NA is described. Diagnosis of HIV infection was used as a model to screen for the infection through detection of anti-HIV antibodies and confirmation of the actual presence of the virus by detecting an HIV-specific RNA target. This combination of a diagnostic screening with a confirmatory test has major advantages: it allows immediate initiation of therapy and counseling and removes the need for the patient to return to the POC facility for either subsequent testing or a final test result. In addition for populations at high risk for HIV infection, it also provides a method to decrease the window between infection and seroconversion, which is a relatively short period when viral loads are highest and transmission (infection of others) is most likely. Other applications could apply to the detection of anti-HPV (subtype 16 and 18) antibodies [29, 30] and HPV subtype-specific DNA [31–33] in oral fluid as a potential indicator for oral cancer. Also, the prospect of a higher complexity device that can combine the detection of antibodies against helmintic *Schistosoma* species, pathogen-derived NA targets and specific glycosylated-proteinaceous antigens can be explored [34–36].

The microfluidic chips are produced by a patented technology (CARD), which is adapted readily for both large- and small-scale production and provides a convenient strategy for rapid modification and testing of small batches of chips for research and development purposes. Different modules were tested and ultimately combined into a single microfluidic chip design for simultaneous detection of nucleic acid (HIV-RNA) and protein (anti-HIV antibody). Alternative methods and modules for several of the on-CARD assay steps described here have been explored (data not shown) and can be integrated depending on the constraints defined for the performance of particular assays. Nucleic acids are detected after amplification; in the example discussed here, RT-PCR was used to amplify an RNA target from HIV. RT-PCR amplification requires a relatively complex heat cycling system; thus we submit that a system capable of performing RT-PCR can be easily adapted for other simpler amplification technologies. To demonstrate this, the system was also successfully tested with a recently commercialized isothermal amplification technology LAMP (results not shown). The only constraint when considering a device with

dry reagents is the requirement that the enzymes and other reagents required for amplification need to be provided with a sufficient stability. The dry reagents tested in this study were obtained from a commercial source (GE Health Care) or were dried using a custom proprietary technology (Tetracore Inc.). The assay-specific reagents for the amplification of the RNA target including the target-specific primers can be supplied to the chip in a microtube attached to the bottom of the CARD. In this open architecture research prototype the tubes are easily installed by the operator. The final design will be a disposable and sealed chip that will be discarded after use as biohazard waste. However, the possibility to change the PCR tube with specific amplification reagents remains and adds flexibility with minimal complexity to the system. For nucleic acid detection the processing of the chip will differ only in the technical details required for the specific method of amplification. Amplicons labeled with digoxigenin (DIG) and biotin (BIO) haptens during amplification can be detected by the rapid LF-based method using phosphorescent upconverting phosphor reporters. Required capture zones and dry UCP reporter can be fully integrated in the LF strips which also can be added to the CARD at a later time point. Multiplexing at the NA level [37] can be implemented in LF format by adding different haptens to the amplification reagent mix [26]. Integration of magnetic beads as an alternative to the silica membrane isolation of nucleic acids has been developed and tested (results not shown) and may improve sensitivity since it allows omitting EtOH-based wash steps [38] and NA elution from the protocol with direct input of all bound NA targets in a microliter size amplification reaction. Moreover, magnetic beads may also be applied to capture and concentrate targets other than NA for multiplex analysis. Important to realize is that the modular approach that can be used in the development of specific CARD microfluidic chips in combination with a scalable production facility conveniently allows iteration and optimization of various assay steps in the process of miniaturization. The model used here to explore the Rheonix system and CARD technology is relevant for rapid POC applications to diagnose and immediately validate HIV infections. Robustness, reproducibility, sensitivity, and specificity issues of the current device require further validation with relevant sets of clinical samples using future closed CARD systems. Especially when moving towards applications that include monitoring of the disease (demanding quantitative determination of low copy numbers of HIV viral RNA), aerosol or other potential contamination sources need to be avoided. When focusing on validation of HIV infection in seroconverted patients prior to drug treatment, the constraints regarding HIV RNA quantitation are considerably less and can be clearly achieved with current device.

Abbreviations

Ab: Antibody
BIO: Biotin
CARD: Chemistry and reagent device (a registered trademark of Rheonix, Inc.)
CF: Consecutive flow
DIG: Digoxigenin
HSLF: High salt lateral flow buffer
LF: Lateral flow
LOC: Lab on a chip
LOD: Limit of detection
NA: Nucleic acid
POC: Point of care
RT-PCR: Reverse transcriptase polymerase chain reaction
RTD: Rapid test device
UCP: Up converting phosphor
Up*link*: a registered trademark of OraSure Technologies Inc.
WMSS: Whole mouth stimulated saliva
RFU: Relative fluorescence units.

Conflict of Interests

Z. Chen and P. Zhou are employed by Rheonix Inc. R. S. Niedbala was a founding member of OraSure Technologies Inc. All of the other authors have no conflict of interests. This statement is made in the interest of full disclosure and not because the authors considerthis to be a conflict of interests.

Acknowledgment

The US National Institute of Health Grant U01DE017855 supported this work.

References

[1] A. B. Hutchinson, G. Corbie-Smith, S. B. Thomas, S. Mohanan, and C. Del Rio, "Understanding the patient's perspective on rapid and routine HIV testing in an inner-city urgent care center," *AIDS Education and Prevention*, vol. 16, no. 2, pp. 101–114, 2004.

[2] A. B. Hutchinson, B. M. Branson, A. Kim, and P. G. Farnham, "A meta-analysis of the effectiveness of alternative HIV counseling and testing methods to increase knowledge of HIV status," *AIDS*, vol. 20, no. 12, pp. 1597–1604, 2006.

[3] J. Pavie, A. Rachline, B. Loze et al., "Sensitivity of five rapid HIV tests on oral fluid or Finger-Stick whole blood: a real-time comparison in a healthcare setting," *PLoS ONE*, vol. 5, no. 7, Article ID e11581, 2010.

[4] T. C. Granade, B. S. Parekh, P. M. Tih et al., "Evaluation of rapid prenatal human immunodeficiency virus testing in rural Cameroon," *Clinical and Diagnostic Laboratory Immunology*, vol. 12, no. 7, pp. 855–860, 2005.

[5] D. Malamud, W. R. Abrams, H. Bau et al., "Oral-based techniques for the diagnosis of infectious diseases," *Journal of the California Dental Association*, vol. 34, no. 4, pp. 297–301, 2006.

[6] C. D. Chin, T. Laksanasopin, Y. K. Cheung et al., "Microfluidics-based diagnostics of infectious diseases in the developing world," *Nature Medicine*, vol. 17, no. 8, pp. 1015–1019, 2011.

[7] S. E. McCalla and A. Tripathi, "Microfluidic reactors for diagnostics applications," *Annual Review of Biomedical Engineering*, vol. 13, pp. 321–343, 2011.

[8] P. L. A. M. Corstjens, Z. Chen, M. Zuiderwijk et al., "Rapid assay format for multiplex detection of humoral immune responses to

infectious disease pathogens (HIV, HCV, and TB)," *Annals of the New York Academy of Sciences*, vol. 1098, pp. 437–445, 2007.

[9] S. Park, Y. Zhang, S. Lin, T.-H. Wang, and S. Yang, "Advances in microfluidic PCR for point-of-care infectious disease diagnostics," *Biotechnology Advances*, vol. 29, no. 6, pp. 830–839, 2011.

[10] R. Cuchacovich, "Clinical applications of the polymerase chain reaction: an update," *Infectious Disease Clinics of North America*, vol. 20, no. 4, pp. 735–758, 2006.

[11] A. Niemz, T. M. Ferguson, and D. S. Boyle, "Point-of-care nucleic acid testing for infectious diseases," *Trends in Biotechnology*, vol. 29, no. 5, pp. 240–250, 2011.

[12] J. R. Krogmeier, I. Schaefer, G. Seward, G. R. Yantz, and J. W. Larson, "An integrated optics microfluidic device for detecting single DNA molecules," *Lab on a Chip*, vol. 7, no. 12, pp. 1767–1774, 2007.

[13] J. S. Marcus, W. F. Anderson, and S. R. Quake, "Parallel picoliter RT-PCR assays using microfluidics," *Analytical Chemistry*, vol. 78, no. 3, pp. 956–958, 2006.

[14] C. J. Easley, J. M. Karlinsey, J. M. Bienvenue et al., "A fully integrated microfluidic genetic analysis system with sample-in-answer-out capability," *Proceedings of the National Academy of Sciences of the United States of America*, vol. 103, no. 51, pp. 19272–19277, 2006.

[15] J. Kim, M. Johnson, P. Hill, and B. K. Gale, "Microfluidic sample preparation: cell lysis and nucleic acid purification," *Integrative Biology*, vol. 1, no. 10, pp. 574–586, 2009.

[16] C. W. Price, D. C. Leslie, and J. P. Landers, "Nucleic acid extraction techniques and application to the microchip," *Lab on a Chip*, vol. 9, no. 17, pp. 2484–2494, 2009.

[17] C. A. Holland and F. L. Kiechle, "Point-of-care molecular diagnostic systems—Past, present and future," *Current Opinion in Microbiology*, vol. 8, no. 5, pp. 504–509, 2005.

[18] P. Zhou, L. Young, and Z. Chen, "Weak solvent based chip lamination and characterization of on-chip valve and pump," *Biomedical Microdevices*, vol. 12, no. 5, pp. 821–832, 2010.

[19] G. Spizz, L. Young, R. Yasmin et al., "Rheonix CARD technology: an innovative and fully automated molecular diagnostic device," *Point of Care*, vol. 11, no. 1, pp. 42–51, 2012.

[20] C. Holm-Hansen, G. Tong, C. Davis, W. R. Abrams, and D. Malamud, "Comparison of oral fluid collectors for use in a rapid point-of-care diagnostic device," *Clinical and Diagnostic Laboratory Immunology*, vol. 11, no. 5, pp. 909–912, 2004.

[21] N. L. Michael, S. A. Herman, S. Kwok et al., "Development of calibrated viral load standards for group M subtypes of human immunodeficiency virus type 1 and performance of an improved AMPLICOR HIV-1 MONITOR test with isolates of diverse subtypes," *Journal of Clinical Microbiology*, vol. 37, no. 8, pp. 2557–2563, 1999.

[22] R. S. Niedbala, H. Feindt, K. Kardos et al., "Detection of analytes by immunoassay using Up-Converting Phosphor Technology," *Analytical Biochemistry*, vol. 293, no. 1, pp. 22–30, 2001.

[23] P. Corstjens, M. Zuiderwijk, A. Brink et al., "Use of up-converting phosphor reporters in lateral-flow assays to detect specific nucleic acid sequences: a rapid, sensitive DNA test to identify human papillomavirus type 16 infection," *Clinical Chemistry*, vol. 47, no. 10, pp. 1885–1893, 2001.

[24] P. Zhou and L. C. Young, *Laminated Microfluidic Structures and Medthod for Making*, U.S. Patent, Rheonix, ithaca, NY, USA, 2009.

[25] T. S. Liang, E. Erbelding, C. A. Jacob et al., "Rapid HIV testing of clients of a mobile STD/HIV clinic," *AIDS Patient Care and STDs*, vol. 19, no. 4, pp. 253–257, 2005.

[26] D. Malamud, H. Bau, S. Niedbala, and P. Corstjens, "Point detection of pathogens in oral samples," *Advances in Dental Research*, vol. 18, no. 1, pp. 12–16, 2005.

[27] C. Liu, X. Qiu, S. Ongagna et al., "A timer-actuated immunoassay cassette for detecting molecular markers in oral fluids," *Lab on a Chip*, vol. 9, no. 6, pp. 768–776, 2009.

[28] S. J. Wu, S. Pal, S. Ekanayake et al., "A dry-format field-deployable quantitative reverse transcriptase-polymerase chain reaction assay for diagnosis of dengue infections," *American Journal of Tropical Medicine and Hygiene*, vol. 79, no. 4, pp. 505–510, 2008.

[29] B. Lu, R. P. Viscidi, J. H. Lee et al., "Human Papillomavirus (HPV) 6, 11, 16, and 18 seroprevalence is associated with sexual practice and age: results from the multinational HPV infection in men study (HIM study)," *Cancer Epidemiology Biomarkers and Prevention*, vol. 20, no. 5, pp. 990–1002, 2011.

[30] S. Desai, R. Chapman, M. Jit et al., "Prevalence of human papillomavirus antibodies in males and females in England," *Sexually Transmitted Diseases*, vol. 38, no. 7, pp. 622–629, 2011.

[31] M. Jentschke, P. Soergel, V. Lange et al., "Evaluation of a new multiplex real-time polymerase chain reaction assay for the detection of human papillomavirus infections in a referral population," *International Journal of Gynecological Cancer*, vol. 22, no. 6, pp. 1050–1056, 2012.

[32] R. Howell-Jones, N. de Silva, M. Akpan et al., "Prevalence of human papillomavirus (HPV) infections in sexually active adolescents and young women in England, prior to widespread HPV immunisation," *Vaccine*, vol. 30, no. 26, pp. 3867–3875, 2012.

[33] N. G. Campos, J. J. Kim, P. E. Castle et al., "Health and economic impact of HPV 16/18 vaccination and cervical cancer screening in Eastern Africa," *International Journal of Cancer*, vol. 130, no. 11, pp. 2672–2684, 2012.

[34] R. J. ten Hove, J. J. Verweij, K. Vereecken, K. Polman, L. Dieye, and L. van Lieshout, "Multiplex real-time PCR for the detection and quantification of *Schistosoma mansoni* and *S. haematobium* infection in stool samples collected in northern Senegal," *Transactions of the Royal Society of Tropical Medicine and Hygiene*, vol. 102, no. 2, pp. 179–185, 2008.

[35] P. L. A. M. Corstjens, L. Van Lieshout, M. Zuiderwijk et al., "Up-converting phosphor technology-based lateral flow assay for detection of Schistosoma circulating anodic antigen in serum," *Journal of Clinical Microbiology*, vol. 46, no. 1, pp. 171–176, 2008.

[36] H. Smith, M. Doenhoff, C. Aitken et al., "Comparison of *Schistosoma mansoni* soluble cercarial antigens and soluble egg antigens for serodiagnosing schistosome infections," *PLoS Neglected Tropical Diseases*, vol. 6, no. 9, Article ID e1815, 2012.

[37] J. Albert and E. M. Fenyo, "Simple, sensitive, and specific detection of human immunodeficiency virus type 1 in clinical specimens by polymerase chain reaction with nested primers," *Journal of Clinical Microbiology*, vol. 28, no. 7, pp. 1560–1564, 1990.

[38] M. K. Hourfar, U. Michelsen, M. Schmidt, A. Berger, E. Seifried, and W. K. Roth, "High-throughput purification of viral RNA based on novel aqueous chemistry for nucleic acid isolation," *Clinical Chemistry*, vol. 51, no. 7, pp. 1217–1222, 2005.

Hindawi Publishing Corporation
BioMed Research International
Volume 2013, Article ID 412370, 9 pages
http://dx.doi.org/10.1155/2013/412370

Research Article

A Pentaplex PCR Assay for the Detection and Differentiation of *Shigella* Species

Suvash Chandra Ojha,[1] Chan Yean Yean,[1] Asma Ismail,[2] and Kirnpal-Kaur Banga Singh[1]

[1] *Department of Medical Microbiology & Parasitology, School of Medical Sciences, Universiti Sains Malaysia, Health Campus, 16150 Kubang Kerian, Kelantan, Malaysia*
[2] *Institute for Research in Molecular Medicine (INFORMM), Universiti Sains Malaysia, Health Campus, 16150 Kubang Kerian, Kelantan, Malaysia*

Correspondence should be addressed to Kirnpal-Kaur Banga Singh; kiren@kck.usm.my

Received 23 November 2012; Revised 6 January 2013; Accepted 11 January 2013

Academic Editor: Arun K. Bhunia

The magnitude of shigellosis in developing countries is largely unknown because an affordable detection method is not available. Current laboratory diagnosis of *Shigella* spp. is laborious and time consuming and has low sensitivity. Hence, in the present study, a molecular-based diagnostic assay which amplifies simultaneously four specific genes to identify *invC* for *Shigella* genus, *rfc* for *S. flexneri*, *wbgZ* for *S. sonnei*, and *rfpB* for *S. dysenteriae*, as well as one internal control (*ompA*) gene, was developed in a single reaction to detect and differentiate *Shigella* spp. Validation with 120 *Shigella* strains and 37 non-*Shigella* strains yielded 100% specificity. The sensitivity of the PCR was 100 pg of genomic DNA, 5.4×10^4 CFU/ml, or approximately 120 CFU per reaction mixture of bacteria. The sensitivity of the pentaplex PCR assay was further improved following preincubation of the stool samples in Gram-negative broth. A preliminary study with 30 diarrhoeal specimens resulted in no cross-reaction with other non-*Shigella* strains tested. We conclude that the developed pentaplex PCR assay is robust and can provide information about the four target genes that are essential for the identification of the *Shigella* genus and the three *Shigella* species responsible for the majority of shigellosis cases.

1. Introduction

Shigellosis continues to be a major health problem in many parts of the world, particularly in underdeveloped and developing countries with poor sanitary systems and improper treatment of water supplies, and also among travelers from industrialized nations [1, 2]. Worldwide, mortality and morbidity due to shigellosis were found to be highest among young children 1 to 5 years of age and the elderly [3–5]. Three species of *Shigella* are responsible for the majority of shigellosis cases: *S. flexneri*, *S. sonnei*, and *S. dysenteriae*. Of these, *S. sonnei* is encountered mostly in industrialized countries and *S. flexneri* in developing countries; *S. dysenteriae* is the only epidemic and pandemic strain [2, 4, 6, 7]. The pathogenesis of shigellosis includes inflammation, ulceration, haemorrhage, tissue destruction, and fibrosis of the colonic mucosa, which result in abdominal pain and diarrhoea/dysentery; in some cases infertility and endometriosis also have been reported [8, 9]. Bacteraemia may occur in people with severe infections, particularly in malnourished children and AIDS patients [10]. A more recent annual estimate of shigellosis throughout the world was estimated to be 90 million incidences and 108,000 deaths [11].

Shigella infection spreads by the faecal-oral route. Because of the low infectious dose (10 to 100 organisms), person-to-person transmission is likely the most common route of infection, as the bacteria can survive gastric acidity better than other enteric bacteria [10, 12]. However, transmission via contaminated water, food, overcrowded communities, food handlers, contaminated swimming pools, and flies also has been documented [8, 13, 14]. Recent increases in the number of cases of shigellosis in many parts of the world are attributed to the emergence of multiple-drug resistant strains. Early and accurate diagnosis of shigellosis coupled with prompt medical intervention is essential for reducing the morbidity and mortality caused by *Shigella* spp.

Shigella spp. are fragile organisms that are excreted in large numbers in the stool, but they die off quickly because stools are acidic [15]. Thus, routine microbiological methods used to identify *Shigella* spp. from stool samples are relatively inefficient, time consuming, and labor intensive, and the diagnosis often remains obscure due to the presence of low numbers of causative organisms, competition from other commensal organisms, and inappropriate sample collection. If samples are collected after antibiotic therapy, growth of the organism may be impaired. Moreover, Dutta et al. [16] and Islam et al. [17] reported the sensitivity of the culture method to be 54% and 74%, respectively, compared to that of the conventional PCR technique. Recent molecular diagnostic techniques based on nucleic acids, such as PCR, have shown tremendous potential for identifying *Shigella* spp. and have been increasingly exploited.

To date, few studies have focused on the rapid diagnosis of shigellosis in underdeveloped and developing countries. However, PCR diagnostic tests have proven to be rapid and effective for the detection and identification to *Shigella* spp. [16–18]. In this study, we searched for genes unique to the *Shigella* serovars and used them to design a pentaplex PCR assay. Our assay differs from conventional multiplex PCRs, which often target the invasion plasmid H (*ipaH*) gene, O antigen synthesis genes, and the 16S rRNA gene for detection of *Shigella* spp. [18–20]; in those cases, the diagnosis is often based on sequence polymorphisms or differences rather than on the absence or presence of a gene. Those methods do not detect *Shigella* at the genus and species level simultaneously. The goal of the present study was to design a pentaplex PCR of *Shigella* spp. with an internal control for the detection of the genus *Shigella* and also for the clinically important *Shigella* spp., namely, *S. flexneri, S. sonnei,* and *S. dysenteriae*.

2. Methods

2.1. Bacterial Strains and Growth Conditions. A total of 120 *Shigella* strains of *S. flexneri* ($n = 95$), *S. sonnei* ($n = 20$), *S. dysenteriae* ($n = 3$) and *S. boydii* ($n = 2$), were used in this study. Pure culture strains were isolated from patients admitted to Hospital Universiti Sains Malaysia (HUSM) from 2001 to 2009. Table 2 lists the *Shigella* spp. reference strains and other bacteria used in this study. Non-*Shigella* strains were used to determine the specificity and robustness of the assay. All the strains were biochemically and serologically confirmed and were stored at −80°C in 16% glycerol.

2.2. Isolation of Shigella Spp. from Clinical Specimens Using a Conventional Method. Stool specimens were inoculated on MacConkey (Oxoid Ltd., UK) and deoxycholate citrate agar (DCA) (Oxoid Ltd., UK) using a sterile inoculating loop. Stools were also enriched in selenite F broth (Oxoid Ltd., UK) and incubated overnight at 37 ± 2°C. The next day, the enriched broth was subcultured on MacConkey agar and DCA and incubated overnight at 37 ± 2°C. Colonies morphologically resembling *Shigella* spp. were further evaluated with biochemical tests using triple sugar iron (Oxoid Ltd., UK), urea agar slant (Oxoid Ltd., UK), methyl red (Oxoid Ltd., UK), Simmon's citrate agar slant (Oxoid Ltd., UK), and sulphur indole motility medium (Oxoid Ltd., UK). Identities of colonies were serologically confirmed by slide agglutination with appropriate group-specific polyvalent antisera followed by type-specific monovalent antisera (Denka-Seiken, Tokyo, Japan). Nonserotypable isolates were further checked using an API 20E kit (BioMerieux, Marcy I'Etoile, France).

2.3. Primer Design for Pentaplex PCR Assay. The gene sequence for *invC* of the genus *Shigella* and gene sequences for *rfc, wbgZ*, and *rfpB* of *S. flexneri, S. sonnei*, and *S. dysenteriae*, respectively, were obtained from GenBank [21] for DNA sequence alignment and primer design. The ClustalW program in Vector NTI version 9.0 software (Invitrogen, Carlsbad, CA, USA) was used to align the DNA sequences. The conserved and non-conserved regions of the DNA sequence alignments were visualized using GeneDoc software [22].

Based on the conserved regions of the alignment, specific primer pairs for the genus *Shigella* were designed to amplify the *invC* gene. Specific primers for *S. flexneri*, *S. sonnei*, and *S. dysenteriae* were designed based on the non-conserved regions of *rfc*, *wbgZ*, and *rfpB* genes, respectively. The four primer pairs were designed in such a way that amplification efficiency was not hindered and amplicon sizes ranging from 211 to 875 bp could be differentiated by agarose gel electrophoresis (Figure 1). The homology of the designed primer sequences was analyzed using BLAST [21]. A primer pair based on the *ompA* gene was designed (1319 bp) and used as an internal control. The primer (AIT BIOTECH, Singapore) sequences for the five genes and expected PCR product sizes are shown in Table 1.

2.4. Pentaplex PCR Assay. The pentaplex PCR assay was standardized using genomic DNA extracted from reference *Shigella* spp. A mixture of DNA from three strains (*S. flexneri* (SH052), *S. sonnei* (SH023), and *S. dysenteriae* (SD375)) that contained the four genes of interest was used as a positive control. DNase-free distilled water was used as a negative control. In addition, a plasmid containing the *ompA* gene (10 pg) was incorporated as an internal control template to rule out false negative results. An internal control (primer pair and template) was incorporated into every reaction mixture, including negative controls.

The colonies isolated from blood agar were inoculated into nutrient agar (Oxoid Ltd., UK) and incubated overnight at 37 ± 2°C. Bacteria lysate was prepared by resuspending one bacterial colony in 30 μL of deionized water, boiling for 5 min, and centrifuging at 8000 ×g for 2 min. Two microliters of supernatant then were used as the DNA template in the pentaplex PCR assays.

The optimized primer concentration for each gene (0.4 pmol for *ompA*, *rfc*, and *rfpB*; 0.3 pmol for *invC*; and 0.2 pmol for *wbgZ*) was used in the pentaplex PCR. The other components used in the PCR were 200 μM dNTPs, 2.5 mM $MgCl_2$, 1X PCR buffer, and 1 U *Taq* DNA polymerase (Promega, Madison, WI, USA). The PCR was performed using a Mastercycler Gradient (Eppendorf, Hamburg, Germany) with one cycle of initial denaturation at 94°C for 3 min,

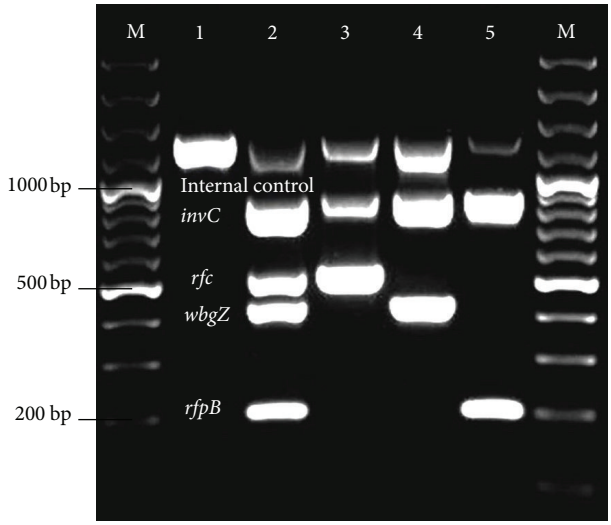

Figure 1: Pentaplex PCR assay profile with reference strains. M, 100 bp plus marker; lane 1, negative control; lane 2, positive control; lane 3, SH052 strain (*rfc S. flexneri*, *invC-Shigella* genus); lane 4, SH031 strain (*invC-Shigella* genus, *wbgZ S. sonnei*); lane 5, SD375 strain (*invC-Shigella* genus, *rfpB S. dysenteriae*); M, 100 bp plus marker.

Table 1: Sequences of primers used for the pentaplex PCR.

Primers	Primer sequence (5′-3′)	Gene target	Location of gene	Amplicon size (bp)	Target identity	GenBank accession number
SgenDF1	TGC CCA GTT TCT TCA TAC GC	*invC*	Plasmid	875	*Shigella* genus	AF386526
SgenDR1	GAA AGT AGC TCC CGA AAT GC					
SflexDF1	TTT ATG GCT TCT TTG TCG GC	*rfc*	Chromosome	537	*Shigella flexneri*	CP000266
SflexDR1	CTG CGT GAT CCG ACC ATG					
SsonDF1	TCT GAA TAT GCC CTC TAC GCT	*wbgZ*	Plasmid	430	*Shigella sonnei*	CP000039
SsonDR1	GAC AGA GCC CGA AGA ACC G					
SdysDF1	TCT CAA TAA TAG GGA ACA CAG C	*rfpB*	Plasmid	211	*Shigella dysenteriae*	CP000640
SdysDR1	CAT AAA TCA CCA GCA AGG TT					
ICDF1	GCA GGC ATT GCT GGG TAA	*ompA*	Plasmid	1319	Internal control	AY305875
ICDR1	ACA CTT GTA AGT TTT CAA CTA CG					

30 cycles of denaturation at 94°C for 30 s, annealing for 30 s at 60°C, and extension at 72°C for 30 s, followed by an extra cycle of annealing at 60°C for 30 s and a final extension at 72°C for 3 min. The PCR products were analyzed by electrophoresis on 1.5% agarose gels (Promega) with 10 mg/mL ethidium bromide (Sigma, USA); they were run at 100 V for 60 min. PCR products were visualized under a UV transilluminator and photographed using an image analyzer (ChemiImager 5500; Alpha Innotech, San Leandro, CA, USA).

2.5. Evaluation of Pentaplex PCR Assay Results. Analytical specificity was evaluated using DNA lysate prepared from pure cultures of 120 *Shigella* strains, 10Gram-positive strains, and 27 Gram negative strains. The analytical sensitivity was evaluated using genomic DNA (1 μg to 10 pg) and also 10^8 to 10^2 CFU/mL obtained from *Shigella* strains. The diagnostic evaluation of the pentaplex PCR was conducted using 95 *S. flexneri*, 20 *S. sonnei*, 3 *S. dysenteriae*, and 2 *S. boydii* strains. The results were compared with those from the conventional culture method, which is considered to be the standard of detection [23].

2.6. Faecal Spiking and Sensitivity. The standardized pentaplex PCR assay designed to detect *Shigella* directly from stool was also tested using stool samples spiked with a known amount of *Shigella* based on slight modification of method described by Houng et al. [18]. Stool samples ($n = 2$, children ≤ 5 years old) were collected from the Department of Medical Microbiology and Parasitology, HUSM, Malaysia, and were pretested for the presence of amplifiable *Shigella* DNA by pentaplex PCR and found to be negative. Five grams of stool were weighed and suspended in 45 mL of normal saline (NS) solution, which corresponds to a 10% mixture. The solution was vortexed for 2 min to obtain a homogenous mixture. Insoluble particulate matter was removed by low-speed centrifugation (1000 ×g) for 3 min, and the supernatant was transferred to a fresh tube. Meanwhile, an overnight culture of *Shigella*-specific strains was grown in nutrient broth (NB)

(Oxoid Ltd., UK) under shaking condition (200 rpm). The bacterial count was estimated to be 10^8 CFU and 10-fold diluted with NS. Next, a 500 μL sample of each dilution of bacterial cells was mixed with 500 μL of the faecal suspension in a new tube. Tubes were vortexed, 1 mL of the mixture was transferred to 9 mL of GNB (Merck, Germany), and the mixture was preincubated at 37 ± 237 ± 2°C for up to 6 h without shaking. At time 0, 2, 4, and 6 h after incubation, 200 μL of mixture was placed in a 0.5 mL microcentrifuge tube and centrifuged at 8000 ×g for 3 min. The supernatant was removed, cells were washed using NS, and lysates were prepared by the boiling method. Two microliters of the lysate supernatant were used for pentaplex PCR evaluation.

2.7. Screening of Clinical Specimens. Stool samples were collected from patients suspected with acute gastroenteritis or dysentery from Department of Medical Microbiology and Parasitology, USM, Malaysia. Approximately 1 g of each faecal sample from 30 patients suspected of dysentery was transferred to 9 mL of GNB broth corresponding to 10% mixture and preincubated at 37°C ± 2°C for 4 h without shaking. Subsequently, 200 μL of the suspension was taken out and placed in 0.5 mL microcentrifuge tube and centrifuged at 8000 ×g for 3 min. The supernatant was discarded and cells were washed with 200 μL of 0.9% NS. Pellet was resuspended with 30 μL of PCR grade water and boiled for 5 min. Two microlitres of the supernatant containing DNA (lysate) were used for thermostabilized multiplex PCR evaluation. A pure culture of strain and a *Shigella* spiked faecal sample served as positive controls whilst a PCR reaction mixture without bacterial DNA template and an unspiked faecal sample from a healthy individual were incorporated as negative controls.

3. Results

We developed a pentaplex PCR assay that simultaneously amplifies four specific genes and one internal control gene in a single reaction; this assay allows detection and differentiation of *Shigella* at the genus and species levels (Table 1). Based on the compatibility of the primers for different genes, the pentaplex PCR was standardized for the *invC* (genus *Shigella*), *rfc* (*S. flexneri*), *wbgZ* (*S. sonnei*), and *rfpB* (*S. dysenteriae*) genes. The fifth primer set (*ompA*) was used for amplification of the internal control to validate the reliability of the assay and to exclude false negative results. Figure 1 shows a representative gel that illustrates differentiation of *Shigella* by genus and species.

All of the primers were positive for the genes targeted by pentaplex PCR but negative for non-*Shigella* strains (Table 2). The optimum concentration of primer needed to amplify uniformly with approximately the same band intensity was 0.4 pmol for *ompA*, *rfc*, and *rfpB*; 0.3 pmol for *invC*; and 0.2 pmol for *wbgZ*. The pentaplex PCR gave the best results when 2.5 mM $MgCl_2$, 200 μM dNTPs, and 1 U *Taq* polymerase were used. The optimal annealing temperature was 60°C.

The pentaplex PCR assay was evaluated for analytical specificity and sensitivity. At the DNA level sensitivity was 100 pg of DNA (Figure 2) and at the bacterial level it was 5.4×10^4 CFU/mL or approximately 120 CFU per reaction mixture of bacteria (Figure 3). The analytical specificity of the pentaplex PCR assay was evaluated using 120 clinical strains of *Shigella* spp. (95 *S. flexneri*, 20 *S. sonnei*, 3 *S. dysenteriae,* and 2 *S. boydii*), 10 Gram positive strains, and 27 Gram negative strains (Table 2).

Of the 120 *Shigella* strains tested, 116 were positive for *invC*. Of the 20 strains of *S. sonnei*, 16 were positive for *wbgZ*. The fact that four strains were *wbgZ* and *invC* negative suggests that the virulence plasmid might have been lost due to long storage time or subculturing [24]. The *rfc* and *rfpB* primers showed 100% sensitivity in identifying their respective strains (Table 3).

The DNA sequencing results of the PCR amplicons for the four genes were aligned using Vector NTI version 9.0 software and then analyzed by BLAST. The results showed that all four PCR amplicons were specific to their respective genes and had 100% sequence identity with the existing GenBank sequences.

The effect of enrichment for *Shigella* count was investigated by spiking normal stool samples with known *Shigella* numbers and incubating the mixture in growth medium. The sample inoculated with 10^3 CFU/mL did not generate any amplicon at time zero (before incubation); however *S. flexneri*, *S. sonnei*, and *S. dysenteriae* produced clear amplicons after 4 h of incubation. This result illustrates that it is possible to detect *Shigella* spp. from samples containing low bacterial concentration by preincubating the samples in growth medium. A preliminary study on the efficacy of the multiplex PCR assay was evaluated using 30 faecal samples which were culturally confirmed negative for *Shigella* spp. No target genes were amplified in the multiplex PCR assay although both the positive and internal controls had amplifications.

4. Discussion

Shigellosis is the most communicable of the bacterial diarrhoeas [11]. This disease occurs as sporadic cases and occasional outbreaks of varying magnitude in developed countries and causes epidemics and endemic disease in developing countries. Because shigellosis is highly contagious, it is crucial to develop a rapid method for identifying the bacteria in order to limit and control outbreaks. Classical methods for determining the presence of bacteria in general are time consuming and labor intensive and have low sensitivity [16, 17, 25–27]. Hence, molecular methods, which offer speed, sensitivity, and specificity, have been developed to address this problem. However, some of these methods are relatively expensive and difficult to perform and require special equipment (e.g., a method combining immunocapture with PCR of bacteria for the detection of *Shigella* spp. [28], seminested PCR [29], PCR-nonradioactive labeling [30], PCR-RFLP [31], and PCR-ELISA [32]). On the other hand, DNA microarray analysis proved to be specific, sensitive, and reproducible, but its application as a diagnostic or epidemiological tool is difficult in view of the elevated cost, instruments and requires a skilled person to perform the test [33].

Table 2: Bacterial species and strains used in this study and results of pentaplex PCR.

Bacterial strains	No. of strains tested	*inv C*[a]	*rfc*	*wbgZ*	*rfpB*	IC (*ompA*)
S. flexneri (ATCC 12022)[b]	1	+	+	−	−	+
S. sonnei (SH031)[c]	1	+	−	+	−	+
S. boydii (ATCC 9207)[b]	1	+	−	−	−	+
S. dysenteriae (SD375)[d]	1	+	−	−	+	+
Salmonella spp.	2	−	−	−	−	+
S. Typhi[c]	3	−	−	−	−	+
S. Paratyphi A[c]	1	−	−	−	−	+
S. Paratyphi B[c]	1	−	−	−	−	+
Klebsiella spp.[c]	2	−	−	−	−	+
K. pneumoniae[c]	2	−	−	−	−	+
E. coli (EPEC)[c]	1	−	−	−	−	+
E. coli (EHEC)[c]	1	−	−	−	−	+
E. coli (ETEC)[c]	1	−	−	−	−	+
E. coli[c]	4	−	−	−	−	+
V. cholerae[c]	3	−	−	−	−	+
V. parahemolyticus[c]	1	−	−	−	−	+
V. fulvalis[c]	1	−	−	−	−	+
V. cholera (wild type)[c]	1	−	−	−	−	+
V. furnissii[c]	1	−	−	−	−	+
P. aeruginosa[c]	3	−	−	−	−	+
P. mirabilis[c]	1	−	−	−	−	+
P. vulgaris[c]	1	−	−	−	−	+
C. freudii[c]	1	−	−	−	−	+
E. cloacae[c]	1	−	−	−	−	+
Y. enterocolitica[c]	1	−	−	−	−	+
Acinetobacter spp.[c]	1	−	−	−	−	+
A. baumannii[c]	1	−	−	−	−	+
S. marcescens[c]	1	−	−	−	−	+
Campylobacter spp.[c]	1	−	−	−	−	+
A. hydrophila[c]	1	−	−	−	−	+
M. morganii[c]	1	−	−	−	−	+
B. cereus[c]	1	−	−	−	−	+
S. aureus[c]	2	−	−	−	−	+
Methylene resistant *S. aureus*[c]	1	−	−	−	−	+
Streptococcus spp. Group A[c]	1	−	−	−	−	+
Streptococcus spp. Group B[c]	1	−	−	−	−	+
Streptococcus spp. Group G[c]	1	−	−	−	−	+
Corynebacterium spp.[c]	1	−	−	−	−	+
Listeria spp.[c]	1	−	−	−	−	+
Lactobacillus spp.[c]	1	−	−	−	−	+
Gardnerella spp.[c]	1	−	−	−	−	+

[a] *Shigella* genus.
[b] Reference strains from American Type Culture Collection (ATCC), Reston, VA, USA.
[c] Department of Medical Microbiology and Parasitology, School of Medical Sciences, Universiti Sains Malaysia.
[d] Obtained from Institute for Medical Research, Malaysia.
"+" is positive; "−" is negative by pentaplex PCR.

To overcome these drawbacks of existing techniques, we developed a pentaplex PCR assay and evaluated its ability to detect and identify three enteropathogenic bacteria species at the genus and species levels. Several previous studies described the development of *Shigella* multiplex PCR, but those assays did not discriminate between *Shigella* at the genus and species levels, nor did they differentiate *Shigella* from closely related pathogens such as *Salmonella*, *Citrobacter*, and enteroinvasive *Escherichia coli* (EIEC) [20, 25, 34].

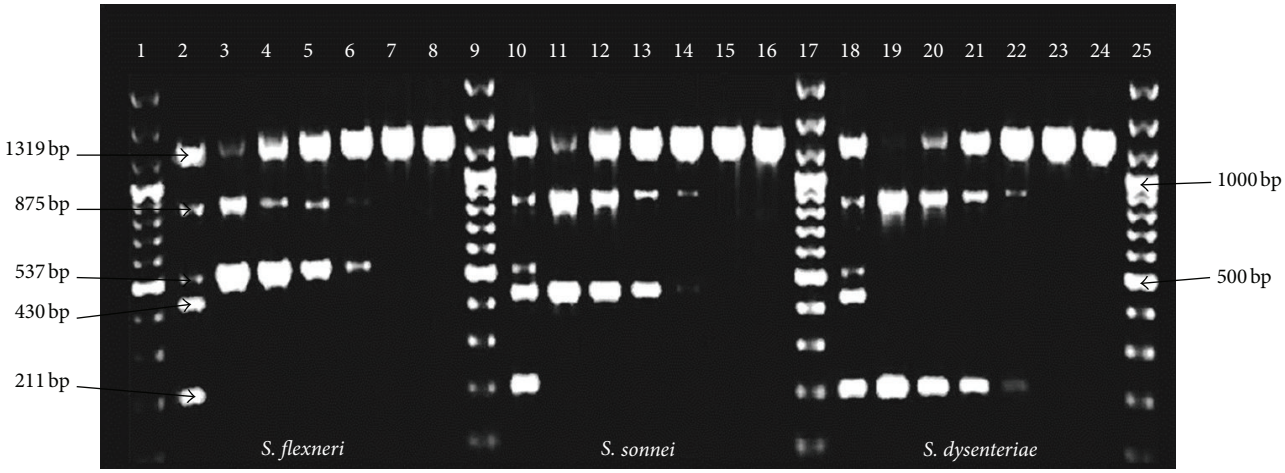

Figure 2: Analytical sensitivity of multiplex PCR at genomic DNA level using reference strains. Lane 1, 100 bp plus marker; lane 2, positive control; lane 3, 100 ng/μL of genomic DNA *S. flexneri*; lane 4, 10 ng/μL of genomic DNA *S. flexneri*; lane 5, 1 ng/μL of genomic DNA *S. flexneri*; lane 6, 100 pg/μL of genomic DNA *S. flexneri*; lane 7, 10 pg/μL of genomic DNA *S. flexneri*; lane 8, 1 pg/μL of genomic DNA *S. flexneri*; lane 9, 100 bp plus marker; lane 10, positive control ; lane 11, 100 ng/μL of genomic DNA *S. sonnei*; lane 12, 10 ng/μL of genomic DNA *S. sonnei*; lane 13, 1 ng/μL of genomic DNA *S. sonnei*; lane 14, 100 pg/μL of genomic DNA *S. sonnei*; lane 15, 10 pg/μL of genomic DNA *S. sonnei*; lane 16, 1 pg/μL of genomic DNA *S. sonnei*; lane 17, 100 bp plus marker; lane 18, positive control ; lane 19, 100 ng/μL of genomic DNA *S. dysenteriae*; lane 20, 10 ng/μL of genomic DNA *S. dysenteriae*; lane 21, 1 ng/μL of genomic DNA *S. dysenteriae*; lane 22, 100 pg/μL of genomic DNA *S. dysenteriae*; lane 23, 10 pg/μL of genomic DNA *S. dysenteriae*; lane 24, 1 pg/μL of genomic DNA *S. dysenteriae*; lane 25, 100 bp plus marker.

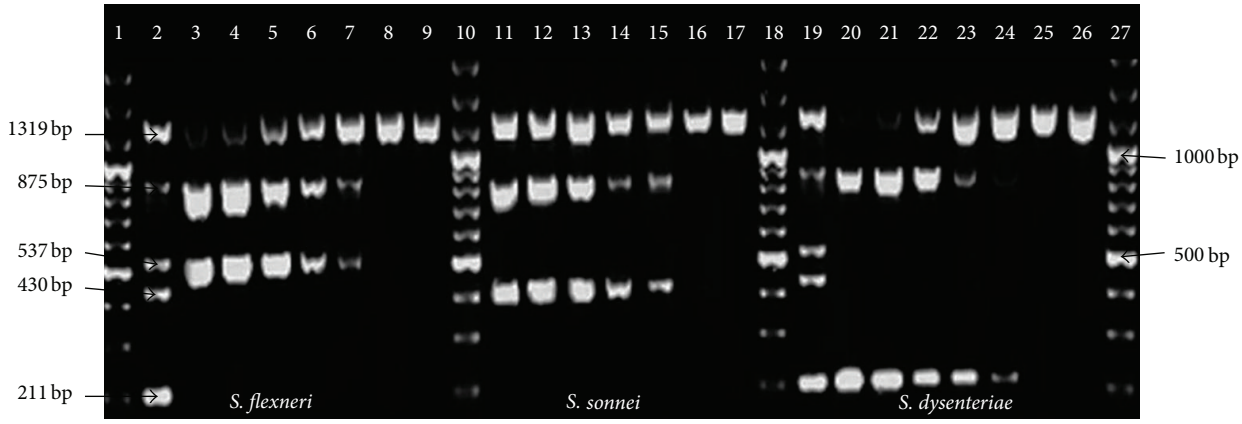

Figure 3: Analytical sensitivity of multiplex PCR at the bacterial level (CFU/mL) using reference strains. Lane 1, 100 bp plus marker; lane 2, positive control; lane 3, 10^8 CFU/mL lysate of *S. flexneri*; lane 4, 10^7 CFU/mL lysate of *S. flexneri*; lane 5, 10^6 CFU/mL lysate of *S. flexneri*; lane 6, 10^5 CFU/mL lysate of *S. flexneri*; lane 7, 10^4 CFU/mL lysate of *S. flexneri*; lane 8, 10^3 CFU/mL lysate of *S. flexneri*; lane 9, 10^2 CFU/mL lysate of *S. flexneri*; lane 10, 100 bp plus Marker; lane 11, 10^8 CFU/mL lysate of *S. sonnei*; lane 12, 10^7 CFU/mL lysate of *S. sonnei*; lane 13, 10^6 CFU/mL lysate of *S. sonnei*; lane 14, 10^5 CFU/mL lysate of *S. sonnei*; lane 15, 10^4 CFU/mL lysate of *S. sonnei*; lane 16, 10^3 CFU/mL lysate of *S. sonnei*; lane 17, 10^2 CFU/mL lysate of *S. sonnei*; lane 18, 100 bp plus Marker; lane 19, Positive control ; lane 20, 10^8 CFU/mL lysate of *S. dysenteriae*; lane 21, 10^7 CFU/mL lysate of *S. dysenteriae*; lane 22, 10^6 CFU/mL lysate of *S. dysenteriae*; lane 23, 10^5 CFU/mL lysate of *S. dysenteriae*; lane 24, 10^4 CFU/mL lysate of *S. dysenteriae*; lane 25, 10^3 CFU/mL lysate of *S. dysenteriae*; lane 26, 10^2 CFU/mL lysate of *S. dysenteriae*; lane 27, 100 bp plus marker.

In our study, primers were designed based on the prevalent species responsible for the majority of shigellosis cases [2, 4, 6, 7]. Four highly specific genes (*invC*, *rfc*, *wbgZ*, and *rfpB*) that can best detect *Shigella* at the genus and species level were identified. Because *invC* is present among all of the *Shigella* spp., *rfc*, *wbgZ*, and *rfpB* were combined with *invC* for speciation of the *Shigella* strains. The primer for *S. flexneri* that targets the *rfc* gene was designed based on Houng et al. [18], and it allows discrimination between *Shigella* and EIEC in faecal samples. Similarly, the three other highly specific primers were designed based on the homologous sequences retrieved from GenBank (NCBI). *S. boydii* species identification was not included in this study because of its low prevalence in developing and industrialized countries. However, the presence of the *invC* band specific for *Shigella* genus and the absence of all other amplicons specific for *Shigella* spp. can be considered to be the detection criteria for *S. boydii*.

Table 3: Summary for evaluation of pentaplex PCR assay carried out using reference strains.

Number of strains evaluated by pentaplex PCR assay		
Bacterial strains	No. of specimen tested	Positive (%) (n = 120)
Shigella genus	120	116 (96.7%)
S. flexneri	95	95 (100%)
S. sonnei	20	16 (80%)
S. dysenteriae	3	3 (100%)

Following the successful application of the primers individually, they were mixed to produce the pentaplex PCR. The mixing of primers in a single tube decreases costs and time and increases the ease of the assay. Although numerous reports of PCR assays for the detection of *Shigella* spp. exist [18, 20, 25, 34], only a few of them have incorporated internal controls to rule out false negatives [35]. According to guidelines for Molecular Diagnostic Methods for Infectious Diseases (MM3-A2), incorporation of an internal control in the reaction is essential for the diagnostic test to exclude false negative result or the presence of inhibitors. In the present study, inclusion of a 1319 bp internal control in the pentaplex PCR assay helped us to rule out false negatives or PCR inhibitors. The primers were designed with great care; BLAST and alignment results of the sequence confirmed that it did not cross-react with closely related species such as enteroinvasive *Escherichia coli* (EIEC) which gives rise to similar illness as shigellosis. However, it was unfortunate that EIEC strain was not available to be tested in this study.

The pentaplex PCR developed in our study successfully amplified all five amplicons from a single reaction tube, and the primers did not interact with each other to produce false negatives. Compatibility of primers with target amplicons was confirmed by sequencing the PCR products derived from the five representative strains. The pentaplex mixture was tested with 120 clinical strains and also against other Gram positive and Gram negative strains to determine the primers' specificity. The primers were found to be highly specific in identifying *Shigella* spp. However, in some cases nonspecific amplicon was weak and fell outside the expected size range for the primers applied and therefore was of no concern. These nonspecific amplifications are likely due to low levels of nonspecific binding between the primers and the bacterial genomic DNA.

The presence of PCR inhibitors in stool samples (e.g., bilirubin, bile salts, and heme in the faeces) may inhibit amplification and limit the usefulness of PCR technique [36, 37]. As reported by Theron et al. [29] and Thong et al. [20], an enrichment procedure prior to PCR enhances the total number of bacteria present, which helps to dilute the PCR inhibitory substances. As stated by the manufacturer of Gram negative broth (GNB), citrate and deoxycholate in the broth act as selective agents and suppress the growth of Gram positive organisms, including some coliform bacteria. The additional step of preincubating spiked faecal sample in GNB helps to eliminate the natural inhibitors and could enhance the viability of *Shigella* spp. in samples [29, 38]. A preliminary study with clinical specimens showed no cross reaction with other non-*Shigella* strains, however, to check the real performance of the developed test, a larger positive sample size need to be further investigated. The 4 h enrichment step would increase the total number of bacteria present and enhance the sensitivity of the assay. The sensitivity level achieved in our study was comparable to that of other studies. For example, Houng et al. [18] detected up to 7.4×10^4 CFU/mL of *Shigella* by amplifying IS 630 sequences, Yavzori et al. [39] detected at 10^4 CFU of *Shigella* per gram of faeces with the use of *virF* primers, and Thong et al. [20] reported a detection level of 5.0×10^4 CFU/mL of *Shigella* by amplifying *ial* and *ipaH* sequences in *Shigella* spp. Thus, the average detection of pentaplex PCR described in this study (5.4×10^4 CFU/mL) is within the common detection limit for *Shigella*.

5. Conclusion

In conclusion, the pentaplex PCR assay developed in this study was able to detect four genes that are essential for the detection and differentiation of *Shigella* at the genus and species levels simultaneously in a single test within 4 h. The built-in internal control in this assay prevented false negative results. The pentaplex PCR assay was highly sensitive and could provide results on the same day that a specimen was submitted for evaluation, which is critical during outbreaks.

Conflict of Interests

The authors declare that they have no conflict of interests.

Acknowledgments

This study was supported by Research University Cluster Grant entitled "Molecular approaches to fundamental studies on biomarkers and development of sustainable rapid nanobiodiagnostics to enteric diseases for low resource settings" (2011–2013). We gratefully acknowledge Institute for Postgraduate Studies, Universiti Sains Malaysia, for providing the fellowship assistance and the Department of Medical Microbiology and Parasitology, School of Medical Sciences, Universiti Sains Malaysia, for providing facilities and isolates.

References

[1] M. L. Bennish and B. J. Wojtyniak, "Mortality due to shigellosis: community and hospital data," *Reviews of Infectious Diseases*, vol. 13, supplement 4, pp. S245–S251, 1991.

[2] S. K. Niyogi, "Shigellosis," *Journal of Microbiology*, vol. 43, no. 2, pp. 133–143, 2005.

[3] A. Hiranrattana, J. Mekmullica, T. Chatsuwan, C. Pancharoen, and U. Thisyakorn, "Childhood shigellosis at King Chulalongkorn Memorial Hospital, Bangkok, Thailand: a 5-year review (1996–2000)," *Southeast Asian Journal of Tropical Medicine and Public Health*, vol. 36, no. 3, pp. 683–685, 2005.

[4] S. M. Faruque, R. Khan, M. Kamruzzaman et al., "Isolation of *Shigella dysenteriae* type 1 and *S. flexneri* strains from surface waters in Bangladesh: comparative molecular analysis of

environmental *Shigella* isolates versus clinical strains," *Applied and Environmental Microbiology*, vol. 68, no. 8, pp. 3908–3913, 2002.

[5] K. K. B. Singh, S. C. Ojha, Z. Z. Deris, and R. A. Rahman, "A 9-year study of shigellosis in Northeast Malaysia: antimicrobial susceptibility and shifting species dominance," *Journal of Public Health*, vol. 19, no. 3, pp. 231–236, 2011.

[6] B. A. Oyofo, M. Lesmana, D. Subekti et al., "Surveillance of bacterial pathogens of diarrhea disease in Indonesia," *Diagnostic Microbiology and Infectious Disease*, vol. 44, no. 3, pp. 227–234, 2002.

[7] D. Sur, T. Ramamurthy, J. Deen, and S. K. Bhattacharya, "Shigellosis: challenges & management issues," *The Indian Journal of Medical Research*, vol. 120, no. 5, pp. 454–462, 2004.

[8] S. Ashkenazi, "*Shigella* infections in children: new insights," *Seminars in Pediatric Infectious Diseases*, vol. 15, no. 4, pp. 246–252, 2004.

[9] V. L. Kodati, S. Govindan, S. Movva, S. Ponnala, and Q. Hasan, "Role of *Shigella* infection in endometriosis: a novel hypothesis," *Medical Hypotheses*, vol. 70, no. 2, pp. 239–243, 2008.

[10] B. R. Warren, M. E. Parish, and K. R. Schneider, "*Shigella* as a foodborne pathogen and current methods for detection in food," *Critical Reviews in Food Science and Nutrition*, vol. 46, no. 7, pp. 551–567, 2006.

[11] World Health Organization, "Initiative for Vaccine Research (IVR)," in *Diarrhoeal Diseases, Shigellosis*, 2009, http://www.who.int/vaccine_research/diseases/diarrhoeal/en/index6.html.

[12] P. O. Ozuah and H. Adam, "*Shigella* update," *Pediatrics in Review*, vol. 19, no. 3, p. 100, 1998.

[13] P. Shears, "*Shigella* infections," *Annals of Tropical Medicine and Parasitology*, vol. 90, no. 2, pp. 105–114, 1996.

[14] B. Edwards, "*Salmonella* and *Shigella* species," *Clinics in Laboratory Medicine*, vol. 19, no. 3, pp. 469–487, 1999.

[15] K. Khalil, S. R. Khan, K. Mazhar, B. Kaijser, and G. B. Lindblom, "Occurrence and susceptibility to antibiotics of *Shigella* species in stools of hospitalized children with bloody diarrhea in Pakistan," *The American Journal of Tropical Medicine and Hygiene*, vol. 58, no. 6, pp. 800–803, 1998.

[16] S. Dutta, A. Chatterjee, P. Dutta et al., "Sensitivity and performance characteristics of a direct PCR with stool samples in comparison to conventional techniques for diagnosis of *Shigella* and enteroinvasive *Escherichia coli* infection in children with acute diarrhoea in Calcutta, India," *Journal of Medical Microbiology*, vol. 50, no. 8, pp. 667–674, 2001.

[17] M. S. Islam, M. S. Hossain, M. K. Hasan et al., "Detection of *Shigella*e from stools of dysentery patients by culture and polymerase chain reaction techniques," *Journal of Diarrhoeal Diseases Research*, vol. 16, no. 4, pp. 248–251, 1998.

[18] H. S. H. Houng, O. Sethabutr, and P. Echeverria, "A simple polymerase chain reaction technique to detect and differentiate *Shigella* and enteroinvasive *Escherichia coli* in human feces," *Diagnostic Microbiology and Infectious Disease*, vol. 28, no. 1, pp. 19–25, 1997.

[19] E. Villalobo and A. Torres, "PCR for detection of *Shigella* spp. in mayonnaise," *Applied and Environmental Microbiology*, vol. 64, no. 4, pp. 1242–1245, 1998.

[20] K. L. Thong, S. L. L. Hoe, S. D. Puthucheary, and R. M. Yasin, "Detection of virulence genes in Malaysian *Shigella* species by multiplex PCR assay," *BMC Infectious Diseases*, vol. 5, no. 8, pp. 1–7, 2005.

[21] GenBank, http://www.ncbi.nlm.nih.gov/.

[22] GeneDoc, http://www.nrbsc.org/downloads/.

[23] *Molecular Diagnostic Methods for Infectious Diseases, Approved Guideline (CLSI MM3-A2)*, vol. 26, 2nd edition, 2006.

[24] R. Schuch and A. T. Maurelli, "Virulence plasmid instability in *Shigella flexneri* 2a is induced by virulence gene expression," *Infection and Immunity*, vol. 65, no. 9, pp. 3686–3692, 1997.

[25] K. R. S. Aranda, U. Fagundes-Neto, and I. C. A. Scaletsky, "Evaluation of multiplex PCRs for diagnosis of infection with diarrheagenic *Escherichia coli* and *Shigella* spp," *Journal of Clinical Microbiology*, vol. 42, no. 12, pp. 5849–5853, 2004.

[26] W. Luo, S. Wang, and X. Peng, "Identification of shiga toxin-producing bacteria by a new immuno-capture toxin gene PCR," *FEMS Microbiology Letters*, vol. 216, no. 1, pp. 39–42, 2002.

[27] V. D. Thiem, O. Sethabutr, L. von Seidlein et al., "Detection of *Shigella* by a PCR assay targeting the *ipaH* gene suggests increased prevalence of shigellosis in Nha Trang, Vietnam," *Journal of Clinical Microbiology*, vol. 42, no. 5, pp. 2031–2035, 2004.

[28] X. Peng, W. Luo, J. Zhang, S. Wang, and S. Lin, "Rapid detection of *Shigella* species in environmental sewage by an immunocapture PCR with universal primers," *Applied and Environmental Microbiology*, vol. 68, no. 5, pp. 2580–2583, 2002.

[29] J. Theron, D. Morar, M. Du Preez, V. S. Brözel, and S. N. Venter, "A sensitive seminested PCR method for the detection of *Shigella* in spiked environmental water samples," *Water Research*, vol. 35, no. 4, pp. 869–874, 2001.

[30] M. P. Jackson, "Detection of shiga toxin-producing *Shigella dysenteriae* type 1 and *Escherichia coli* by using polymerase chain reaction with incorporation of digoxigenin-11-dUTP," *Journal of Clinical Microbiology*, vol. 29, no. 9, pp. 1910–1914, 1991.

[31] C. I. B. Kingombe, M. L. Cerqueira-Campos, and J. M. Farber, "Molecular strategies for the detection, identification, and differentiation between enteroinvasive *Escherichia coli* and *Shigella* spp," *Journal of Food Protection*, vol. 68, no. 2, pp. 239–245, 2005.

[32] O. Sethabutr, M. Venkatesan, S. Yam et al., "Detection of PCR products of the ipaH gene from *Shigella* and enteroinvasive *Escherichia coli* by enzyme linked immunosorbent assay," *Diagnostic Microbiology and Infectious Disease*, vol. 37, no. 1, pp. 11–16, 2000.

[33] D. R. Call, "Challenges and opportunities for pathogen detection using DNA microarrays," *Critical Reviews in Microbiology*, vol. 31, no. 2, pp. 91–99, 2005.

[34] M. J. Farfán, T. A. Garay, C. A. Prado, I. Filliol, M. T. Ulloa, and C. S. Toro, "A new multiplex PCR for differential identification of *Shigella flexneri* and *Shigella sonnei* and detection of *Shigella* virulence determinants," *Epidemiology and Infection*, vol. 138, no. 4, pp. 525–533, 2010.

[35] O. G. Gómez-Duarte, J. Bai, and E. Newell, "Detection of *Escherichia coli*, *Salmonella* spp., *Shigella* spp., *Yersinia enterocolitica*, *Vibrio cholerae*, and *Campylobacter* spp. enteropathogens by 3-reaction multiplex polymerase chain reaction," *Diagnostic Microbiology and Infectious Disease*, vol. 63, no. 1, pp. 1–9, 2009.

[36] L. Rossen, P. Nørskov, K. Holmstrøm, and O. Rasmussen, "Inhibition of PCR by components of food samples, microbial diagnostic assays and DNA-extraction solutions," *International Journal of Food Microbiology*, vol. 17, no. 1, pp. 37–45, 1992.

[37] I. Wilson, "Inhibition and facilitation of nucleic acid amplification," *Applied and Environmental Microbiology*, vol. 63, no. 10, pp. 3741–3751, 1997.

[38] W. I. Taylor and D. Schelhart, "Effect of temperature on transport and plating media for enteric pathogens," *Journal of Clinical Microbiology*, vol. 2, no. 4, pp. 281–286, 1975.

[39] M. Yavzori, D. Cohen, R. Wasserlauf, R. Ambar, G. Rechavi, and S. Ashkenazi, "Identification of *Shigella* species in stool specimens by DNA amplification of different loci of the *Shigella* virulence plasmid," *European Journal of Clinical Microbiology and Infectious Diseases*, vol. 13, no. 3, pp. 232–237, 1994.

Hindawi Publishing Corporation
BioMed Research International
Volume 2013, Article ID 270457, 5 pages
http://dx.doi.org/10.1155/2013/270457

Research Article

Urine Cell-Free DNA Integrity as a Marker for Early Prostate Cancer Diagnosis: A Pilot Study

Valentina Casadio,[1] Daniele Calistri,[1] Samanta Salvi,[1] Roberta Gunelli,[2] Elisa Carretta,[1] Dino Amadori,[1] Rosella Silvestrini,[1] and Wainer Zoli[1]

[1] *IRCCS Istituto Scientifico Romagnolo per lo Studio e la Cura dei Tumori (IRCCS IRST), Via P. Maroncelli 40, 47014 Meldola, Italy*
[2] *Department of Urology, Morgagni Pierantoni Hospital, Via C. Forlanini 34, 47121 Forli, Italy*

Correspondence should be addressed to Valentina Casadio; v.casadio@irst.emr.it

Received 19 October 2012; Revised 8 January 2013; Accepted 9 January 2013

Academic Editor: Tavan Janvilisri

Circulating cell-free DNA has been recognized as an accurate marker for the diagnosis of prostate cancer, whereas the role of urine cell-free DNA (UCF DNA) has never been evaluated in this setting. It is known that normal apoptotic cells produce highly fragmented DNA while cancer cells release longer DNA. We thus verified the potential role of UCF DNA integrity for early prostate cancer diagnosis. UCF DNA was isolated from 29 prostate cancer patients and 25 healthy volunteers. Sequences longer than 250 bp (*c-Myc*, *BCAS1*, and *HER2*) were quantified by real-time PCR to verify UCF DNA integrity. Receiver operating characteristic (ROC) curve analysis revealed an area under the curve of 0.7959 (95% CI 0.6729–0.9188). At the best cut-off value of 0.04 ng/μL, UCF DNA integrity analysis showed a sensitivity of 0.79 (95% CI 0.62–0.90) and a specificity of 0.84 (95% CI 0.65–0.94). These preliminary findings indicate that UCF DNA integrity could be a promising noninvasive marker for the early diagnosis of prostate cancer and pave the way for further research into this area.

1. Introduction

Early diagnosis plays an important role in the treatability of patients with different tumor types in terms of disease-free and overall survival. Prostate cancer has a high incidence and represents the second cause of death from cancer in men after lung cancer. Early diagnosis is thus essential, especially in view of the slow natural history of the disease and its potential curability in the initial hormone-dependent phase. Noninvasive diagnostic procedures have a higher patient compliance and a lower cost than invasive screening programs. At present, the only noninvasive approach currently used for the diagnosis of prostate cancer is the determination of PSA (prostate-specific antigen) in blood, which has been shown to reduce prostate cancer mortality. However, the use of PSA has recently been questioned because of its low accuracy, especially in terms of specificity. False positive results lead to overtreatment in individuals, with consequently higher healthcare costs and psychological distress [1–5]. Although great efforts have been made to improve the diagnostic accuracy of PSA, the search continues for new molecular markers, proteins, or genetic and epigenetic alterations [6, 7] to be used in this setting.

New accurate and cost-effective diagnostic approaches are needed to enhance or replace standard techniques for prostate cancer diagnosis. Cell-free nucleic acids have proven useful for early cancer diagnosis and positive results have also been published on serum and plasma cell-free DNA and RNA as sources of tumor-specific markers [8, 9]. Circulating cell-free DNA has been shown to play an important diagnostic role in colon [10] and lung cancer [11], and a number of studies have also highlighted its potential usefulness in prostate cancer [12–14]. Urine cell-free (UCF) DNA as a source of tumor biomarkers has not been adequately investigated in prostate cancer and only a few recent studies have discussed its potential importance for early bladder cancer diagnosis [15–17].

It has been shown that DNA from normal apoptotic cells is highly fragmented, whereas DNA from necrotic cancer

Table 1: Case series.

	Number	Age (yrs)		Median PSA (range)	Gleason score		Pathological stage			
		<70	≥70		≤6	>6	pT2a	pT2b	pT3a	pT3c
Healthy individuals	25	15	10	—	—	—	—	—	—	—
Prostate cancer patients	29	20	9	7.5 (3.19–33)	12	17	2	14	10	3

cells maintains its integrity [18]. Taking this into account and also considering recent results on bladder cancer highlighting the importance of UCF DNA integrity for early diagnosis [15], we investigated the ability of this marker to distinguish between prostate cancer patients and healthy individuals by analyzing UCF-DNA fragments longer than 250 bp in 3 regions is known to be frequently amplified in solid tumors, including prostate cancer: *c-Myc* (8q24.21), *HER2* (17q12.1), and *BCAS1* (20q13.2) [19–21].

2. Materials and Methods

2.1. Case Series. This pilot study was composed of 54 individuals, 29 at first diagnosis of prostate cancer and 25 healthy individuals (control group) matched to patients for age. Subjects with previous or concomitant urogenital diseases or cancers were excluded from the study. Healthy individuals underwent transrectal ultrasound (TRUS) to exclude the presence of prostate cancer. Participants were recruited from the Department of Urology of Morgagni, Pierantoni Hospital (Forli) and all provided written informed consent to take part in the study, which was reviewed and approved by the local Ethics Committee. Median age was 65 years for patients and 66 for healthy individuals. All patients underwent radical prostatectomy. The Gleason score and pathological stage were evaluated after surgical removal of the tumor. Twelve patients had a Gleason score of ≤6 and 17 patients had a score of >6. Two patients had pT2a tumors, 14 pT2b, 10 pT3a, and 3 pT3c. The median PSA value was 7.5 (range 3.19–33) (Table 1).

2.2. Urine Collection. First-morning-void urine samples were collected for UCF DNA analysis. For prostate cancer patients, specimens were collected before radical prostatectomy. All patients and controls were instructed to give clean-catch urine samples, which were maintained at 4°C for a maximum of 3 hours. Thirty milliliter aliquots of urine were centrifuged at 850 g for 10 minutes and the supernatants were transferred to cryovials and immediately stored at −80°C until use.

2.3. UCF DNA Analysis. DNA was extracted and purified from 2 mL of supernatant by Qiamp DNA minikit (Qiagen, Milan, Italy) according to the manufacturer's instructions. At the same time, DNA was extracted from a human bladder cancer cell line (MCR) using the same minikit and quantified by spectrophotometry (NanoDrop ND-1000, Celbio, Milan, Italy).

Real-time PCR reactions were carried out by Rotor Gene 6000 detection system (Corbett Research, St. Neots, UK) using IQ SYBR green (Biorad, Milan, Italy). Sequences longer than 250 bp corresponding to 3 oncogenes were analyzed as follows: *c-Myc* (locus 8q24.21, amplification product 264 bp), *BCAS1* (locus 20q.13.2, amplification product 266 bp), and *HER2* (locus 17q12.1, amplification product 295 bp). A short 125 bp fragment of *STOX1* (locus 10q21.3) was analyzed to check for potential PCR inhibition. Primer sequences were as follows: *c-Myc* fw TGGAGTAGGGACCGCATATC, rev ACCCAACACCACGTCCTAAC; *BCAS1* fw GGGTCAGAG CTTCCTGTGAG, rev CGTTGTCCTGAAACAGAGCA; *HER2* fw CCAGGGTGTTCCTCAGTTGT, rev TCAGTA TGGCCTCACCCTTC; *STOX1* fw GAAAACAGGGCAGCA AGAAG, rev CAGACAGCATGGAGGTGAGA. PCR conditions for the oncogenes were as follows: 95°C for 3 minutes followed by 45 cycles at 94°C for 40 seconds, 56°C for 40 seconds, and 72°C for 1 minute. PCR conditions'for the short *STOX1* sequence were as follows: 95°C for 90 seconds followed by 45 cycles at 94°C for 40 seconds and 54°C for 1 minute. All real-time PCR reactions were performed in duplicate on 10 ng of each UCF DNA sample. Various amounts of DNA from the MCR cell line (0.01, 0.1, 1, 5, 10, and 20 ng) were also analyzed to construct a standard curve. The UCF DNA value for each sample was obtained by Rotor Gene 6000 detection system software using standard curve interpolation. The analysis was repeated if the difference between duplicate samples was greater than 1 cycle threshold. The final UCF DNA integrity value was obtained by summing the three oncogene values. Real-time experiments were performed independently in duplicate on the same 8 samples to test assay variability. The coefficients of variation (CV) were then calculated for *c-Myc*, *HER2*, *BCAS*, and *STOX1*. Real-time PCR analyses were performed in accordance with MIQE guidelines (remarks to the MIQE checklist are included as Supplementary Table 1 available online at http://dx.doi.org/10.1155/2013/270457) [22].

2.4. Statistical Analysis. The relationship between UCF DNA integrity values in the two subgroups was analyzed using a nonparametric ranking statistic test. The most discriminating cut-off values between healthy individuals and cancer patients were identified using receiver operating characteristic (ROC) curve analysis. True positive rates (sensitivity) were plotted against false positive rates (1-specificity) for all classification points. Accuracy was measured by the area under the ROC curve (AUC), which represents an average probability of correctly classifying a case chosen at random. Study endpoints were sensitivity (the proportion of cancer patients who were correctly identified by the test or procedures) and specificity (the proportion of healthy individuals who were correctly identified), with their 95% confidence intervals (CIs) [23]. P values < 0.05 were considered statistically significant. Statistical analyses were performed using SPSS statistical software (version 12.0, SPSS GmbH Software).

Table 2: UCF DNA integrity in healthy individuals and prostate cancer patients.

	Number	UCF DNA integrity (ng/μL) Median values (range)	Mean values (range)	P^*
Healthy individuals	25	0.007 (0–0.141)	0.023 (0–0.141)	0.0004
Prostate cancer patients	29	0.129 (0–5.379)	0.533 (0–5.379)	

*Wilcoxon-Mann-Whitney test.

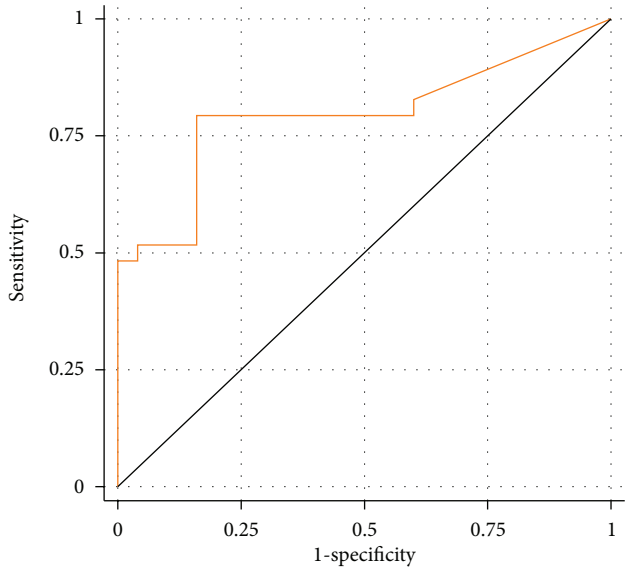

Figure 1: ROC curve of UCF DNA integrity.

3. Results

Total free DNA showed a median value of 6 ng/μL (range 2–36 ng/μL). There was no statistically significant difference between total urine cell free DNA in cancer patients and healthy individuals ($P = 0.1200$ Wilcoxon-Mann-Whitney test).

The ROC curve for total free DNA showed an AUC of 0.6262 (Supplementary Figure 1). UCF DNA integrity analysis was feasible and results were evaluable for all 54 individuals. The 125 bp *STOX1* sequence was amplified in all samples, thus excluding the presence of PCR inhibitors. Values showed a wide variability in both healthy individuals and cancer patients, with a partial overlapping. However, median values were significantly lower (about 20-fold, $P = 0.0004$) in healthy than in cancer patients (Table 2).

ROC curve analysis of UCF DNA integrity showed an AUC of 0.7959 (0.6729–0.9188) for healthy individuals and cancer patients (Figure 1). Detailed analysis of sensitivity and specificity highlighted a different accuracy for the various UCF DNA cut-off values, with a sensitivity of 0.79 for 0.03 and 0.04 cutoffs which decreased at the highest cut-off values and a specificity of 0.84 which remained consistent for all cutoffs from 0.03 to 0.06 (Table 3).

Table 3: Sensitivity and specificity of different UCF DNA integrity cut-off values.

Cutoff (ng/μL)	Sensitivity	Specificity
0.03		
n	23/29	21/25
Rate (95% CI)	0.79 (0.62–0.90)	0.84 (0.65–0.94)
0.04		
n	23/29	21/25
Rate (95% CI)	0.79 (0.62–0.90)	0.84 (0.65–0.94)
0.05		
n	19/29	21/25
Rate (95% CI)	0.66 (0.47–0.80)	0.84 (0.65–0.94)
0.06		
n	17/29	21/25
Rate (95% CI)	0.59 (0.41–0.74)	0.84 (0.65–0.94)

Table 4: Area under ROC curve for each single gene and for UCF DNA integrity.

	AUC (95% CI)	P^*
c-Myc	0.7862 (0.6595–0.9129)	NS**
BCAS1	0.7076 (0.5771–0.8381)	
HER2	0.7779 (0.6625–0.8934)	
UCF DNA integrity	0.7959 (0.6729–0.9188)	

*Chi-square test.
**NS: not significant.

UCF DNA integrity did not significantly vary between younger (<70 years) and older individuals (data not shown). The analysis of UCF DNA as a function of tumor characteristics did not highlight any significant differences between patients with a Gleason score of ≤6 and those with a score of >6 or between pT2 and pT3 patients (data not shown).

The median PSA value in the patients analyzed was 7.5. Sixteen patients had a PSA value between 4 and 10, considered as a "gray zone," and 12 of these had a positive UCF DNA result, with a sensitivity of 0.75 (data not shown). We also performed ROC curve analysis for each gene in order to verify the role of single genes in determining test accuracy; AUC values were as follows: 0.7862 for *c-MYC* (95% CI: 0.6595–0.9129) 0.7779 for *HER2* (95% CI: 0.6625–0.8934) and 0.7076 for BCAS (95% CI: 0.5771–0.8381) (Table 4). However, the AUC values observed for the different genes were not statistically different (chi-square test).

4. Discussion

In recent years increasing efforts have been made to identify new diagnostic markers and to develop noninvasive diagnostic approaches that can be used additionally or as an alternative to common invasive tests to increase diagnostic accuracy for solid tumors. Important results have been obtained for lung [11] and colon cancer [10]. In a urological

setting, studies performed to improve the early noninvasive diagnosis of prostate cancer have highlighted the usefulness of specific DNA alterations (methylation or mutations) in blood to identify cancer patients [12, 24, 25], but the potential of cell-free DNA in urine has been never investigated.

Starting from recent results on the diagnostic relevance of urine cell free DNA for bladder cancer [15–17], we extended the research to prostate cancer, hypothesizing that long DNA in urine may have two different origins: necrotic bladder cancer cells [15] or necrotic prostate cancer cells. We excluded that DNA fragments passing through the glomerular filtration barrier could influence our analysis because these fragments are short, as demonstrated by SU and coworkers [26]. Our results also showed that urine DNA integrity is capable of distinguishing between prostate cancer patients and healthy individuals with an accuracy of about 80%, similar to that observed for bladder cancer. Such findings are seemingly in contrast to those of Ellinger and coworkers who found a positive correlation between prostate cancer and the presence of short DNA fragments in blood [25]. The difference between cell free DNA in urine or blood remains unclear and should be investigated by comparing DNA integrity determined in blood and urine samples from the same patients.

We also analyzed the diagnostic accuracy of DNA integrity of three oncogenes (*c-MYC*, *HER2*, and *BCAS1*) which are known to be involved in the development of bladder cancer. A comparison of ROC curves revealed that *c-MYC* had the highest AUC, a finding supported by evidence that *c-MYC* is involved in prostate tumorigenesis [27]. Furthermore, literature data on CGH array and copy number alterations highlight a high frequency of gain at 8q24 region where the *c-MYC* oncogene maps [19, 28–30], which could explain the higher number of copies of long *c-MYC* fragments in urine samples from prostate cancer patients than in those from healthy individuals. Lower diagnostic accuracy was observed for *HER2* and decreased further for *BCAS1*, but the AUC values observed for the different genes were not significantly different.

The main limitation of this potentially important diagnostic finding is that it was obtained from a pilot study on a relatively small number of individuals. However, our results are being validated in a large confirmatory study ongoing at our institute. The advantage of the proposed approach is that cell free DNA, as previously shown [15], can be easily detected in a very small amount of urine. Moreover, unlike protein or RNA, it has good stability and is an inexpensive noninvasive method whose results are obtainable in about two working days. In the future it could be used as a test on its own or, thanks to its high specificity, could help to unmask cases of false positive PSA, especially in the subgroup of individuals with *grey zone* PSA values, thus reducing the number of unnecessary invasive diagnostic tests (e.g., prostate biopsy) carried out.

5. Conclusions

The results obtained in the present work indicate that urine cell-free DNA integrity is a potentially good marker for the early diagnosis of noninvasive prostate cancers, with an overall diagnostic accuracy of about 80%. This preliminary finding paves the way for confirmatory studies on larger case series.

Conflict of Interests

The authors have no conflict of interests to declare.

Acknowledgment

The authors thank Grainne Tierney for editing the paper.

References

[1] S. A. Strope and G. L. Andriole, "Prostate cancer screening: current status and future perspectives," *Nature Reviews Urology*, vol. 7, no. 9, pp. 487–493, 2010.

[2] F. H. Schröder, J. Hugosson, M. J. Roobol et al., "Prostate-cancer mortality at 11 years of follow-up," *New England Journal of Medicine*, vol. 366, no. 11, pp. 981–990, 2012.

[3] F. H. Schröder, J. Hugosson, T. L. J. Tammela et al., "ERSPC Screening and prostate-cancer mortality in a randomized European study," *New England Journal of Medicine*, vol. 360, no. 13, pp. 1320–1328, 2009.

[4] E. A. M. Heijnsdijk, A. Der Kinderen, E. M. Wever, G. Draisma, M. J. Roobol, and H. J. De Koning, "Overdetection, overtreatment and costs in prostate-specific antigen screening for prostate cancer," *British Journal of Cancer*, vol. 101, no. 11, pp. 1833–1838, 2009.

[5] O. W. Brawley, D. P. Ankerst, and I. M. Thompson, "Screening for prostate cancer," *CA Cancer Journal for Clinicians*, vol. 59, no. 4, pp. 264–273, 2009.

[6] J. Groskopf, S. M. J. Aubin, I. L. Deras et al., "APTIMA PCA3 molecular urine test: development of a method to aid in the diagnosis of prostate cancer," *Clinical Chemistry*, vol. 52, no. 6, pp. 1089–1095, 2006.

[7] T. Wu, E. Giovannucci, J. Welge, P. Mallick, W. Y. Tang, and S. M. Ho, "Measurement of GSTP1 promoter methylation in body fluids may complement PSA screening: a meta-analysis," *British Journal of Cancer*, vol. 105, no. 1, pp. 65–73, 2011.

[8] H. Schwarzenbach, D. S. B. Hoon, and K. Pantel, "Cell-free nucleic acids as biomarkers in cancer patients," *Nature Reviews Cancer*, vol. 11, no. 6, pp. 426–437, 2011.

[9] K. Jung, M. Fleischhacker, and A. Rabien, "Cell-free DNA in the blood as a solid tumor biomarker-A critical appraisal of the literature," *Clinica Chimica Acta*, vol. 411, no. 21-22, pp. 1611–1624, 2010.

[10] R. Mead, M. Duku, P. Bhandari, and I. A. Cree, "Circulating tumour markers can define patients with normal colons, benign polyps, and cancers," *British Journal of Cancer*, vol. 105, no. 2, pp. 239–245, 2011.

[11] P. Ulivi, L. Mercatali, W. Zoli et al., "Serum free DNA and COX-2 mRNA expression in peripheral blood for lung cancer detection," *Thorax*, vol. 63, no. 9, pp. 843–844, 2008.

[12] J. Ellinger, D. C. Müller, S. C. Müller et al., "Circulating mitochondrial DNA in serum: a universal diagnostic biomarker for patients with urological malignancies," *Urologic Oncology*, vol. 30, no. 4, pp. 509–515, 2012.

[13] E. Gordian, K. Ramachandran, I. M. Reis, M. Manoharan, M. S. Soloway, and R. Singal, "Serum free circulating DNA is a useful

biomarker to distinguish benign versus malignant prostate disease," *Cancer Epidemiology Biomarkers and Prevention*, vol. 19, no. 8, pp. 1984–1991, 2010.

[14] H. Schwarzenbach, C. Alix-Panabières, I. Müller, N. Letang, J.-P. Vendrell, and X. Rebillard, "Cell-free tumor DNA in blood plasma as a marker for circulating tumor cells in prostate cancer," *Clinical Cancer Research*, vol. 15, no. 3, pp. 1032–1038, 2009.

[15] V. Casadio, D. Calistri, M. Tebaldi et al., "Urine Cell-Free DNA integrity as a marker for early bladder cancer diagnosis: preliminary data," *Urologic Oncology*, 2012.

[16] M. Zancan, F. Galdi, F. Di Tonno et al., "Evaluation of cell-free DNA in urine as a marker for bladder cancer diagnosis," *International Journal of Biological Markers*, vol. 24, no. 3, pp. 147–155, 2009.

[17] T. Szarvas, I. Kovalszky, K. Bedi et al., "Deletion analysis of tumor and urinary DNA to detect bladder cancer: urine supernatant versus urine sediment," *Oncology Reports*, vol. 18, no. 2, pp. 405–409, 2007.

[18] S. Jahr, H. Hentze, S. Englisch et al., "DNA fragments in the blood plasma of cancer patients: quantitations and evidence for their origin from apoptotic and necrotic cells," *Cancer Research*, vol. 61, no. 4, pp. 1659–1665, 2001.

[19] A. S. Ishkanian, C. A. Mallof, J. Ho et al., "High-resolution array CGH identifies novel regions of genomic alteration in intermediate-risk prostate cancer," *Prostate*, vol. 69, no. 10, pp. 1091–1100, 2009.

[20] J. D. Oxley, M. H. Winkler, D. A. Gillatt, and D. S. Peat, "Her-2/neu oncogene amplification in clinically localised prostate cancer," *Journal of Clinical Pathology*, vol. 55, no. 2, pp. 118–120, 2002.

[21] Y. Tabach, I. K. Sakin, Y. Buganim et al., "Amplification of the 20q chromosomal arm occurs early in tumorigenic transformation and may initiate cancer," *PLoS ONE*, vol. 6, no. 1, Article ID e14632, 2011.

[22] S. A. Bustin, V. Benes, J. A. Garson et al., "The MIQE guidelines: minimum information for publication of quantitative real-time PCR experiments," *Clinical Chemistry*, vol. 55, no. 4, pp. 611–622, 2009.

[23] P. M. Bossuyt, J. B. Reitsma, D. E. Bruns et al., "Towards complete and accurate reporting of studies of diagnostic accuracy: the STARD initiative," *Clinical Chemistry*, vol. 49, no. 1, pp. 1–6, 2003.

[24] A. Altimari, A. D. Grigioni, E. Benedettini et al., "Diagnostic role of circulating free plasma DNA detection in patients with localized prostate cancer," *American Journal of Clinical Pathology*, vol. 129, no. 5, pp. 756–762, 2008.

[25] J. Ellinger, P. J. Bastian, K. I. Haan et al., "Noncancerous PTGS2 DNA fragments of apoptotic origin in sera of prostate cancer patients qualify as diagnostic and prognostic indicators," *International Journal of Cancer*, vol. 122, no. 1, pp. 138–143, 2008.

[26] Y. H. Su, M. Wang, D. E. Brenner et al., "Human urine contains small, 150 to 250 nucleotide-sized, soluble DNA derived from the circulation and may be used in the detection of colorectal cancer," *Journal of Molecular Diagnostics*, vol. 6, no. 2, pp. 101–107, 2004.

[27] M. Yeager, N. Chatterjee, J. Ciampa et al., "Identification of a new prostate cancer susceptibility locus on chromosome 8q24," *Nature Genetics*, vol. 41, no. 10, pp. 1055–1057, 2009.

[28] J. Sun, W. Liu, T. S. Adams et al., "DNA copy number alterations in prostate cancers: a combined analysis of published CGH studies," *Prostate*, vol. 67, no. 7, pp. 692–700, 2007.

[29] W. Liu, C. C. Xie, Y. Zhu et al., "Homozygous deletions and recurrent amplications implicate new genes involved in prostate cancer," *Neoplasia*, vol. 10, no. 8, pp. 897–907, 2008.

[30] M. van Duin, R. van Marion, K. Vissers et al., "High-resolution array comparative genomic hybridization of chromosome arm 8q: evaluation of genetic progression markers for prostate cancer," *Genes Chromosomes and Cancer*, vol. 44, no. 4, pp. 438–449, 2005.

Hindawi Publishing Corporation
BioMed Research International
Volume 2013, Article ID 834790, 9 pages
http://dx.doi.org/10.1155/2013/834790

Research Article

Development of a Novel System for Mass Spectrometric Analysis of Cancer-Associated Fucosylation in Plasma α_1-Acid Glycoprotein

Takayuki Asao,[1] Shin Yazawa,[1,2] Toyo Nishimura,[2] Takashi Hayashi,[3] Hideyuki Shimaoka,[4] Abby R. Saniabadi,[5] and Hiroyuki Kuwano[1]

[1] *Department of General Surgical Science, Gunma University Graduate School of Medicine, Maebashi 371-8511, Japan*
[2] *Tokushima Research Institute, Otsuka Pharmaceutical Co., Ltd., Tokushima 771-0192, Japan*
[3] *Institute of Biomedical Innovation, Otsuka Pharmaceutical Co., Ltd., Tokushima 771-0192, Japan*
[4] *S-BIO Business Division, Sumitomo Bakelite Co., Ltd., Tokyo 140-0002, Japan*
[5] *JIMRO Co., Ltd., Tokyo 151-0063, Japan*

Correspondence should be addressed to Shin Yazawa; syazawa@titan.ocn.ne.jp

Received 3 November 2012; Accepted 13 December 2012

Academic Editor: Tavan Janvilisri

Human plasma α_1-acid glycoprotein (AGP) from cancer patients and healthy volunteers was purified by sequential application of ion-exchange columns, and N-linked glycans enzymatically released from AGP were labeled and applied to a mass spectrometer. Additionally, a novel software system for use in combination with a mass spectrometer to determine N-linked glycans in AGP was developed. A database with 607 glycans including 453 different glycan structures that were theoretically predicted to be present in AGP was prepared for designing the software called AGPAS. This AGPAS was applied to determine relative abundance of each glycan in the AGP molecules based on mass spectra. It was found that the relative abundance of fucosylated glycans in tri- and tetra-antennary structures (FUCAGP) was significantly higher in cancer patients as compared with the healthy group ($P < 0.001$). Furthermore, extremely elevated levels of FUCAGP were found specifically in patients with a poor prognosis but not in patients with a good prognosis. In conclusion, the present software system allowed rapid determination of the primary structures of AGP glycans. The fucosylated glycans as novel tumor markers have clinical relevance in the diagnosis and assessment of cancer progression as well as patient prognosis.

1. Introduction

The two main classes of glycosidic linkages to proteins involve either N-glycans or O-glycans through asparagine or serine and threonine, respectively. The N-linked glycans attached to the protein contain a trimannosyl pentasaccharide, Manα1,6[Manα1,3]Manβ1,4GlcNAcβ1,4GlcNAc ($[\text{Man}]_3[\text{GlcNAc}]_2$) as the common core structure, and are classified into three main groups, high mannose, complex and hybrid types [1]. The complex-type glycans have no mannose residues other than those in the common core structure but have antennae or branches with N-acetyllactosamine residues at the reducing termini attached to the common core structure.

α_1-Acid glycoprotein (AGP, orosomucoid) possessing the complex type glycans is the major plasma glycoprotein with a molecular weight of 41–43 kDa. Further, this glycoprotein has highly branched N-linked glycans, bi-, tri-, and tetra-antennary glycans including elongated tetra-antennary glycans with repeating lactosamine structures having (sialyl) Le^X determinant, (NeuAcα2,3)Galβ1,4[Fucα1,3]GlcNAcβ [2].

Recently, we reported on AGP glycoforms in plasma samples from cancer patients with malignancies that differed in the degree of branching and the extent of fucosylation as determined by crossed affinoimmunoelectrophoresis (CAIE) with Con A lectin and *Aleuria aurantia* lectin (AAL) and

anti-AGP antibody [3]. Accordingly, patients with advanced malignancies who had AGP glycoforms containing highly fucosylated branched glycans for long periods after surgery were found to have a poor prognosis, while patients without such glycoforms were expected to have a good prognosis irrespective of their clinical stages.

However, in the past, the purification of AGP has commonly involved chromatography on metal chelate affinity gel and anti-AGP immobilized affinity gel, ion-exchange chromatography, CAIE with Con A lectin, hot phenol extraction, and sulphosalicylic acid precipitation [4–8]. Further, more recently, purification and characterization of glycans on AGP have been done with the aid of capillary electrophoresis [9, 10], but most of these methods are unsuitable for processing a large number of plasma samples in a short period of time. The CAIE method we recently introduced can process plasma samples without purification for investigating glycoforms because AGP can be identified by means of an anti-AGP antibody but still is not applicable to large numbers of samples if rapid processing is required [3]. This experience also indicated that better data on disease progression and outcome of postoperative patients with malignancies could be obtained from changes of plasma AGP glycoforms than from changes in the level of plasma AGP. Hence investigation of glycan structures associated with these changes became a major focus of interest and inspired us to develop an automated method for rapid processing of a large number of test samples.

With the above background in mind, in this study, we developed a simple method for the purification of plasma AGP and obtained N-linked glycans labeled with a highly sensitive agent for mass spectrometry [11–13] after digestion of AGP with trypsin and PNGase F. There are several methods available for determining glycan structures of AGP based on spectra from mass spectrometry [14]. However, most of these seem to be difficult for carrying out comprehensive analysis of glycan structures without some knowledge of the intrinsic structures in the individual glycoconjugates. The main interest in this study was the glycosylation process of AGP glycans because there is a need for adequate knowledge on the glycans that are expected to be present in plasma AGP [3]. Therefore, first, we developed a simple method to purify plasma AGP and then analyzed N-glycans by means of mass spectrometry together with constructing operation software (AGPAS) to assist analysis of glycans in AGP. At the same time, we evaluated AGPAS by investigating glycan structures and their relative abundance in plasma AGP from cancer patients whose glycoforms had been identified previously [3].

Since it was clearly demonstrated in our previous study that no obvious difference between patients with respect to AGP levels in plasma samples and their clinicopathologic background after surgery, it must be postulated with high probability that changes in glycosylation of the AGP molecule after surgery could indeed be used as a novel parameter for monitoring and predicting the fate of tumor-bearing patients.

2. Materials and Methods

2.1. Materials. DEAE Sepharose Fast Flow, SP Sepharose Fast Flow, HiTrap Desalting, HiTrap DEAE FF, and HiTrap SP FF were obtained from GE Healthcare (Amersham Place, UK). PNGase F was from Roche Applied Science (Indianapolis, USA). Anti-human AGP rabbit serum was obtained from DAKO (Carpinteria, CA, USA) and peroxidase-conjugated anti-human AGP was from Abcam (Cambridge, UK). Human AGP was purchased from SIGMA (St. Louis, MO, USA). Trypsin, DTT, 2,5-dihydroxybenzoic acid, and other reagents were obtained from Wako Pure Chemicals Co. (Tokyo, Japan). BlotGlyco was from Sumitomo Bakelite Co. (Tokyo, Japan). Blood samples were obtained from patients with various types of malignancies who were admitted to the Gunma University Hospital (Maebashi, Japan) along with the guideline for informed consent and approval from the Ethics Committee of Gunma University. Details of clinicopathological features of the patients for follow-up studies were described previously [3]. Blood samples were also obtained from randomly selected volunteers as a healthy control group. Each plasma sample was stored at −80°C until use. Protein was determined with a DC protein assay kit (Bio-Rad, Richmond, CA, USA) using bovine serum albumin as a standard. SDS-polyacrylamide gel electrophoresis was carried out using a 10/20 gradient gel (MultiGel II Mini, Cosmo Bio Co. Ltd., Tokyo, Japan). After electrophoresis, the gel was transferred to an Immobilon PVDF membrane (Millipore, Bedford, MA, USA) in a Trans-Blot SD cell (Bio-Rad). The membrane was stained with Coomassie Brilliant Blue for detecting protein bands. For detecting AGP molecule, the membrane was blocked with PBS containing 5% skim milk and then the membrane was incubated with peroxidase-conjugated anti-human AGP and stained with the VECTASTAIN ABC kit (Vector Laboratories, Inc., Burlingame, CA, USA) according to the manufacturer's instruction.

2.2. Preparation and Purification of N-Glycans from Purified Plasma AGP. N-Glycans released from purified AGP preparation were labeled according to the protocol of the glycosylation kit (BlotGlyco) with a slight modification. A lyophilized AGP preparation purified from 500 μL of human plasma was dissolved in 50 μL of H_2O, 25 μL of the solution (20–200 μg AGP) was mixed with 2.5 μL of 1 M ammonium bicarbonate, 2.5 μL of 120 mM DTT, and 25 μL of sample to be analyzed, and the mixture was incubated at 60°C for 30 min. Then 5 μL of 123 mM of iodoacetamide was added and the mixture was allowed to stand under dark at room temperature for 1 h followed by addition of 5 μL of 400 units of trypsin and incubation at 37°C for 1 h. After heating at 90°C for 5 min, 27 units of PNGase F was added and the mixture was incubated overnight at 37°C. After heating at 90°C for 5 min, 20 μL of the mixture was used for the following labeling step. The mixture containing N-glycans released enzymatically from AGP was treated with BlotGlyco kit to prepare methyl esterified and aoWR-labeled N-glycans according to the manufacturer's instruction and labeled glycans were obtained as a 50 μL of the solution.

2.3. Sandwich-Type ELISA of Plasma AGP. The AGP levels were measured by a sandwich-type ELISA using anti-human AGP and horseradish peroxidase-conjugated anti-human AGP as described previously [3].

2.4. Mass Spectrometric Analysis. One μL of the sample solution was mixed with 1 μL of 2,5-dihydroxybenzoic acid (10 mg in acetonitrile/water, 1 : 1, v/v) and an aliquot was deposited on a MALDI target plate and allowed to dry. Mass spectrometric data were obtained using an AB Sciex MALDI TOF/TOF TM 5800 System (Applied Biosystems, Inc., Foster City, CA, USA). All spectra in the mass range of m/z 1,000 to 4,550 were obtained using a positive reflectron mode. Deisotopic masses for each peak were picked by Data Explorer software (Applied Biosystems) and exported as a mass peak list with each value of both the centroid mass and the corresponding area to the operation software, AGPAS described below.

3. Results and Discussion

3.1. Purification of Plasma AGP. Pooled human plasma (50 mL) was dialyzed against 0.02 M of citrate-phosphate buffer (pH 4.0) overnight at 4°C. After centrifugation of the dialyzed plasma at 10,000 rpm for 20 min at 4°C, the supernatant was applied to a 10 × 50 cm of DEAE-Sepharose FF column equilibrated with 0.02 M of citrate-phosphate buffer (pH 4.0) and the column was washed with the same buffer until absorbance of the eluate reached the baseline level. Then the column was washed with 0.02 M citrate-phosphate buffer (pH 7.0) containing NaCl at concentration of 0.2 M and 0.5 M, respectively. The concentrations of AGP in each fraction were monitored by means of a sandwich-ELISA method. Fractions containing AGP were eluted from the column when the column was washed with 0.02 M citrate-phosphate buffer (pH 7.0) containing 0.2 M NaCl (Figure 1(a)). All fractions containing AGP were pooled and dialyzed against 0.02 M of citrate-phosphate buffer (pH 4.0) overnight at 4°C. The dialyzed, pooled fractions were then applied to an SP-Sepharose FF column (2 × 20 cm) equilibrated with 0.02 M citrate-phosphate buffer (pH 4.0). AGP bound to the column was eluted when the column was washed with 0.02 M of citrate-phosphate buffer (pH 4.8, Figure 1(b)). This purification procedure yielded a preparation that showed a single protein band with an approximate 47 KDa on an SDS-PAGE (Figure 1(c), lane 3) and reacted with anti-human AGP antibody (Figure 1(c), lane 4). The procedure allowed over 1,000 purification fold of AGP.

For the purification of AGP in small amounts from a large number of samples, the aforementioned purification procedure was slightly modified with a sequential use of two different ion-exchange and desalting cartridge columns. A 0.5 mL sample was applied to a HiTrap Desalting, equilibrated with 0.02 M citrate-phosphate buffer (pH 4.0), and fractions at the first peak were then applied to a HiTrap DEAE FF. Fractions containing AGP were eluted with the same buffer containing 0.2 M NaCl as described above and pooled fractions were passed through two joined HiTrap Desalting columns. The eluate containing AGP was then applied to a HiTrap SP FF and AGP was eluted in the same manner as described above. The eluted fractions were lyophilized and purified AGP was then dissolved in distilled water and used for the preparation of labeled N-glycans followed by mass spectrometric analyses described above. In order to ensure a full dose of released N-glycans from AGP, levels of AGP in the purified preparations from a large number of samples were measured in advance by means of ELISA using anti-AGP antibody [3]. All the preparations for labeling and MS analysis were shown to contain adequate amounts of glycans and their labeled ones, respectively (data not shown) indicating that less than 1 μL of the labeled preparations allowed to analyze most of the N-glycans expressed on the AGP molecule irrespective of their preparations both from healthy controls and patients with cancer as described below.

The present method allowed purification of plasma AGP, and by using cartridge columns, the entire process was completed within an hour. AGP was obtained at the same purity as mentioned above. With the aid of an anti-AGP antibody-immobilized column, AGP at almost the same purity could be obtained, but it was found that some of the AGP with hypersialylated glycans were hard to react with anti-AGP antibody, passing through the column during the purification process (S. Yazawa, unpublished observations).

3.2. Operation Software, AGPAS. The obtained mass spectrometric data were processed by using the assisting software we called AGPAS not only to determine N-linked glycan structures of plasma AGP automatically from the corresponding centroid masses, but also to calculate the relative abundance of individual glycans from the corresponding area relative to the total hit area. For a mass spectrometric analysis, every sample was digested with trypsin and PNGase F and then the resulting N-glycans were labeled by means of BlotGlyco. After labeling with the aoWR reagent, an exact ms of each glycan was changed as follows: MW of a labeled glycan = [an exact ms] – [H_2O(18.0105)] + [aoWR(447.223)] + [CH_3(14.0156) × n] + [H(1.0078)], where n indicates the number of N-acetylneuraminic acid residues.

To determine the primary structures of N-glycans in AGP, the GlycoMod Tool in the ExPASY (http://web.expasy.org/glycomod/) was available, but it was not always convenient or easy to obtaine suitable results. Therefore, a database for constructing the operation software, AGPAS, was established to facilitate selection of N-glycans present in the AGP molecule with the following steps.

Step 1. Extract N-glycans from the GlycoMod Tool available through the ExPASy. N-Glycans having glycoform masses from 1,000 to 4,550 monoisotopic values were extracted by using the GlycoMod Tool and 4,193 glycans were selected in total.

Step 2. Select N-glycans of AGP. Every conceivable glycan theoretically expressed on the AGP molecule was selected based on the background knowledge. The corresponding glycans were classified as bi-, tri-, and tetra-antennary structures extending from the common core trimannosyl pentasaccharide structure attached to the protein core. These glycans are reported to consist of galactose (Gal), *N*-acetylglucosamine (GlcNAc), fucose (Fuc), and N-acetylneuraminic acid (NeuAc) residues as for [Hexose], [HexNAc], [Deoxyhexose], and [NeuAc] expressed in the GlycoMod Tool, respectively, in the case specialized for AGP glycan structures [3]. For

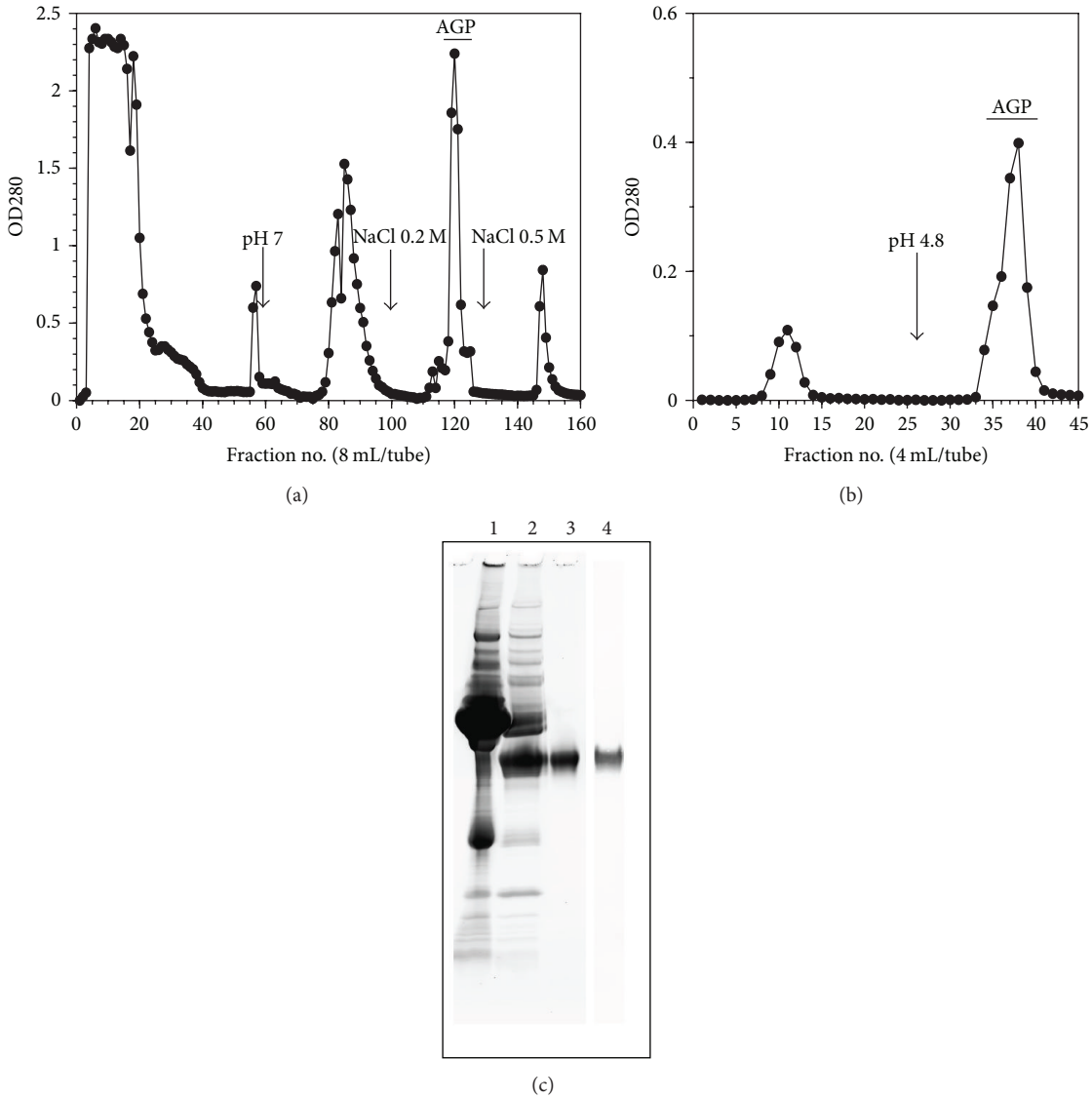

Figure 1: Purification of plasma AGP from pooled human plasma. (a) Ion-exchange chromatography of human plasma on a DEAE-Sepharose FF column (10 × 50 cm) equilibrated with 0.02 M citrate phosphate buffer, pH 4.0. Fifty mL of the dialyzed plasma sample was applied to the column. Fractions were assayed for protein (•) and AGP concentrations. AGP appeared only in the fractions eluted with 0.02 M citrate-phosphate buffer, pH 7.0 containing 0.2 M NaCl (—). (b) Ion-exchange chromatography of the eluate from DEAE-Sepharose FF column on an SP-Sepharose FF column (2 × 20 cm) equilibrated with 0.02 M citrate-phosphate buffer, pH 4.0. Ten mL of the pooled and dialyzed samples were applied to the column. Fractions were assayed for protein (•) and AGP concentration. AGP appeared in the eluate of citrate-phosphate buffer at pH 4.8 (—). (c) 10/20 SDS-polyacrylamide gel electrophoresis of purified AGP preparations. Lane 1: pooled plasma sample; lane 2: DEAE-Sepharose FF eluted fractions (0.2 M NaCl, pH 7.0); lanes 3, 4: DEAE- (0.2 M NaCl, pH 7.0) and SP- (pH 4.8) Sepharose FF eluted fractions. After electrophoresis, the gel was blotting on the membrane and each lane on the membrane was stained with Coomassie Brilliant Blue (lanes 1–3) and anti-human AGP antibody (lane 4). See the details in the Text.

setting a database factoring all the N-glycans expected to be present in an AGP molecule, each glycan except the common core structure was identified by using four-digit (FD) numbers indicating the number of each residue in order of Gal, GlcNAc, Fuc, and NeuAc such as FD number *abcd* for the glycan, $[\mathrm{Gal}]_a[\mathrm{GlcNAc}]_b[\mathrm{Fuc}]_c[\mathrm{NeuAc}]_d + [\mathrm{Man}]_3[\mathrm{GlcNAc}]_2$. In addition, among the number of these residues, five conditional equations essential for proceeding glycosylation of AGP glycans were proposed as follows: $a \leq b$, $2 \leq b \leq 7$, $c \leq b - 1$, $d \leq 4$, and $a \geq d$ in $[\mathrm{Gal}]_a$ $[\mathrm{GlcNAc}]_b$ $[\mathrm{Fuc}]_c$ $[\mathrm{NeuAc}]_d$ (FD number *abcd*). After N-glycans corresponding to these equations were selected, the FD numbers for these N-glycans were assigned individually with their corrected MW values using software from the Visual Basic Editor in Excel (Microsoft, ver.2010, Redmond, WA, USA). Since fucosylated AGP contained only α-1,3-fucosylated linkages attached to GlcNAc in the tri- and tetra-antennary glycan structures [2, 3], no α-1,3- or α-1,6-fucosylated bi-antennary structures, nor α-1,6-fucosylated tri- or tetra-antennary structures should be present in AGP. It

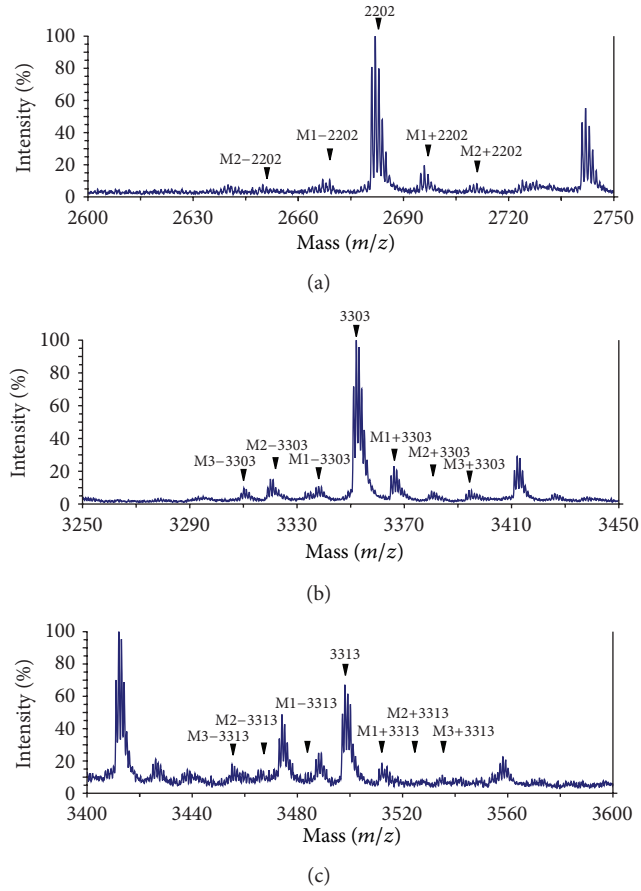

Figure 2: Mass spectra of methylated forms of AGP glycans derived from methyl esterification of sialylated glycans during the labeling process. Several de- (M−) and over- (M+) methylated glycans were detected around the exact labeled glycans. Purified AGP was prepared and labeled from 500 μL of plasma sample and an aliquot (ca. one-fiftieth) was used for MS analysis. See the details in the text.

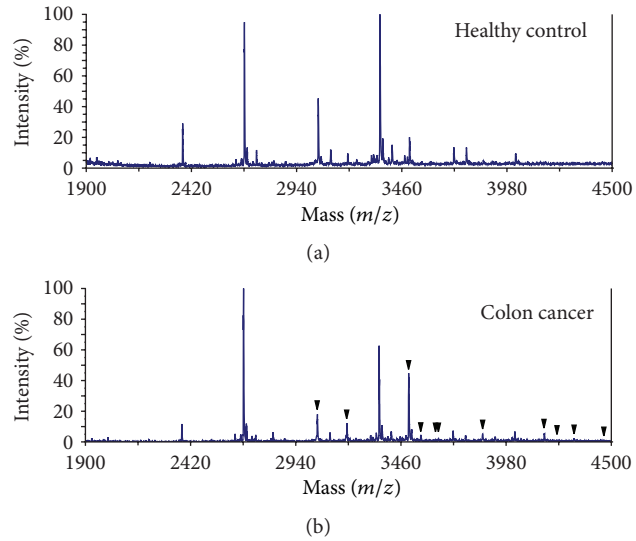

Figure 3: Mass spectra of AGP glycans isolated from a healthy control and a patient with colon cancer. Black triangles indicate fucosylated tri- and tetra-antennary glycans assigned. Purified AGP was prepared and labeled from 500 μL of plasma samples and an each aliquot (ca. one-fiftieth) was used for MS analysis.

is likely that aberrant α-1,3-fucosylated biantennary glycans, and glycans having FD numbers *X21X* ($X \leq 2$) existed but were not omitted from the database. Then, 453 glycans in total were selected.

Step 3. Determine the major sialylated AGP glycans. From the results of mass spectrometric analysis of randomly selected 100 samples, forty-five glycans for which the relative abundance was more than 0.1% and the number of Gal residues was more than one for sialylation were selected from N-glycans of AGP described in Step 2 as the major sialylated AGP glycans.

Step 4. Create methylated glycans. During mass spectrometric analysis, a series of unidentified spectra corresponding to a group of unknown masses before and after the exact MW of sialylated glycans at $\pm 14.0156 \times n$ m/z intervals (n = numbers of [NeuAc] residues) were observed (Figure 2). These were thought to represent methylated glycans formed from methyl esterification of the sialic acid residues attached to glycans through the labeling process undertaken in this study. Therefore, as additional glycans in the database, methylated glycans of which the numbers were theoretically calculated as lower and higher than those of [NeuAc] residues in the aforementioned major glycans with [NeuAc] residues (45 species from Step 3) were added to the database (154 glycans in total). Further, to simplify identification of these methylated glycan structures, the letter M was added to the original four-digit numbers. Therefore, methylated subpeaks such as M1−2202 indicating FD number 2202 structure with one deficient methyl residue and M4+4424 indicating FD number 4424 structure with four excess methyl residues were predicted to be present.

Step 5. Sum up N-glycans in the database of AGPAS. From original (452 glycans from Step 2) and additional (154 glycans, Step 4) AGP N-glycans, the numbers of glycans in the database of AGPAS approached 607 in total. Relative abundance of methylated glycans was added to the original glycans in case of making summary counts of relative abundance of individual AGP glycans. Individual centroid masses were automatically corrected based on their exact masses by using the aforementioned equation. Each corresponding area was transferred to the AGPAS for assigning labeled glycans and calculating their relative abundance. Data were then processed to identify FD numbers of glycans and to calculate their relative abundance, individually, and then a table indicating the relative abundance of bi-, tri-, and tetra-antennary glycans together with their respective fucosylated forms appeared. More than 100 peaks hit the glycans present in the database and the relative abundance of glycans totally hit was 54.63 ± 15.82% (n = 102).

Table 1: Relative abundances of N-glycans with bi-, tri-, and tetra-antennary chains and their fucosylated ones in plasma AGP from healthy controls and colorectal cancer patients.

Glycan structure	Numbers of [GlcNAc]	Numbers of [Fuc]	Relative abundance (%)# Normal (n = 35)	Relative abundance (%)# Cancer (n = 67)	P value
Bi-antennary	2	0	36.12 ± 15.52	42.07 ± 14.03	n.s.
Tri-antennary	3	0–2	47.10 ± 12.69	42.54 ± 13.03	n.s.
	3	0	37.44 ± 12.57	25.84 ± 9.76	<0.001
	3	1	8.26 ± 3.63	14.60 ± 5.42	<0.001
	3	2	1.40 ± 1.05	2.10 ± 1.06	<0.001
Fuc-tri-antennary	3	1-2	**9.66 ± 3.02**	**16.69 ± 5.42**	**<0.001**
Tetra-antennary	4	0–3	15.03 ± 7.69	13.15 ± 4.08	n.s.
	4	0	7.95 ± 4.15	5.41 ± 2.19	<0.001
	4	1	1.42 ± 1.16	2.32 ± 1.30	<0.001
	4	2	0.57 ± 0.50	0.66 ± 0.57	n.s.
	4	3	0.29 ± 0.28	0.34 ± 0.36	n.s.
Fuc-tetra-antennary	4	1–3	**2.28 ± 1.65**	**3.32 ± 1.82**	**<0.01**
	5–7	0–6	1.63 ± 1.24	1.58 ± 0.91	n.s.
Tri- + tetra-antennary	3–7	0	62.12 ± 17.09	55.69 ± 14.88	n.s.
Fuc-(tri- + tetra-antennary)*	3–7	1–6	**18.68 ± 6.33**	**23.02 ± 5.7**	**<0.001**

#Calculated based on the hit area to the total one. *FUCAGP: fucosylated (tri + tetra)-antennary glycans/total glycans × 100.

3.3. Mass Spectrometric Analysis of Plasma AGP Glycans from Healthy Volunteers and Cancer Patients. To evaluate the AGPAS operation software for assisting determination of glycans structures of AGP, mass spectrometric analyses of AGP glycans from healthy volunteers and patients with colorectal cancers were conducted. When mass spectra from a healthy individual and a patient with colon cancer were compared (Figure 3), signals with common masses, but different intensity, were observed in both samples. Fucosylated glycans attached to the tri-, and tetra-antennary structures seemed to increase in the cancer patient. In our previous study [3], we found that the levels of plasma AGP were not important, but the degree of branching and the extent of fucosylation in AGP glycans were very useful for predicting outcome of postoperative cancer patients. Therefore, in this study, relative abundance of each glycan both in healthy individuals (n = 35) and in patients with colorectal cancer (n = 67) was determined by using the AGPAS. Accordingly, the relative abundance of every glycan was obtained and then the individual structures were tallied simultaneously as bi-, tri-, and tetra-antennary together with their fucosylated glycans based on the second number of individual FD numbers, because it could preferentially define glycan structures from bi-, tri-, and tetra-antennary glycans (Table 1). It was clearly indicated the relative abundance of all the fucosylated tri-antennary glycans including mono- (b = 3, c = 1 in $[\text{GlcNAc}]_b$ $[\text{Fuc}]_c$) and difucosylated (b = 3, c = 2 in $[\text{GlcNAc}]_b$ $[\text{Fuc}]_c$) structures and their total was significantly higher (P < 0.001) in cancer patients as compared with healthy controls even though the relative abundance of afuco-tri-antennanry glycans (b = 3, c = 0 in $[\text{GlcNAc}]_b$ $[\text{Fuc}]_c$) in cancer patients was significantly low (P < 0.001). A difference between healthy controls and cancer patients was also observed in monofucosylated (b = 4, c = 1 in $[\text{GlcNAc}]_b$ $[\text{Fuc}]_c$) and their afuco- (b = 4, c = 0 in $[\text{GlcNAc}]_b$ $[\text{Fuc}]_c$) tetra-antennary glycans (P < 0.001). Further, the relative abundance of fucosylated tetra-antennary glycans including mono-, di-, and tri-fucosylated (b = 4, c = 1–3 in $[\text{GlcNAc}]_b$ $[\text{Fuc}]_c$) glycans (P < 0.01) and fucosylated tri- plus tetra-antennary glycans (FUCAGP, P < 0.001) was significantly higher in cancer patients versus healthy controls. Therefore, it was evident that AGP glycans from cancer patients, most of whom had undergone operation and received chemotherapy periodically, were considerably fucosylated irrespective of their clinical status. It was, of particular interest, that the level of FUCAGP in cancer patients was significantly higher than the level in healthy controls but that no such a difference was present in the tri- plus tetra-antennary glycans (b = 3–7, c = 0 in $[\text{GlcNAc}]_b[\text{Fuc}]_c$). It should be appropriate to mention here that AGP glycoforms have been investigated in patients with noncancerous diseases, and elevated plasma AGP and fucosylated AGP were associated with inflammation [2, 15–22].

3.4. Mass Spectrometric Analysis of Plasma AGP Glycans in Followed Up Cancer Patients. Previously, follow-up studies of AGP glycans were undertaken in cancer patients over a long period after surgery, and their glycoforms were determined periodically, while their progress was monitored. Although demographic factors and plasma AGP level were not related to prognosis, based on fucosylation and branching indices, an individual patient's chance of survival could be predicted with the lowest misclassification rate (0.0666, P < 0.0001) [3]. While certain AGP glycoform could be a good prognostic marker for malignant disease, patients whose AGP glycoforms were highly fucosylated with branched glycans had a

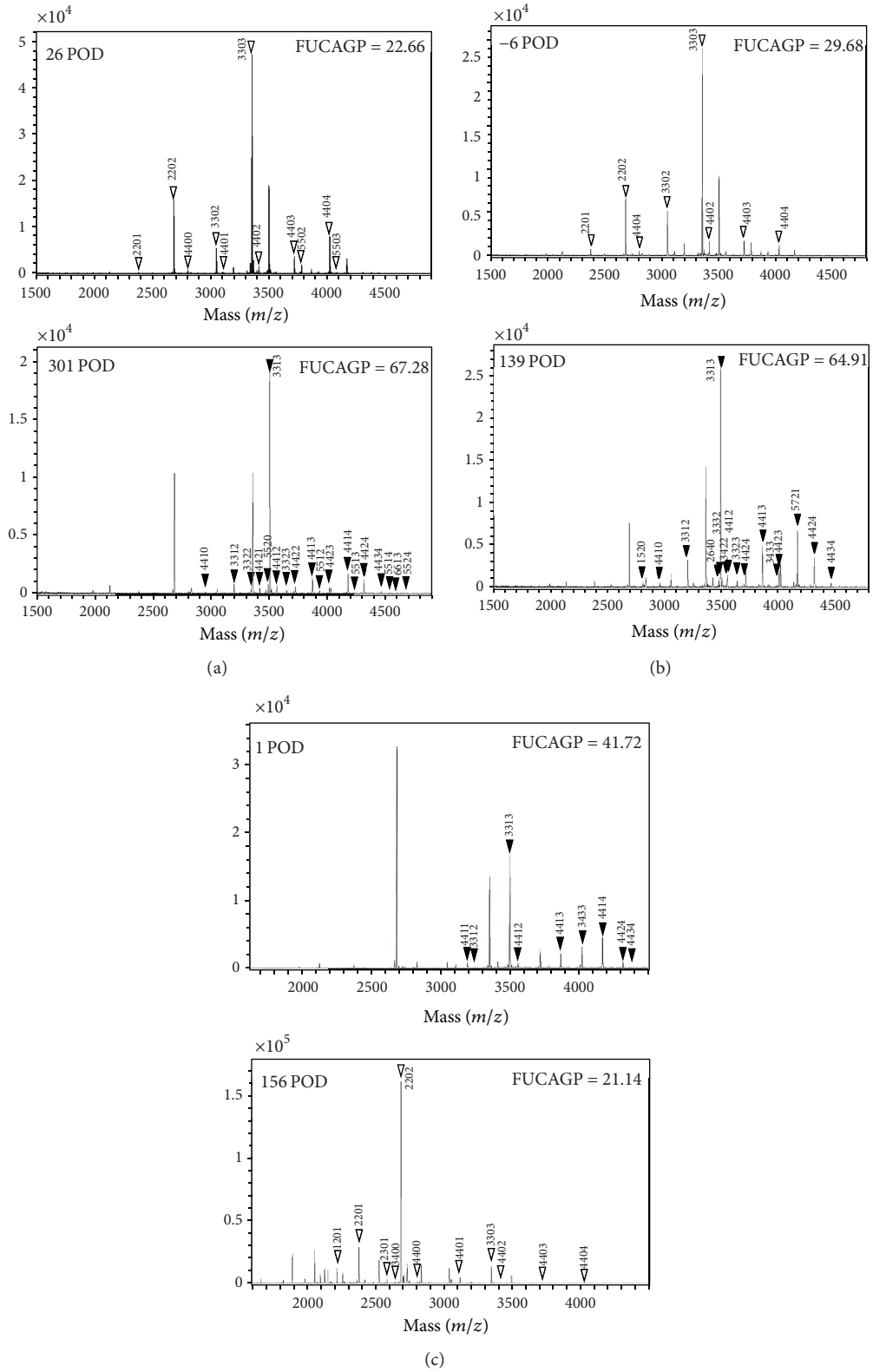

Figure 4: Mass spectra of AGP glycans isolated from followed up patients with advanced cancer. Patients with a poor prognosis, stage IV colon cancer with recurrence (a), rectal cancer with recurrence (b), and stage IIIA lung cancer (c). Purified AGP was prepared and labeled from 500 μL of plasma samples and an each aliquot (ca. one-fiftieth) was used for MS analysis. White and black triangles indicate defucosylated and fucosylated tri- and tetra-antennary glycans assigned, respectively. POD, postoperative days.

poor prognosis, died due to disease recurrence. Therefore, it was of particular interest to identify glycan structures having clinical relevance in the management of cancer patients. AGP glycans from a patient with stage IV colon cancer who had recurrence at 31 postoperative days (POD) and died were analyzed at 26 and 301 POD. The level of FUCAGP increased by more than threefold between 26 and 301 POD, reflecting levels of glycans, namely, FD numbers 3313, 4422, 4413, 4423, 4414, and 4424, together with relatively decreased expressions of 3302, 3303, 4403, and 4404 glycans (Figure 4(a)). Changes in glycoforms in this patient were associated with the degree of branching and the extent of fucosylation over the cut-off values at 301 POD [3]. Similarly, mass spectrometric analyses of AGP glycans from a patient with rectal cancer who had recurrence at 90 POD were also done both at 6 days before operation and at 139 POD. FUCAGP levels increased by more than twofold in line with an increase in the expressions of fucosylated tri-antennary glycans (FD numbers 3313, 3312, 3332) and fucosylated tetra-antennary glycans (4424, 4413, 4424 and 4434), along with decreases of 3302, 3303, 4403, or 4404 glycans (Figure 4(b)). In contrast, AGP glycans from a patient with stage IIIA lung cancer but with a good prognosis changed differently and fucosylated glycans such as 3313, 4414, 3433, 4413, 4424, 4411, and 4412 decreased markedly between 1 and 156 POD together with a fall of FUCAGP level (Figure 4(c)). In line with these observations, relative abundance of FUCAGP in patients who had AGP with either low degrees of branching or low level of fucosylation for a long period after operation was observed to be as low as those in healthy control. Therefore, all these mass spectrometric analyses in following up cancer patients showed that the primary structures of AGP glycans are in agreement with results from AGP glycoforms and that the FUCAGP index could be a postoperative marker for diagnosis and assessment of cancer progression. The newly developed AGPAS could be valuable software for a rapid determination of AGP glycan structures following mass spectrometric analyses. A detailed analysis of AGP glycans is now in progress with large numbers of plasma samples from cancer patients under various medications.

4. Conclusions

The functions of plasma AGP and its potential physiological significance as an acute phase protein have generated significant interest. However, most studies have focused on its highly glycosylated N-glycan structures along with recent developments of glycomics as well as approaches from proteomics [2, 17, 19, 22–29]. The detailed structures which were prepared from both healthy controls and patients with various diseases have been incompletely reported [14, 30–34]. Previously, we demonstrated that glycoforms of plasma AGP from cancer patients changed depending on the patients' clinical status and that any patient whose glycans contained highly fucosylated branched structures for long periods of time after operation showed a poor prognosis. In contrast, it was found that patients who had AGP glycoforms without such changes showed a good prognosis regardless of their clinical stages [3]. The present study demonstrated that assessment of primary structures of AGP glycans by following mass spectrometric analysis could be established with the aid of our newly developed software, AGPAS, which factors a database consisting of 607 N-glycans that were theoretically expected to be present in glycans of AGP. At the same time, a reliable purification method for plasma AGP by sequential use of ion-exchange cartridges was developed and followed by specifically labeling cleaved N-glycans from purified AGP. Therefore, relative abundance of all the glycans as well as bi-, tri-, and tetra-antennary glycans was simultaneously determined with their related sugar residues. It was clearly demonstrated that relative abundance of fucosylated AGP was significantly elevated in cancer patients and that mono- and difucosylated tri-antennary and monofucosylated tetra-antennary glycans were predominantly present in cancer patients. Furthermore, increased relative abundance of fucosylated AGP was found specifically in patients with a poor prognosis, consistent with not only our previous analyses of AGP glycoforms in large numbers of cancer patients but also follow-up studies of glycoforms in the same patients. The methods applied in this study seemed to be appropriate for processing large numbers of plasma samples to determine a biomarker in AGP glycans. In this endeavor, the operation software, AGPAS, should be valuable for screening plasma samples to identify biomarkers of cancer prognosis or progression based on AGP glycans with fucosylated structures.

Conflict of Interests

The authors have no conflict of interests.

References

[1] J. F. G. Vliegenthart and J. Motreuil, "Primary structure of glycoprotein glycans," in *Glycoproteins*, J. Montreuil, J. F. G. Vliegenthart, and H. Schachter, Eds., pp. 13–28, Elsevier, Amsterdam, The Netherlands, 1995.

[2] W. van Dijk, E. C. Havenaar, and E. C. M. Brinkman-van der Linden, "Alpha 1-acid glycoprotein (orosomucoid): pathophysiological changes in glycosylation in relation to its function," *Glycoconjugate Journal*, vol. 12, no. 3, pp. 227–233, 1995.

[3] S. Hashimoto, T. Asao, J. Takahashi et al., "α_1-Acid glycoprotein fucosylation as a marker of carcinoma progression and prognosis," *Cancer*, vol. 101, no. 12, pp. 2825–2836, 2004.

[4] P. Laurent, L. Miribel, J. Bienvenu, C. Vallve, and P. Arnaud, "A three-step purification of human alpha 1-acid glycoprotein," *FEBS Letters*, vol. 168, no. 1, pp. 79–83, 1984.

[5] J. Chan and D. Yu, "One-step isolation of alpha 1-acid glycoprotein," *Protein Expression and Purification*, vol. 2, no. 1, pp. 34–36, 1991.

[6] F. Hervé, M. C. Millot, C. B. Eap, J. C. Duché, and J. P. Tillement, "Two-step chromatographic purification of human plasma α1-acid glycoprotein. Its application to the purification of rare phenotype samples of the protein and their study by chromatography on immobilized metal chelate affinity adsorbent," *Journal of Chromatography B*, vol. 678, no. 1, pp. 1–14, 1996.

[7] I. Rydén, G. Skude, A. Lundblad, and P. Påhlsson, "Glycosylation of α_1-acid glycoprotein in inflammatory disease: analysis by high-pH anion-exchange chromatography and concanavalin A crossed affinity immunoelectrophoresis," *Glycoconjugate Journal*, vol. 14, no. 4, pp. 481–488, 1997.

[8] T. R. McCurdy, V. Bhakta, L. J. Eltringham-Smith, S. Gataiance, A. E. Fox-Robichaud, and W. P. Sheffield, "Comparison of methods for the purification of alpha-1 acid glycoprotein from human plasma," *Journal of Biomedicine and Biotechnology*, vol. 2011, Article ID 578207, 9 pages, 2011.

[9] S. Ongay, I. Lacunza, J. C. Diez-Masa, J. Sanz, and M. de Frutos, "Development of a fast and simple immunochromatographic method to purify alpha-1-acid glycoprotein from serum for analysis of its isoforms by capillary electrophoresis," *Analytica Chimica Acta*, vol. 663, no. 2, pp. 206–212, 2010.

[10] K. Shimura, M. Tamura, T. Toda, S. Yazawa, and K.-I. Kasai, "Quantitative evaluation of lectin-reactive glycoforms of α_1-acid glycoprotein using lectin affinity capillary electrophoresis with fluorescence detection," *Electrophoresis*, vol. 32, no. 16, pp. 2188–2193, 2011.

[11] R. Uematsu, J. I. Furukawa, H. Nakagawa et al., "High throughput quantitative glycomics and glycoform-focused proteomics of murine dermis and epidermis," *Molecular and Cellular Proteomics*, vol. 4, no. 12, pp. 1977–1989, 2005.

[12] Y. Kita, Y. Miura, J. I. Furukawa et al., "Quantitative glycomics of human whole serum glycoproteins based on the standardized protocol for liberating N-glycans," *Molecular and Cellular Proteomics*, vol. 6, no. 8, pp. 1437–1445, 2007.

[13] Y. Miura, M. Hato, Y. Shinohara et al., "BlotGlycoABC, an integrated glycoblotting technique for rapid and large scale clinical glycomics," *Molecular and Cellular Proteomics*, vol. 7, no. 2, pp. 370–377, 2008.

[14] T. Imre, T. Kremmer, K. Héberger et al., "Mass spectrometric and linear discriminant analysis of N-glycans of human serum alpha-1-acid glycoprotein in cancer patients and healthy individuals," *Journal of Proteomics*, vol. 71, no. 2, pp. 186–197, 2008.

[15] J. E. Hansen, V. A. Larsen, and T. C. Bøg-Hansen, "The microheterogeneity of alpha-1-acid glycoprotein in inflammatory lung disease, cancer of the lung and normal health," *Clinica Chimica Acta*, vol. 138, no. 1, pp. 41–47, 1984.

[16] P. Hrycaj, M. Sobieska, S. Mackiewicz, and W. Muller, "Microheterogeneity of alpha 1-acid glycoprotein in early and established rheumatoid arthritis," *Journal of Rheumatology*, vol. 20, no. 12, pp. 2020–2024, 1993.

[17] T. W. De Graaf, M. E. van der Stelt, M. G. Anbergen, and W. van Dijk, "Inflammation-induced expression of sialyl Lewis X-containing glycan structures on α_1-acid glycoprotein (orosomucoid) in human sera," *The Journal of Experimental Medicine*, vol. 177, no. 3, pp. 657–666, 1993.

[18] E. C. Havenaar, J. S. Axford, E. C. M. Brinkman-van Der Linden et al., "Severe rheumatoid arthritis prohibits the pregnancy-induced decrease in α3-fucosylation of α_1-acid glycoprotein," *Glycoconjugate Journal*, vol. 15, no. 7, pp. 723–729, 1998.

[19] H. G. Jorgensen, M. A. Elliott, R. Priest, and K. D. Smith, "Modulation of sialyl Lewis X dependent binding to E-selection by glycoforms of alpha-1-acid glycoprotein expressed in rheumatoid arthritis," *Biomedical Chromatography*, vol. 12, no. 6, pp. 343–349, 1998.

[20] W. van Dijk, C. Koeleman, B. van het Hof, D. Poland, C. Jakobs, and J. Jaeken, "Increased α3-fucosylation of α1-acid glycoprotein in patients with congenital disorder of glycosylation type IA (CDG-Ia)," *FEBS Letters*, vol. 494, no. 3, pp. 232–235, 2001.

[21] T. Zimmerman-Belsing, U. Feldt-Rasmussen, G. From, H. Perrild, and T. C. Bøg-Hansen, "Long-term pathologic changes of alpha 1-acid glycoprotein (orosomucoid) glycoforms in autoimmune thyroid disease," *Autoimmunity*, vol. 35, no. 7, pp. 441–447, 2002.

[22] F. Ceciliani and V. Pocacqua, "The acute phase protein α_1-acid glycoprotein: a model for altered glycosylation during diseases," *Current Protein and Peptide Science*, vol. 8, no. 1, pp. 91–108, 2007.

[23] K. M. Chiu, R. F. Mortensen, A. P. Osmand, and H. Gewurz, "Interactions of α1-acid glycoprotein with the immune system. I Purification and effects upon lymphocyte responsiveness," *Immunology*, vol. 32, no. 6, pp. 997–1005, 1977.

[24] J. M. H. Kremer, J. Wilting, and L. H. M. Janssen, "Drug binding to human α_1-acid glycoprotein in health and disease," *Pharmacological Reviews*, vol. 40, no. 1, pp. 1–47, 1988.

[25] C. Libert, P. Brouckaert, and W. Fiers, "Protection by α_1-acid glycoprotein against tumor necrosis factor-induced lethality," *Journal of Experimental Medicine*, vol. 180, no. 4, pp. 1571–1575, 1994.

[26] T. Fournier, N. Medjoubi-N, and D. Porquet, "Alpha-1-acid glycoprotein," *Biochimica et Biophysica Acta*, vol. 1482, no. 1-2, pp. 157–171, 2000.

[27] A. Mackiewicz and K. Mackiewicz, "Glycoforms of serum alpha-1-acid glycoprotein as markers of inflammation and cancer," *Glycoconjugate Journal*, vol. 12, no. 3, pp. 241–247, 1995.

[28] I. Rydén, P. Påhlsson, A. Lundblad, and T. Skogh, "Fucosylation of α_1-acid glycoprotein (orosomucoid) compared with traditional biochemical markers of inflammation in recent onset rheumatoid arthritis," *Clinica Chimica Acta*, vol. 317, no. 1-2, pp. 221–229, 2002.

[29] D. C. W. Poland, J. J. G. Vallejo, H. W. M. Niessen et al., "Activated human PMN synthesize and release a strongly fucosylated glycoform of α_1-acid glycoprotein, which is transiently deposited in human myocardial infarction," *Journal of Leukocyte Biology*, vol. 78, no. 2, pp. 453–461, 2005.

[30] K. Higai, Y. Aoki, Y. Azuma, and K. Matsumoto, "Glycosylation of site-specific glycans of α_1-acid glycoprotein and alterations in acute and chronic inflammation," *Biochimica et Biophysica Acta*, vol. 1725, no. 1, pp. 128–135, 2005.

[31] S. Ongay, C. Neusüß, S. Baas, J. C. Diez-Masa, and M. De Frutos, "Evaluation of the effect of the immunopurification-based procedures on the CZE-UV and CZE-ESI-TOF-MS determination of isoforms of intact α-1-acid glycoprotein from human serum," *Electrophoresis*, vol. 31, no. 11, pp. 1796–1804, 2010.

[32] T. Kremmer, É. Szöllösi, M. Boldizsár et al., "Liquid chromatographic and mass spectrometric analysis of human serum acid alpha-1-glycoprotein," *Biomedical Chromatography*, vol. 18, no. 5, pp. 323–329, 2004.

[33] M. Nakano, K. Kakehi, M. H. Tsai, and Y. C. Lee, "Detailed structural features of glycan chains derived from α1-acid glycoproteins of several different animals: the presence of hypersialylated, O-acetylated sialic acids but not disialyl residues," *Glycobiology*, vol. 14, no. 5, pp. 431–441, 2004.

[34] A. Kuno, Y. Ikehara, Y. Tanaka et al., "Multilectin assay for detecting fibrosis-specific glyco-alteration by means of lectin microarray," *Clinical Chemistry*, vol. 57, no. 1, pp. 48–56, 2011.

Hindawi Publishing Corporation
BioMed Research International
Volume 2013, Article ID 289295, 8 pages
http://dx.doi.org/10.1155/2013/289295

Research Article

Microsphere Suspension Array Assays for Detection and Differentiation of Hendra and Nipah Viruses

Adam J. Foord, John R. White, Axel Colling, and Hans G. Heine

Australian Animal Health Laboratory, CSIRO Animal, Food and Health Sciences, Geelong, VIC 3220, Australia

Correspondence should be addressed to Hans G. Heine; hans.heine@csiro.au

Received 19 October 2012; Accepted 25 December 2012

Academic Editor: Arun K. Bhunia

Microsphere suspension array systems enable the simultaneous fluorescent identification of multiple separate nucleotide targets in a single reaction. We have utilized commercially available oligo-tagged microspheres (Luminex MagPlex-TAG) to construct and evaluate multiplexed assays for the detection and differentiation of Hendra virus (HeV) and Nipah virus (NiV). Both these agents are bat-borne zoonotic paramyxoviruses of increasing concern for veterinary and human health. Assays were developed targeting multiple sites within the nucleoprotein (N) and phosphoprotein (P) encoding genes. The relative specificities and sensitivities of the assays were determined using reference isolates of each virus type, samples from experimentally infected horses, and archival veterinary diagnostic submissions. Results were assessed in direct comparison with an established qPCR. The microsphere array assays achieved unequivocal differentiation of HeV and NiV and the sensitivity of HeV detection was comparable to qPCR, indicating high analytical and diagnostic specificity and sensitivity.

1. Introduction

Bats harbour a wide range of viruses that have been implicated in spill over events into other mammalian hosts resulting in highly virulent and often fatal zoonoses. Henipa-, filo-, lyssa-, and coronaviruses are some of the most notable examples [1]. The henipaviruses HeV and NiV are bat-borne paramyxoviruses which have been responsible for severe disease outbreaks in humans, horses, and pigs [2]. HeV was first identified in Australia in 1994 as the cause of fatal infection in horses and humans [3]. The closely related NiV was subsequently identified as the causative agent of infections in pigs and humans in Malaysia in 1998-99 [4]. The fruit bat (*Pteropus* spp.) is the only known natural reservoir of these two viruses. NiV infections in humans have been identified in several countries including Malaysia, Singapore, Bangladesh, and India with mortality up to and exceeding 75% in some of these epidemics [2]. Evidence for this virus or henipa-like viruses in bat populations in other South-East Asian locations have also been provided [5–7]. Henipa-like genomic sequences have also been detected in African bats [8] and Cedar paramyxovirus (CedPV), a novel henipa-like virus, was recently isolated in Australia [9]. HeV is endemic in Australian *Pteropus* bats and can spread directly from bats to horses, causing severe disease. Human HeV infection has so far only resulted from close contact with the blood, body fluids, and tissues of infected horses. Although bats appear to be unaffected by HeV there is a high case-fatality rate in both humans and horses and spill-over events from bats to horses are occurring with increasing regularity [10, 11]. The wide range of viruses and their enormous genome sequence variation and evolution pose a challenge to the development of molecular diagnostic assays. Although next generation sequencing can identify viruses without any prior knowledge of their sequence [12], this approach is still not practical for screening larger numbers of samples in a diagnostic context. Various combinations of conventional PCR and sequencing, or qPCR, have been used for virus identification [12, 13]. Highly conserved genes and sequences within, or across, virus species in combination with degenerate PCR primer sequences have broadened the range of viruses detectable by a single PCR [14]. The nature of these generic PCR assays necessitates the use of highly degenerate primers which can lead to a reduction in sensitivity and still requires confirmation of any resulting PCR products by DNA sequencing. Nevertheless, qPCR is highly specific, sensitive, and suitable

Table 1: Oligonucleotides for HeV and NiV microsphere array assays.

Name	Function	Sequence (5′-3′)	Position ([a])
	N-gene		
D-358	PCR-Fwd	TTTGAMGAGGCGGCTAGTTT	125–144
D-368	PCR-Rev	CATCAARCCTTCCATCTCCTC	499–479
D-676	TSPE-henipa (*MTAG-A057)	(*)-GCRGCAACWGCTACTTTGAC	188–207
D-679	TSPE-HeV (*MTAG-A061)	(*)-ACTAATAGCCCAGAACTGAGATG	236–258
D-680	TSPE-NiV (*MTAG-A067)	(*)-ACTAATAGTCCAGAGCTCAGATG	236–258
	P-gene		
D-550	PCR-Fwd	ACATACAACTGGACCCARTGGTT	2698–2720
D-551	PCR-Rev	CACCCTCTCTCAGGGCTTGA	2794–2775
D-641	TSPE Henipa (*MTAG-A051)	(*)-ACAGACGTTGTATACCATG	2721–2739

([a]) Positions are relative to the HeV genome (GenBank accession number: NC_001906). TSPE denotes target-specific primer extension.
(*) denotes sequence of 3′ extension containing anti-TAG sequence complementary to TAG sequence on microsphere as defined by particular MTAG-A# (Luminex Corporation, USA).

for automation and screening of large sample numbers. However, the limited multiplexing capability of qPCR, typically no more than 2-3 combined assays, requires the setup of various and frequently, constituently different qPCR reactions when screening for multiple viruses. Microsphere suspension array assays offer advantages over qPCR in the level of readily achievable multiplexing. This allows for the simultaneous screening of many targets (up to 100 markers in the Luminex system) in a single reaction and has become a valuable tool for investigation of disease syndromes. Various assay panels for nucleic acid detection have been developed for medical or veterinary applications, including respiratory viral diseases [15], gastroenteritis pathogens [16], cystic fibrosis [17], biothreat agents [18, 19], and vesicular diseases of livestock [20]. Polymerase chain reaction amplification of the regions of interest forms the first step of these assays. Proprietary polystyrene microspheres that contain dyes displaying distinct spectral characteristics form the substrate for these assays. Luminex MagPlex-TAG microspheres (Luminex Corporation) contain unique 24 nucleotide DNA "antiTAG" sequences covalently coupled to their surface. This facilitates hybridization of specifically amplified and labeled products containing complementary "TAG" sequences and allows identification by association with particular microsphere sets in a flow cytometry-based detection system. Microsphere suspension array assays can be designed as a modular system and combined into assay panels of increasing complexity to increase the range for detection of different viruses.

Here we report the development of microsphere array assays for detection and differentiation of RNA from HeV and NiV isolates and their analytical and diagnostic performance. Furthermore, we demonstrated the utility of these assays as modules for detection of HeV in Australian horses. Our intention is to include these assays in future development of multiplex assay panels for investigating infectious diseases, syndromes in livestock, and zoonoses.

2. Materials and Methods

2.1. Viruses and Diagnostic Samples. Viruses used in this study were HeV (hendra virus/ Australia/horse/Hendra/1994, six HeV isolates from four of the 2011 outbreaks in Queensland and New South Wales, Australia); NiV (Nipah virus/Malaysia/1998, Nipah virus/Bangladesh/2004); Cedar paramyxovirus; nonrelated paramyxovirus (Tioman, Sendai, Menangle, Rinderpest, and J virus); other viruses (West Nile, Kunjin, Murray valley encephalitis, and Japanese encephalitis virus). All viruses were held as stocks at the Australian Animal Health Laboratory (AAHL). Diagnostic samples used in this study included blood, tissue, and swabs from horses submitted to AAHL during several outbreaks of HeV in the Australian States of Queensland and New South Wales in 2011. Further samples from time-course experimental studies on a limited number of HeV-infected horses were also used [21]. To assist with an appropriate statistical analysis of the collective data, swab samples from submissions of quarantined European horses, presumed to be negative for HeV, were also utilized. Nucleic acid was isolated from each sample using the MagMAX 96 Viral RNA Extraction Kit (Life Technologies Cat. No. AM1836-5).

2.2. Microsphere Suspension Array Primer Design. The primer designs (Table 1) were based on the alignments of the available 17 HeV sequences (GenBank accession numbers: HM044317, HM044318, HM044319, HM044320, HM044321, JN255800, JN255801, JN255802, JN255803, JN255804, JN255805, JN255806, JN255812, JN255814, JN255817, JN255818, NC001906) and 20 NiV sequences (GenBank accession numbers AF376747, AJ564621, AJ564622, AJ564623, AJ627196, AY029767, AY029768, AY858110, AY988601, FJ513078, FN869553, JN808857, JN808858, JN808859, JN808860, JN808861, JN808862, JN808863, JN808864, NC002728) using Geneious Pro software [23]. Primers were designed for two independent assays specific for either a 375 nucleotide region of the N-gene coding sequence (CDS) or 97 nucleotide region of the P-gene CDS of HeV and NiV (Figure 1). The N-gene assay accommodated three target-specific primer extension (TSPE) primers, one for generic detection of both HeV and NiV, and one specific for HeV or NiV only. The P-gene assay based on a qPCR assay [24] contains only a single TSPE primer for detection

```
          1                   20    64                  83    112                     134    355                 375
          |                    |    |                   |     |                       |      |                   |
HeV       UUUGACGAGGCGGCUAGUUU/../GCGGCAACAGCUACUUUGAC/../ACUAAUAGCCCAGAACUGAGAUG/../GAGGAGAUGGAAGGUUUGAUG
NiV-M     .....A...............//..A.....U...........//.........U.....G..C.....//..............C......
NiV-B     .....A...............//..G.....U...........//.........U.....G..C.....//..............C......
          -----*-------------->//--*-----*---------->//---------*-----*--*---->//<-------------*------
                D-358                   D-676                     D-679/D-680                 D-368
```

(a) N-gene

```
          1                       24                  42    78                  97
          |                       |                   |     |                   |
HeV       ACAUACAACUGGACCCAAUGGUUACAGACGUUGUAUACCAUG/../UCAAGCCCUGAGAGAGGGUG
NiV-M     ................G........................//.....................
NiV-B     ................G........................//.....................
          -----------------*---->------------------>//<-------------------
                D-550                   D-641                   D-551
```

(b) P-gene

Figure 1: Design of oligonucleotides for henipavirus N-gene- (a) and P-gene- (b) specific microsphere array assays. Representative virus sequences are HeV (NC_001906), NiV-Malaysia (NC_002728), and NiV-Bangladesh (AY988601). Sequence gaps (sequences not displayed) outside target regions are indicated by //. Regions of sequence identity are marked by dash (-) and differences are marked (*) in the primer target regions. PCR primers forward (D-358) and reverse (D-368) are flanking the 375 nucleotide N-gene amplicon, and PCR primers forward (D-550) and reverse (D-551) are flanking the 97 nucleotide P-gene amplicon. Only the gene-specific target sequences and not the TAG extensions are displayed for TSPE primers (D-676, D-679, D-680, and D-641). All TSPE primers were designed to extend in forward orientation.

of both HeV and NiV. The incorporation of degenerate nucleotides was utilized to facilitate generic amplification and detection of all known HeV and NiV isolates. The design of two independent assays served as a contingency in the event of diagnostic failure should virus sequences change in an individual assay target region.

2.3. Microsphere Suspension Array Assay Procedure

2.3.1. Primary PCR. Single-step reverse transcription PCR (RT-PCR) was performed using Superscript III One-Step RT-PCR with Platinum Taq kit (Invitrogen) with the following conditions: 25 μL volume, 200 nM forward and reverse primers, and 2.0 mM $MgSO_4$. Thermal cycling conditions were 30 min at 48°C (RT reaction), 2 min at 94°C (Taq activation), 45 cycles of 30 sec at 94°C, 40 sec at 50°C, and 40 sec at 68°C, followed by 68°C for 7 min. RT-PCR was performed separately for each target using the same conditions for both N and P-gene assays. The unincorporated dNTPs and primers from the initial RT-PCR were removed by treating with ExoSAP-IT (Affymetrix). Twenty-five microliters of RT-PCR were treated with 10 μL ExoSAP-IT and incubated at 37°C for 30 min, followed by 10 min at 80°C to inactivate the enzymes.

2.3.2. Target-Specific Primer Extension (TSPE). Linear amplification was then performed in the presence of biotin-labeled cytosine with the required TSPE primers present in a given reaction mix. The treated RT-PCR products were then combined for TSPE reactions. The 5′ ends of the TSPE primers were designed to contain 24 base TAG sequences complementary to the particular microsphere sets, whereas the remainder of the primer sequence was designed to bind to targets within the RT-PCR product. Biotin-dCTP was incorporated in the reaction to allow detection by streptavidin-R-phycoerythrin (SA-PE). Each TSPE reaction contained 5 μL of Exo-SAP-treated RT-PCR product, 0.75 U *Tsp* DNA polymerase (Invitrogen), 25 nM TSPE primer 5 μM dATP/dTTP/dGTP and biotin-dCTP (Invitrogen), 1X *Tsp* DNA polymerase reaction buffer (Invitrogen), and 4.0 mM $MgCl_2$. Thermocycling was performed at 95°C for 2 min, followed by 30 cycles of 94°C for 30 s, 50°C for 30 s, and 72°C for 40 s with a final extension at 72°C for 5 min.

2.3.3. Microsphere Hybridisation. Products from the TPSE reactions were multiplexed with relevant MagPlex-TAG microspheres (Luminex MagPlex-TAG). Five microliters of TSPE reaction were hybridized in 50 μL 1X hybridization buffer (0.2 M NaCl/0.1 M Tris/0.08% Triton X-100, pH 8.0) with 500 each (microspheres/microsphere set/well) of the appropriate MagPlex-TAG microspheres containing the antitag complimentary to the 5′ TAG on the TSPE primer. The hybridization mixture was incubated at 96°C for 90 sec and 37°C for 30 min. The microsphere mixture was transferred to a black-sided 96-well Bio-Plex flat bottom plate (Bio-Rad) and washing of magnetic microspheres was performed using an automated plate washer (Bio-Plex pro II wash station; Bio-Rad).

2.3.4. Microsphere Identification and Fluorescence Detection. Seventy-five microlitres of 1X hybridization buffer containing 2 mg/L streptavidin-R-phycoerythrin (Invitrogen) were added to each plate well and the mixture was incubated in the dark at 37°C for 15 min. Instrument procedure was as described by the manufacture; briefly, 50 μL of the microsphere/TSPE/streptavidin-R-phycoerythrin mixture was injected into a Bio-Plex 200 instrument (Bio-Rad), at a sample plate temperature of 37°C. Each assay plate was analysed in a Bio-Plex 200 fluorometer (Bio-Rad) running

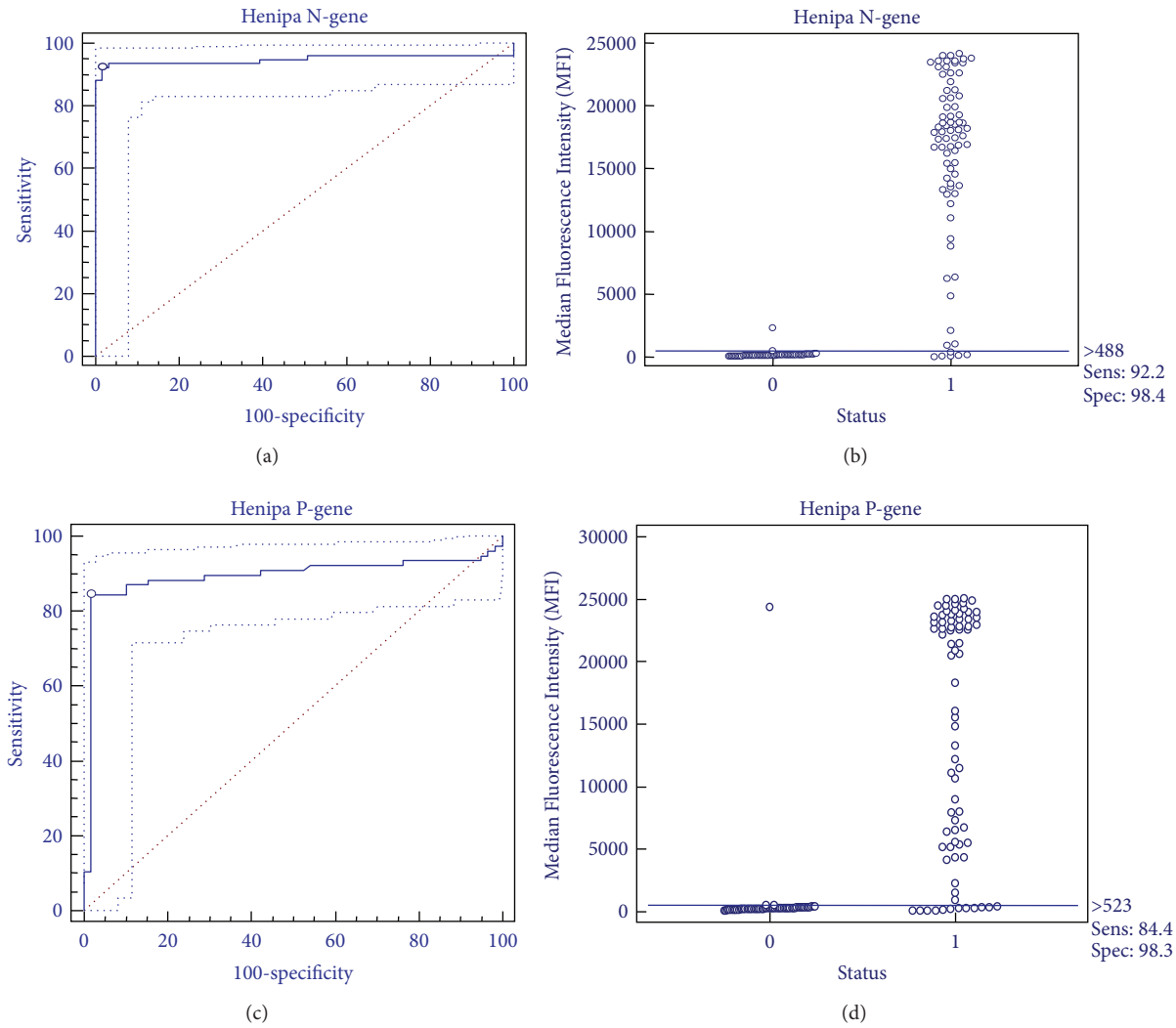

Figure 2: Diagnostic performance characteristics of microsphere array assays. Accuracy of microsphere array assays specific for the henipa N-gene (a, b) and henipa P-gene (c, d) was determined by receiver operating characteristic (ROC) curve analysis (a, c) using qPCR assay as reference standard. Distribution of positive (1) and negative (0) values are shown (b, d).

at high RP1 target setting with 100 of each microsphere set analysed per well. Fluorescence was measured as units of Median Fluorescence Intensity (MFI). A positive result was initially defined as a value greater than three times the MFI obtained from a known HeV negative control.

2.4. qPCR Assays. A HeV N-gene-specific qPCR assay [24] was used for comparative assessment of the microsphere assays. Assay conditions and oligonucleotides were as described in the paper. Cut-off values were cycle threshold (CT) ≤ 40 for positive and CT ≥ 45 for negative. Results with CT values between 40 and 45 were deemed indeterminate.

2.5. Statistical Analysis. Statistical analyses were performed using Microsoft Excel 2007 and MedCal Version 12.3.0.0. ROC curve analysis was performed using 77 positive and 61 negative samples by qPCR for the henipa N- and P-gene microsphere array assay. For this analysis infected and noninfected horses were given the statuses 1 and 0, respectively. The area under the ROC curve (AUC) (Figure 2) was 0.948 for the henipa N (at cutoff > 488MFI) and 0.893 for the P-gene microsphere array assay (at a cut-off of > 523MFI). In the ROC analysis, values of $0.9 < \text{AUC} < 1$ are considered highly accurate. A perfect test with a Se and Sp of 100% would have an AUC of 1 and be in the upper left corner of the graph [25]. An interactive dot diagram was plotted using results of the henipa N- and P-gene microsphere array assays in relation to the infected (1) and noninfected (0) category, to show false negative and false positive results at cut-offs with highest combined Se and Sp.

3. Results and Discussion

3.1. Analytical Specificity of Microsphere Suspension Array Assays. The analytical specificity of the N- and P-gene-based microsphere array assays was assessed using RNA extracted

Table 2: Detection of HeV in experimentally infected horses.

Day	Microsphere array assay		qPCR ([a])	LAMP ([a])
	Henipa N (MFI)	Henipa P (MFI)	(Ct)	(U/Pos)
Horse 1				
0	148	213	U	U
1	185	256	U	U
2	**20 858**	**23 745**	**37.5**	U
3	**22 088**	**24 593**	**34.7**	**Pos**
4	**22 828**	**24 049**	**35.9**	**Pos**
5	**23 734**	**24 985**	**29.5**	**Pos**
6	**23 856**	**25 197**	**32.8**	**Pos**
Horse 2				
0	219	104	U	U
1	197	296	U	**Pos**
2	**22 304**	**23 547**	**36.3**	**Pos**
3	**22 983**	**23 625**	**32.4**	**Pos**
4	**11 638**	**8 142**	**38.9**	**Pos**
5	**23 063**	**24 068**	**34.3**	**Pos**
6	**22 914**	**23 333**	**31.1**	**Pos**
7	**23 024**	**24 284**	**28.1**	**Pos**
8	**22 900**	**24 145**	**29.2**	**Pos**
9	**22 900**	**24 951**	**35.2**	**Pos**
Horse 3				
0	186	301	U	U
1	221	288	U	U
2	**10 734**	375	42*	**Pos**
4	**1 271**	**2 251**	41.4*	**Pos**
5	**5 406**	**7 018**	43*	**Pos**
6	**1 804**	**8 019**	U	U
7	**16 731**	**20 575**	**37.7**	**Pos**
Pos control	23228	23451		
NTC	226	298		

Comparison of microsphere array assays performed on archival RNA extracted from daily nasal swabs of experimentally infected horses [21].
([a]) Comparison with qPCR and loop-mediated amplification (LAMP) assay results [22] in retrospective analysis. Day indicates sampling day after challenge. MFI: median fluorescence intensity; U: undetected; Pos: positive reaction; * indicates qPCR indeterminate results; NTC: no template control. All positive results are in bold .

from different virus isolates and nonrelated laboratory reference virus strains (listed in Materials and Methods). HeV and NiV isolates were positive in the generic henipavirus assays and their corresponding virus type-specific assays. All other tested viruses including CedPV were negative in the N- and P-gene assays. Although the recently isolated CedPV from Australian bats has been suggested as a henipa-like virus, it is quite distinct from HeV and NiV. Importantly, CedPV contained multiple sequence changes in each of the N- and P-gene primer regions for HeV and NiV. HeV and NiV are phylogenetically closely related having nucleotide sequence identities of 68.2% for whole genome, 78.4% for N-gene, and 70.0% for P-gene CDS, whereas the more distantly related CedPV has identities of only 47.5–48.1% for whole genome, 60.5–60.2% for N-gene, and 42.5–42.4% for P-gene CDS.

3.2. Analytical Sensitivity of Microsphere Suspension Array Assays. The analytical sensitivity of the microsphere array assays was assessed in direct comparison to the HeV specific qPCR assay by determining the limit of detection using tenfold serially diluted RNA template derived from HeV (Hendra virus/horse/Hendra/1994) and NiV (Nipah virus/Malaysia/1998). The microsphere suspension array assays had a dynamic range for detection equal to qPCR and were at least as sensitive as qPCR (data not shown). The fitness of microsphere array assays for the sensitive detection of HeV infection was further confirmed using archival samples from horses experimentally infected with HeV [21]. Results were compared with qPCR and loop-mediated amplification (LAMP) assays [22] (Table 2). HeV was detected by microsphere array assays as early as qPCR or LAMP assays, two days after infection. There was excellent correlation between the N- and P-gene microsphere assays. Day 2 results for horse 3 were the only occasion where an N-gene positive sample was negative in the corresponding P-gene assay. Overall, the utility of microsphere assays was confirmed by the high level of sensitivity as was apparent with positive results at days 2, 4, and 5 in horse 3 when

Table 3: Diagnostic evaluation of microsphere array assays for HeV detection.

Microsphere array assay (archival RNA)	HeV qPCR assay[a] (original diagnostic results)		
	Positive	Negative	Indeterminate
Henipa N-gene positive	72	4	4
Henipa N-gene negative	5[b]	57	3
Total (n = 145)	77	61	7
Henipa P-gene positive	65	2	1
Henipa P-gene negative	12[b]	57	6
Total (n = 143)[c]	77	59	7

Retrospective analysis of results from microsphere array assays on archival RNA of diagnostic submissions in comparison with original qPCR diagnostic results. Preliminary cut-off values (241 MFI for the N-gene and 518 MFI for the P-gene) were derived from results of the negative horse population.
([a]) HeV qPCR negatives include presumed HeV negative samples.
([b]) Five samples categorised HeV qPCR positive in the originally diagnostic assay were negative in both Henipa N- and P-gene assay of archival RNA. All five samples were HeV negative when archival RNA was retested by qPCR (indicating likely degradation of the archival RNA in these samples).
([c]) Two samples from the presumed HeV negative population were not available for the henipa P assay.

corresponding qPCR indicated indeterminate or undetected results.

3.3. Diagnostic Evaluation of Microsphere Suspension Array Assays. Assays were evaluated in a retrospective analysis of archival diagnostic horse samples (n = 145). Expected negative values for each of the microsphere array assays were obtained from presumed negative horse samples (n = 40). The mean MFI (+3STD) of these samples was 121 (+120) for the henipa N-gene assay, 126 (+141) for the HeV N-gene assay, 145 (+147) for the NiV N-gene assay, and 257 (+261) for the henipa P-gene assay. Archival RNA from diagnostic submissions obtained during investigations of HeV in horses in Australia in 2011 was tested and results then correlated with the original diagnostic results obtained from qPCR assays (Table 3). Five HeV qPCR positive samples in the originally diagnostic assay were negative in both the henipa N- and P-gene assay of archival RNA (Table 3). When archival RNA was retested by qPCR all five samples were HeV negative, most likely due to degradation of the archival RNA from these samples. This indicates that the diagnostic performance of the microsphere array assays may have been underestimated in the retrospective analysis of microsphere array assays on archival RNA in comparison with original qPCR diagnostic results. Out of 7 HeV indeterminate samples (by qPCR), the henipa N-gene microsphere assay returned 4 positive and 3 negative results and the henipa P-gene 6 negative and 1 positive result. An advantage of these microsphere array assays was the clear differentiation between positive and negative results and an ability to resolve unambiguous results as exemplified by clear resolution of the indeterminate results observed at the limit of detection in qPCR.

For ROC curve analysis (Figure 2), all of the samples positive in the N-gene henipa-specific microsphere assay were also positive in the HeV specific N-gene assay and none of these were found to be positive in the NiV-specific N-gene assay. HeV-specific positive and negative values in all assays were generally well separated, so changes from optimal cutoff values did not significantly change results in a ROC curve analysis (results not shown). For the N-gene henipa-specific assay the optimal ROC curve calculated cutoff MFI = 488 yielded sensitivity (Se) and specificity (Sp) readings of 92.2 (95% CI 83.8–97.1) and 98.4 (95% CI 91.2–100.0), respectively (Figures 2(a) and 2(b)). For the P-gene henipa-specific assay the calculated optimal cutoff MFI 523 gave an Se of 84.4 (95% CI 74.4–91.7) and an Sp of 98.3 (95% CI 90.9–100.0) (Figures 2(c) and 2(d)). The analysis of Sp and Se data for the HeV-specific assay showed near identical results to the generic henipa N-gene assay (data not shown). The ROC curve determined that negative cut-offs for all four assays were also found to exceed the highest MFI values obtained in an analysis of 40 presumed HeV negative horse swab samples in each assay. Direct comparison of all assays by ROC curve analysis using qPCR assay as reference standard identified the Henipa and HeV N-gene assays as the best performers for HeV detection. Assay accuracy for the henipa N, HeV-N and henipa P-gene assays was 0.941, 0.940, and 0.874, respectively, for samples n = 96 samples (qPCR confirmed), increasing to 0.948, 0.946, and 0.893 for n = 136 samples including 40 presumed negative samples unconfirmed by qPCR.

The HeV N-gene test exhibited the higher Se producing less false negative results. The Sp was similar for both tests. High Se is highly desirable for a test that diagnoses zoonotic and potentially fatal disease. As the reference test (qPCR) may be imperfect, it cannot be assumed that the status of the samples is 100% accurate. Evaluation of further field samples from infected and noninfected horses would be required to obtain more robust estimates for Se and Sp.

4. Conclusions

The microsphere array assay modules were specific for HeV and NiV. Based on sequence conservation of target regions, these assays should detect all known HeV and NiV isolates. Furthermore, the N-gene assay reliably differentiated HeV and NiV. The analytical sensitivity of the microsphere

array assays matched that of qPCR assays in the limit of detection study, the detection of virus in experimentally infected horses, and in the retrospective analysis of diagnostic field samples. The microsphere array assays are based on an open diagnostic platform allowing a high degree of customisation. This facilitates the expansion of individual assay components into larger and more complex arrays and the update of assays in response to new and emerging viruses. The microsphere array assays offer advantages over qPCR in the level of readily achievable multiplexing. Assays can be designed as a modular system and combined into assay panels of increasing complexity. This ensures that assay sensitivity and specificity are not adversely affected by difficulties often observed in multiplexed qPCR reactions. This study demonstrated the utility of the microsphere array assays for detection of HeV. Our aim is to incorporate these HeV and NiV microsphere array assays as modules in future higher multiplexed microsphere arrays. This will facilitate the development of syndrome-based assay panels for disease investigation and agent surveillance in horse, bat, pig, and human populations.

Conflict of Interests

The authors declare that there is no conflict of interests.

Acknowledgments

The authors wish to thank the AAHL PCR Group for release of retrospective test samples and associated qPCR data and Vicky Boyd for her earlier involvement in reagent optimisation and valuable ongoing advice and assistance. Dr. Glenn Marsh kindly provided the virus isolates needed for analysis of assay performance. Linda Wright is also thanked for retrieving required test sample IDs from the AAHL diagnostic archive as is Dr. Brian Meehan for his support and encouragement throughout this study.

References

[1] C. H. Calisher, J. E. Childs, H. E. Field et al., "Bats: important reservoir hosts of emerging viruses," *Clinical Microbiology Reviews*, vol. 19, no. 3, pp. 531–545, 2006.

[2] G. A. Marsh and L. F. Wang, "Hendra and Nipah viruses: why are they so deadly?" *Current Opinion in Virology*, vol. 2, no. 3, pp. 242–247, 2012.

[3] K. Murray, P. Selleck, P. Hooper et al., "A morbillivirus that caused fatal disease in horses and humans," *Science*, vol. 268, no. 5207, pp. 94–97, 1995.

[4] K. B. Chua, K. J. Goh, K. T. Wong et al., "Fatal encephalitis due to Nipah virus among pig-farmers in Malaysia," *The Lancet*, vol. 354, no. 9186, pp. 1257–1259, 1999.

[5] S. Wacharapluesadee, B. Lumlertdacha, K. Boongird et al., "Bat Nipah virus, Thailand," *Emerging Infectious Diseases*, vol. 11, no. 12, pp. 1949–1951, 2005.

[6] J. M. Reynes, D. Counor, S. Ong et al., "Nipah virus in Lyle's flying foxes, Cambodia," *Emerging Infectious Diseases*, vol. 11, no. 7, pp. 1042–1047, 2005.

[7] I. Sendow, H. E. Field, J. Curran et al., "Henipavirus in Pteropus vampyrus bats, Indonesia," *Emerging Infectious Diseases*, vol. 12, no. 4, pp. 711–712, 2006.

[8] D. T. S. Hayman, R. Suu-Ire, A. C. Breed et al., "Evidence of henipavirus infection in West African fruit bats," *PLoS ONE*, vol. 3, no. 7, Article ID e2739, 2008.

[9] G. A. Marsh, C. de Jong, J. A. Barr et al., "Cedar virus: a novel henipavirus isolated from Australian bats," *PLOS Pathogens*, vol. 8, no. 8, Article ID 100283, 2012.

[10] I. Smith, A. Broos, C. de Jong et al., "Identifying Hendra virus diversity in pteropid bats," *PLoS ONE*, vol. 6, no. 9, Article ID e25275, 2011.

[11] Queensland Horse Council, "Hendra Virus," http://www qldhorsecouncil.com/QHC%20Documents/Notifiable%20Diseases%20Information%20Sheets/Hendra%20Virus.pdf.

[12] J. F. Drexler, V. M. Corman, M. A. Muller et al., "Bats host major mammalian paramyxoviruses," *Nature Communications*, vol. 3, article 796, 2012.

[13] K. S. Baker, S. Todd, G. Marsh et al., "Co-circulation of diverse paramyxoviruses in an urban African fruit bat population," *Journal of General Virology*, vol. 93, part 4, pp. 850–856, 2012.

[14] S. Tong, S. W. W. Chern, Y. Li, M. A. Pallansch, and L. J. Anderson, "Sensitive and broadly reactive reverse transcription-PCR assays to detect novel paramyxoviruses," *Journal of Clinical Microbiology*, vol. 46, no. 8, pp. 2652–2658, 2008.

[15] P. Jokela, H. Piiparinen, L. Mannonen et al., "Performance of the Luminex xTAG respiratory viral panel fast in a clinical laboratory setting," *Journal of Virological Methods*, vol. 182, no. 1-2, pp. 82–86, 2012.

[16] J. Liu, G. Kibiki, V. Maro et al., "Multiplex reverse transcription PCR Luminex assay for detection and quantitation of viral agents of gastroenteritis," *Journal of Clinical Virology*, vol. 50, no. 4, pp. 308–313, 2011.

[17] M. A. Johnson, M. J. Yoshitomi, and C. S. Richards, "A comparative study of five technologically diverse CFTR testing platforms," *Journal of Molecular Diagnostics*, vol. 9, no. 3, pp. 401–407, 2007.

[18] I. Janse, J. M. Bok, R. A. Hamidjaja et al., "Development and comparison of two assay formats for parallel detection of four biothreat pathogens by using suspension microarrays," *PLoS ONE*, vol. 7, no. 2, Article ID e31958, 2012.

[19] Y. Yang, J. Wang, H. Wen et al., "Comparison of two suspension arrays for simultaneous detection of five biothreat bacterial in powder samples," *Journal of Biomedicine and Biotechnology*, vol. 2012, Article ID 831052, 8 pages, 2012.

[20] B. J. Hindson, S. M. Reid, B. R. Baker et al., "Diagnostic evaluation of multiplexed reverse transcription-PCR microsphere array assay for detection of foot-and-mouth and look-alike disease viruses," *Journal of Clinical Microbiology*, vol. 46, no. 3, pp. 1081–1089, 2008.

[21] G. A. Marsh, J. Haining, T. J. Hancock et al., "Experimental infection of horses with Hendra virus/Australia/horse/2008/Redlands," *Emerging Infectious Diseases*, vol. 17, no. 12, pp. 2232–2238, 2011.

[22] A. J. Foord, D. Middleton, and H. G. Heine, "Hendra virus detection using Loop-Mediated Isothermal Amplification," *Journal of Virological Methods*, vol. 181, no. 1, pp. 93–96, 2012.

[23] A. B. Drummond AJ, S. Buxton, M. Cheung et al., "Geneious v5.4," 2012, http://www.geneious.com/.

[24] K. S. Feldman, A. Foord, H. G. Heine et al., "Design and evaluation of consensus PCR assays for henipaviruses," *Journal of Virological Methods*, vol. 161, no. 1, pp. 52–57, 2009.

[25] M. Greiner, D. Pfeiffer, and R. D. Smith, "Principles and practical application of the receiver-operating characteristic analysis for diagnostic tests," *Preventive Veterinary Medicine*, vol. 45, no. 1-2, pp. 23–41, 2000.

Hindawi Publishing Corporation
BioMed Research International
Volume 2013, Article ID 703048, 12 pages
http://dx.doi.org/10.1155/2013/703048

Review Article

Microvesicles as Potential Ovarian Cancer Biomarkers

Ilaria Giusti, Sandra D'Ascenzo, and Vincenza Dolo

Department of Life, Health and Environmental Sciences, University of L'Aquila, 67100 L'Aquila, Italy

Correspondence should be addressed to Vincenza Dolo; vincenza.dolo@univaq.it

Received 12 October 2012; Accepted 10 December 2012

Academic Editor: Tavan Janvilisri

Although the incidence of ovarian cancer is low (i.e., less than 5% in European countries), it is the most lethal gynecologic malignancy and typically has a poor prognosis. To ensure optimal survival, it is important to diagnose this condition when the pathology is confined to the ovary. However, this is difficult to achieve because the first specific symptoms appear only during advanced disease stages. To date, the biomarker mainly used for the diagnosis and prognosis of ovarian cancer is CA125; however, this marker has a low sensitivity and specificity and is associated with several other physiological and pathological conditions. No other serum ovarian cancer markers appear to be able to replace or complement CA125, and the current challenge is therefore to identify novel markers for the early diagnosis of this disease. For this purpose, studies have focused on the microvesicles (MVs) released from tumor cells. MVs may represent an ideal biomarker because they can be easily isolated from blood, and they have particular features (mainly regarding microRNA profiles) that strongly correlate with ovarian cancer stage and may be effective for early diagnosis.

1. Introduction

For many years, it was believed that communication between cells exclusively depends on the release of specific soluble or immobilized mediators and their corresponding receptors. Such a process may involve cell-to-cell contact or the release of mediators into the blood, other bodily fluids (endocrine interactions), or the microenvironment to form gradients (paracrine interactions) [1]. When it was discovered that cells were able to secrete vesicles, it was thought that this was a form of waste elimination. However, it is now known that vesicles represent signaling packages that are able to convey messages to stimulate/inhibit neighboring cells and modify the surrounding microenvironment [2]. The term "rececrine" has been suggested to describe this signaling method, which specifically refers to the secretion of receptors carried by microvesicles (MVs) and their transfer to target cells where they may exert specific functions [3]. There is also increasing evidence for the involvement of MVs in various physiological and pathological events, such as the immune response, cellular differentiation, and vascular and cancer pathologies [4].

Cells can release different types of vesicles, the most important of which are apoptotic bodies, exosomes, and shed MVs (Figure 1) [1, 5, 6]; the last two types are primarily involved in the exchange of messages between cells. This paper mainly focuses on the role of MVs as potential clinical biomarkers and also contains a brief overview of all types of vesicles.

The term "apoptotic bodies" was coined in 1972 [7]. The release of apoptotic bodies from cell membrane is the final consequence of cell fragmentation during apoptosis. Apoptotic bodies have irregular shapes, ranging between 1 and 5 μm in size, and may contain intact organelles and fragmented DNA and histones which, according to Mathivanan et al. [5], are used as unique protein markers to identify these types of vesicles [6]. To date, there is no standard protocol for the isolation of apoptotic bodies [6].

Exosomes, which were first described in 1981 [8], are cup shaped and range from 30 to 100 nm in size. These are produced inside the cell before releasing from multivesicular bodies; they express typical endosomal compartment proteins [2]. However, it is possible that their cup-shaped morphology is the consequence of fixation procedures used for transmission electron microscopy (TEM) analysis [9], as TEM is the gold standard for determining the size of a vesicle. Exosomes are isolated through differential centrifugation followed by sucrose gradient ultracentrifugation,

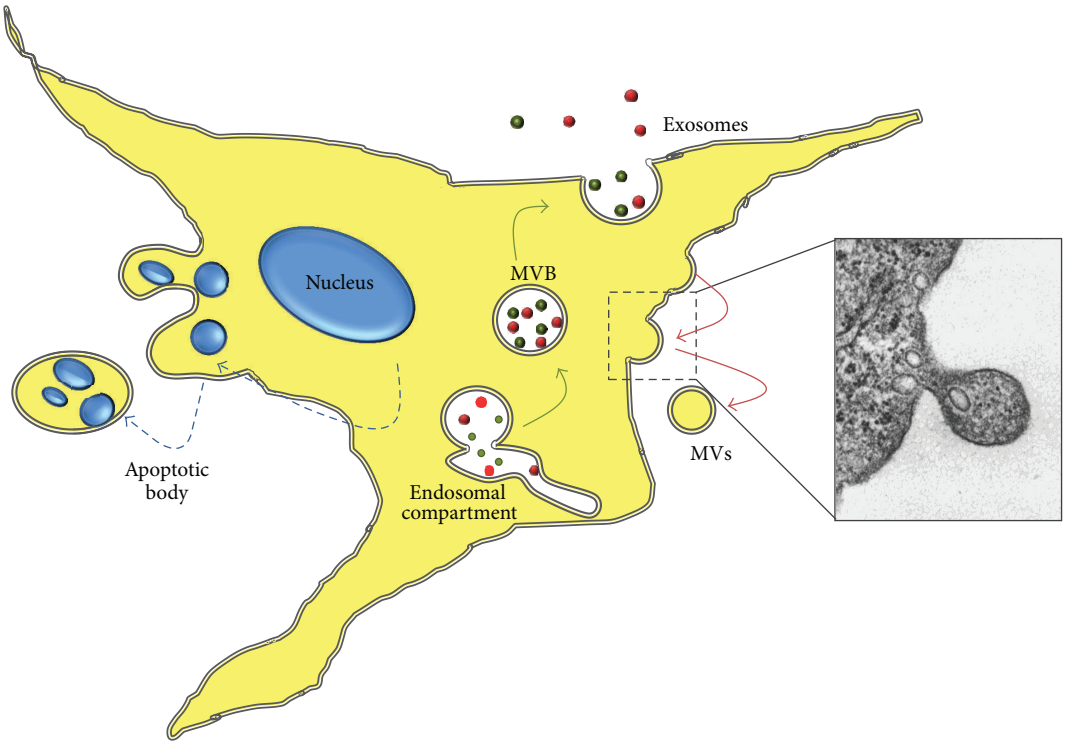

Figure 1: Schematic view of vesicles released from cells. Inset: microvesicle release from human fibroblast plasma membrane (personal original unpublished data).

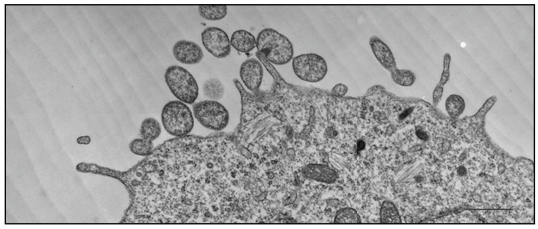

Figure 2: Transmission electron micrograph of the microvesicle shedding process from B16 mouse melanoma cells. Scale bar: 500 nm (personal original unpublished data).

for which their density is between 1.10 and 1.21 g/mL, or through immunoaffinity capture. Typical markers of exosomes include CD63, CD81, CD9, LAMP1, TSG101, Alix, and HSC70 [5]. In addition, exosome membranes are characterized by a low level of phosphatidylserine exposure. Other lipids found in these membranes include cholesterol, ceramide, and sphingomyelin, and lipid rafts are also contained within these membranes [5]. Exosomes have been mainly studied in cancer and immune cells [6]. The ability of exosomes to interact with cells may be due to several potential mechanisms, including direct cellular contact, which is mediated by the interaction of exosomal membranes with target cell receptors, the binding of exosomal membrane proteins released by protease-mediated cleavage to target cell surface receptors, and endocytosis by fusion with target cells [5, 10]. A multitude of pathways may then be activated following cellular interactions with exosomal molecules, including mRNA, microRNA (miRNA), and proteins (e.g., cytoskeletal proteins, heat shock proteins, adhesion molecules, tetraspanins, and proteins involved in signal transduction, transcription regulation, and antigen presentation); induced pathways basically depend on cellular origin of exosomes; exosomes from cancer cells, for example, modulate immune response, stimulate angiogenesis, and are involved in stroma remodeling contributing to tumor progression [5, 11, 12].

MVs were first described in 1964 [13] and have been intensively studied during the last two decades. These vesicles can have different shapes and range between 100 and 1,000 nm in size, although a low-end size cut-off has not been well established [5, 6]. MVs differ from exosomes, and in addition to their different size variations, the main difference between these types of vesicles is that MVs are formed by the regulated release from outward budding or blebbing of the plasma membrane (inset of Figures 1 and 2). These vesicles may also be isolated by differential centrifugation or capture-based assays [14, 15], and several proteins may be used as MV markers, including flotillin-2, selectins, integrins, CD40, and metalloproteinases [5, 16]; specific marker for MVs has not yet been identified. Moreover, MV membranes are characterized by a high level of exposure of phosphatidylserine, which is translocated from the inner to the outer surface leaflet [17].

Although no standard MV isolation protocols are available, most groups use centrifugation conditions ranging from 18,000 to 100,000 ×g for times ranging from 30 to 60 min

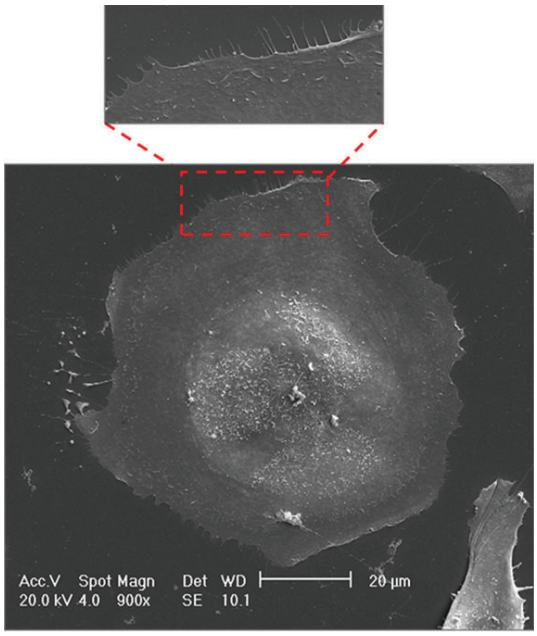

Figure 3: Scanning electron micrograph of human normal ovarian surface epithelium (OSE). The phenomenon of MV shedding is very much reduced in normal cells. Inset: there are no evident microvesicles at the edge of the normal cells (personal original unpublished data).

[6]. However, it is possible that these conditions pellet mixed vesicle populations because the size distribution of MVs overlaps with that of apoptotic bodies and exosomes at their upper and lower limits, respectively. For this reason, it may be appropriate to combine differential centrifugation with sucrose gradient ultracentrifugation to remove exosomes or to proceed by immunoisolation.

MV cargos include proteins, such as enzymes, growth factors, growth factor receptors, cytokines and chemokines [1], lipids, and nucleic acids, including mRNA, miRNA, ncRNA, and genomic DNA [18, 19]. Various studies of the molecular characterization of MVs have demonstrated similarities and differences with respect to the molecular composition of the cells of origin, suggesting that MVs are not simply miniature parental cells [1, 20]. For example, MVs in human glioma contain a plethora of proteins, cytokines, chemokines, and transcripts that are uniquely contained within vesicles and are undetectable (or expressed in different quantities) in the corresponding parental cells [19].

MVs have been widely studied in several normal cell types, including platelets, red blood cells, and endothelial cells, but have been primarily studied in cancer cells [6, 21, 22]. Importantly, MVs are more easily detectable after the acquisition of a tumorigenic phenotype, as they are shed at low levels in normal and parental cells [23]. In normal cells, indeed, shedding phenomenon occurs in very selected areas of plasma membrane (Figure 3), whereas in tumor cells, a lot of MVs are released from the entire cell surface (Figure 4(a)), especially from invading cellular edges (Figure 4(b)) (personal unpublished original data).

MVs play a role in many aspects of tumor progression, including the following.

(i) MVs contribute to the progression of cancer cells. The ability of a tumor cell to modify the extracellular matrix is important for enabling tumor progression and invasion, and MVs appear to promote the proteolytic cascade required for the localized degradation of the extracellular matrix through lytic enzymes such as uPA, MMPs, and cathepsins [24]. It has been demonstrated that cancer-derived MVs contain such proteases; for example, prostate carcinoma cell lines release MVs that reach uPA activity levels and are able to adhere to and degrade collagen IV and reconstitute the basal membrane (Matrigel) [25]. Furthermore, MVs from ovarian ascites are rich in MMPs and uPA, the activation of which leads to increased extracellular matrix degradation and facilitates tumor cell invasion and metastasis [26]. Ovarian cancer cell lines release lytic enzymes as well, and the amount and level of proteolytic activity associated with shed vesicles correlate with the *in vitro* invasiveness of cancer cells [23].

(ii) MVs are involved in tumorigenesis too. Indeed, the addition of MVs from PC3 cells (a human prostate cancer cell line with high metastatic potential) to the poorly invasive prostate cancer cell line LnCaP enhanced the adhesive and invasive capabilities of the latter cell type [25].

(iii) MVs help tumor cells evade apoptosis. Some MVs contain caspase 3, which is one of the main apoptotic enzymes. It has been postulated that tumor cells may escape apoptosis by preventing the intracellular accumulation of caspase 3 through the release of MVs containing this enzyme [27]. This hypothesis was confirmed by the observation that cells, if MV release is inhibited, accumulate caspase 3 and undergo apoptosis [28].

(iv) MVs contribute to the induction of transformation. It was demonstrated that glioma cancer cells could transfer through MVs a truncated, oncogenic form of EGFR to glioma cells lacking this receptor and that this transfer was able to transform recipient cells [11]. More recently, it was demonstrated that MVs derived from human cancer cells (i.e., breast carcinoma and glioma cells) may play an important role in oncogenesis, as they were shown to be capable of transforming normal fibroblasts and epithelial cells to adopt the typical cancer cell characteristics (e.g., anchorage-independent growth and enhanced survival capability) through the transfer of the cross-linking enzyme tissue-transglutaminase (tTG) [16].

(v) MVs promote drug resistance. It was reported that chemoresistant cancer cell lines express more genes related to shedding as compared to chemosensitive cells. Moreover, experiments using the chemotherapeutic agent doxorubicin confirmed the existence of drug accumulation and expulsion through MVs [29],

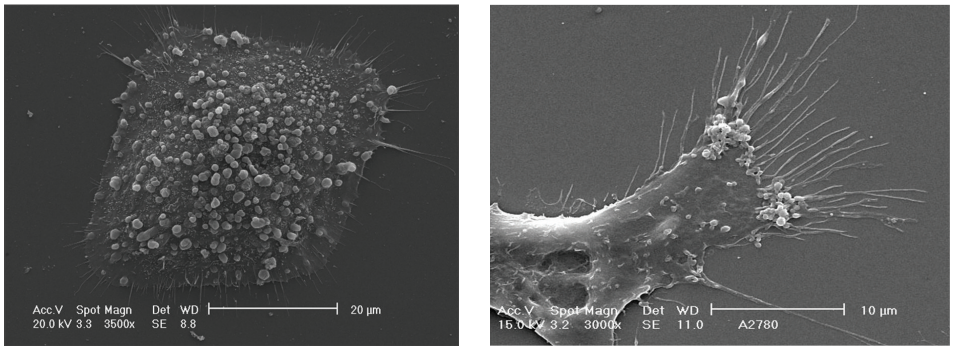

(a) (b)

Figure 4: Scanning electron micrograph of OVCA 432 (a) and A2780 (b). It's evident the enormous release of microvesicles with heterogeneous dimensions ranged between 300–100 nm. (a) The microvesicles shedding is visible on whole cell body in OVCA 432; (b) the phenomenon is more evident at the edge of cells (personal original unpublished data).

which suggests that MVs released from tumor cells contribute to cellular survival.

(vi) MVs contribute to immunoescape. There are many examples demonstrating how the shedding of MVs mediates interactions between cancer and immune cells to modulate the immune response. MVs released from some cancer cells, such as those of oral cancer, can act as carriers for Fas ligand, which induces apoptosis in T-cells and prevents their cytotoxic effects on tumor cells [30–32]. Moreover, MVs released from human melanoma and colorectal carcinoma cells following fusion with monocytes inhibited differentiation and promoted immunosuppressive cytokine release in the monocytes [32]. Furthermore, some cancer cells (such as squamous cell carcinoma) use MVs to escape from complement-induced lysis; the release of MVs containing CD46, a membrane complement inhibitor cofactor protein, can inactivate complement complexes by inducing the inactivation of C4b and C3b [33].

(vii) MVs promote the induction of angiogenesis. It is well known that tumor growth and survival depends on the formation of new blood vessels that infiltrate the tumor mass [34]. MVs shed from tumor cells may transmit proangiogenic stimuli to endothelial cells through various mechanisms; for example, proangiogenic cargo may be released into the tumor microenvironment or directly transferred to recipient endothelial cells [1]. Some studies have demonstrated that cancer cell MVs can induce the secretion of several proangiogenic factors in stromal fibroblasts to induce endothelial cell proliferation and therefore angiogenesis [35]. It has also been demonstrated that MVs released from tumor cells bearing the EGFR are able to activate the VEGF/VEGFR pathway in endothelial cells [36]. MVs are a rich source of the MMP stimulant EMMPRIN, which is able to promote the angiogenic ability of endothelial cells [37], the proangiogenic growth factor VEGF, FGF-2 [22, 38], and proteases (e.g., uPA, MMPs, and cathepsin B) [15, 22, 25, 39]. Degradation of the basal membrane and extracellular matrix via the actions of lytic enzymes favors angiogenesis and new vessel formation [40]. Moreover, cancer cell-released MVs may contain several molecules (such as sphingomyelin) which could reprogram the endothelial cell response and stimulate their angiogenic ability [41, 42]. Alternatively, cancer-derived MVs taken up by endothelial cells can turn on VEGF production, inducing autocrine stimulation [36].

In summary, it is clear that MVs are able to directly and indirectly modulate the behavior of surrounding cells through their delivery of proteins and nucleic acids. Moreover, the effects that MVs have on target cells have been extensively studied, although it remains unclear how MVs interact with target cells, that is, whether they fuse with the plasma membrane or are taken up by endocytosis.

2. MV Isolation from Biological Fluids

The quantity and molecular characteristics of circulating MVs reflect not only their cellular origin but also the stimulus that triggered their release. Thus, the isolation and analysis of circulating MVs, which are released into bodily fluids exposed to primary tumors (e.g., blood, urine, saliva, ascites, pleural effusion, and spinal fluid), may provide the opportunity to assess pathological and cancer-related biological information. Furthermore, this type of analysis may enable rapid and repeated evaluation without the need for invasive procedures such as surgical biopsy, which can be affected by sampling error [1, 18, 43]. MVs have also been studied to identify a potential association with the prognosis of several pathologies, including thrombosis, sepsis, coronary artery syndrome, multiple sclerosis, and some cancer types [44–48].

As a result of studies in which it was assessed the half-life in the bloodstream of labeled MVs, it has been hypothesized that MVs have a lifespan of about 15–60 min in the blood circulation [49, 50]; the rapid elimination could be because they are rapidly taken up by recipient cells. It is also possible

that other forms of bioelimination may exist, for example, due to the interaction of phosphatidylserine exposed on their surface with phagocytic system. Nevertheless, it is not possible to exclude the possibility that biological activities of MVs may persist long enough (some days perhaps) giving the chance to perform desired analysis [1].

To date, there are no validated methods for the isolation, identification, characterization, or detection/quantification of circulating MVs. Moreover, it must be noted that the presence of MVs derived from nontumor cells in bodily fluids may be a further complicating factor that requires the development of strategies enabling selectively isolate tumor-derived MVs, which may represent a relatively small fraction of the total number of isolated MVs [18]. The lack of adequate validation methods greatly limits the potential use of MVs as clinical markers, although several studies have been conducted to assess the reliability of this approach [43, 51–54].

It appears to be important to standardize the pre-analytical procedures in order to study biological fluids, as centrifugation procedures or the choice of a specific anticoagulant may affect the reproducibility of MV analyses. Time and storage temperature may also be critical parameters, although the freezing of plasma (useful for large scale analysis) for more than one year was shown to minimally affect the recovery of MVs [43]. Two main strategies have been proposed for the isolation of MVs, and these include techniques based on MV physical properties and those based on MV biochemical features. In the former approach, size and density are used as reference parameters, and serial centrifugations and flotation in sucrose gradients, which is occasionally combined with size-exclusion chromatography, are mainly used, although size discrimination based on dielectrophoresis sorting has been employed as well. In the latter approach, magnetophoretic sorting or immunoaffinity chromatography are used [18].

Cytometry is the most widely used method to detect and quantify MVs in biological fluids because it uses both size and affinity measurements (through conjugation with specific fluorescent antibodies). The number of MVs is important because these numbers seem to correlate with various pathologies and nonphysiological conditions and may aid in the diagnosis and determination of prognosis of these conditions. However, it must be noted that vesicles smaller than 200 nm cannot be distinguished from instrumental noise; thus, exosomes and smaller MVs cannot be detected using this technique. Nevertheless, there have been many studies that have standardized and improved MV analysis through the use of flow cytometry [6, 55, 56]. More recently, a novel strategy based on the differential light scattering of different size particles solved in a fluid medium (NanoSight) has been used to detect and quantify MVs [18].

Initially, annexin V was used as a marker for MVs; however, evidence for a substantial proportion of annexin V-negative MVs was found [6, 57]. Thus, alternative labeling was proposed based on the cellular source of the MVs [4, 58, 59].

3. MVs as Cancer Biomarkers

A biomarker, or biological marker, is a substance whose detection is used as an indicator of a biological state and whose changes are correlated with the progression or the response of the disease to a given therapeutic treatment. Ideally, a biomarker should be specifically associated with a particular disease. Consequently, it should be able to discriminate between two pathological or physiological conditions even if they are similar. It would also be convenient if the biomarker could be identified in a biological sample that is easily obtainable, for example, blood, urine, or saliva. Moreover, biomarker expression levels should be able to predict aspects of the corresponding pathological/physiological condition. Moreover, for routine use, noninvasive detection methods that are accurate, fast, and potentially inexpensive should exist [60].

As previously mentioned, many studies have been conducted to better understand the role of circulating MVs in various clinical conditions. The best characterized MVs are those derived from platelets and endothelial cells, and their alterations (mainly elevated levels) are involved in numerous clinical disorders such as cardiovascular diseases (e.g., hypertension, atherosclerosis, and congestive heart failure) [61–63], autoimmune diseases (e.g., rheumatoid arthritis, vasculitis, type I diabetes mellitus, and multiple sclerosis) [64–67], and hematological and cerebrovascular diseases [68, 69].

However, in recent years, tumor MVs have gained attention as potential biomarkers because tumor cells are able to constitutively release large amounts of MVs bearing tumor-specific antigens into the bloodstream and other bodily fluids. For example, solid tumors that are difficult to reach and detect may reveal their presence by releasing MVs, and the presence of tumor-derived MVs in biological fluids may also be useful for detecting metastases [70]. Moreover, in addition to protein antigens, MVs are able to carry RNAs, particularly miRNAs. miRNAs and other molecular features of MVs represent a unique combination representative of the cancer cells from which they were derived [20]; thus, their presence in cancer-derived MVs may serve as a novel source of disease-related information and possibly as unique, specific, and identifiable cancer biomarkers that may prove useful for screening and diagnosis [1]. Tumor-specific markers, such as mucin in adenocarcinoma, may also be used in the early detection of cancers [27].

MVs have been detected in the circulation of patients with several cancers, such as breast, ovarian, lung, prostate, colorectal, and gastric cancers [27]. In gastric cancer, MVs are notably increased in patients with stage IV disease. MV levels are also elevated in cancers with associated thromboses, such as colorectal carcinoma, breast cancer, and pancreatic adenocarcinoma [71, 72]. In patients with bladder cancer, MVs were isolated from urine and were identified eight proteins whose levels were elevated with respect to healthy controls, which indicated that the protein composition of urine MVs could be used for the early detection of this pathology [73]. MVs from patients with glioblastoma demonstrated high levels of CD133 and the transcript encoding the oncogenic

form of EGFRvIII. Furthermore, it is intriguing that tumor removal correlates with the disappearance of circulating MVs [19, 74] and that MVs may maintain proteins with the same functional state (e.g., phosphorylation) as those typical of their parental cancer cells. This property may be potentially utilized to follow the effects of some anticancer drugs [40].

Some studies have been conducted to assess the use of MVs in prognosis too; in patients with disseminated breast and pancreatic cancer with higher levels of TF (Tissue Factor) and MUC1 (epithelial mucin) in MVs was shown a lower survival rate at 3–9 months followup compared to those with low TF-activity and no MUC1 expression [71]. In patients with hormone-refractory prostate cancer, platelet MVs levels were predictive of outcome; overall survival was significantly shorter in those patients with MVs level above the cut-off compared to those patients whose level was below it [75]. Patients with gastric cancer at stage IV showed higher levels of MVs compared to controls, and plasma levels might be useful to predict metastasis formation [72].

In the future, the use of MVs as serum biomarkers may facilitate cancer diagnosis in controversial cases and help to avoid the use of invasive procedures, primarily those involving surgical biopsies of organs in which repeated biopsies are unrealistic (e.g., the pancreas, ovaries, or central nervous system) [18]. It has been hypothesized that because the molecular profiles of cancer cells change with disease progression, MVs may be useful for disease staging or even to evaluate the response to therapy by permitting an accurate assessment of a patient's responsiveness and personalization of treatment [18]. The analysis of MVs may also be used to detect tumor recurrence [18, 70]. Moreover, if we assume that MVs are representative of the molecular features of the parental cancer cells, their profiling may be useful for creating targeted and personalized anticancer therapies. For example, in some tumors, including ovarian, breast, and gastric cancers, the level of the HER-2/neu oncogenic receptor was elevated, and the protein was detected in MVs in the serum, which suggests that these patients may benefit from current therapeutic treatments targeting HER-2 [18, 76].

Although the results presented to date are undoubtedly promising, further investigation is required to determine the feasibility of the use of MVs as circulating cancer biomarkers. Furthermore, the routine use of MVs in diagnosis and prognosis requires some additional precautionary notes. First, the development of sensible instruments is needed to be able to isolate all of the MVs from an analyzed sample (e.g., the blood or other bodily fluids exposed to tumors). Second, because samples will contain MVs derived from nontumor cells, advanced strategies with greater specificity are needed to target and isolate pathological MVs that may be diluted in the biological sample.

4. MV-Associated miRNAs as Possible Biomarkers for Human Ovarian Cancer

Ovarian cancers comprise a heterogeneous group of neoplasias that are mostly epithelial cancers characterized by mucinous, serous, endometrioid, and clear cell subtypes and are derived from ovarian surface epithelium or inclusion cysts. However, these cancers also include sarcomas and sex-cord stromal, germ cell, and mixed tumors, which may be rare [77]. Ovarian cancer is the most lethal gynecologic malignancy and is characterized by poor prognosis with an overall 5-year survival rate of approximately 50%. If the cancer is diagnosed while confined to the ovary, the 5-year survival rate could become 90%, but this occurs only in a small percentage of patients (approximately 20%) [78, 79]. Ovarian cancer can be identified at the following four stages: stage I, the cancer is limited to one or both ovaries; stage II, the cancer is present in one or both ovaries as well as in pelvic extensions or implants; stage III, peritoneal implants are present outside of the pelvis or are limited to the pelvis with an extension to the small bowel or omentum, and there may also be metastasis on the liver surface; stage IV, distant metastases to the parenchymal compartment of the liver or outside of the peritoneal cavity are present [80].

The ovarian cancer diagnosis is often delayed because the first specific symptoms, which are mainly related to the presence of large tumors or extensive ascites, appear only during an advanced disease stage [81–83]. However, early diagnosis is fundamental for offering patients a better chance of being cured using available therapies, such as surgery or, in some cases, chemotherapy with the combination of platinum and taxane. The more a tumoral mass is reduced by surgery, the more often the following chemotherapy is effective [84]. Unfortunately, tumor recurrence frequently occurs, and patients can develop resistance to additional therapies [79].

Currently, imaging methods such as computer tomography-positron emission tomography (CT-PET), fluorodeoxyglucose-PET (FDG-PET), magnetic resonance, transvaginal and transabdominal sonography, and the serum marker CA 125 are used as diagnostic tools [79]. CA 125 is undoubtedly the most carefully studied and extensively used biomarker despite being characterized as having low sensitivity and specificity [85]. Many gynecologic and nongynecologic pathological conditions showed increased serum levels for this marker such as endometriosis and adenomyosis, pelvic, peritoneal, pleural, and musculoskeletal inflammatory diseases, hepatitis, and pancreatitis [81, 86]. In addition, physiological conditions such as menstruation or pregnancy can be associated with elevated CA 125 levels [81], and it should be noted that the CA 125 level remains normal in some women with ovarian cancer [81].

Biomarker specificity is fundamental to be sure that the patient really has this specific pathology, because a definitive diagnosis often requires abdominal surgery; thus, there can be a great negative impact on women who have false-positive results [87]. CA 125 remains the most effective biomarker despite studies that have searched for alternative and potentially useful serum biomarkers, including CA 19-9, CA 15-3, CA 72-4, CEA, HE4, lysophosphatidic acid (LPA), Haptoglobin-α (HP-α), Bikunin, and OVX1 [81, 87]. With the exception of HE4, which appears to have high sensitivity even at early stages, all of these markers have shown disadvantages, such as poor correlation with the clinical course or low

specificity [81]. In fact, no other ovarian cancer serum marker appears to be able to replace or complement CA 125, which highlights the need to find a novel marker for this disease. Furthermore, the discovery of alternative serum biomarkers for early diagnosis is vitally important.

One new insight into ovarian cancer biomarker identification occurred after the discovery of miRNAs. miRNAs are small (19–25 nucleotides), single-stranded, noncoding RNAs that are responsible for gene expression regulation at the posttranscriptional level. In animals, miRNAs act by inhibiting mRNA translation at the initiation or elongation step, which blocks the translation of mRNAs from several important genes into corresponding proteins [88]. Their regulatory functions mainly affect cell proliferation and differentiation and cell cycle regulation [89]. It has been widely shown that abnormal miRNA levels are associated with many pathologies, including cardiovascular disease, diabetes, rheumatoid arthritis, and cancer [90]. The role of miRNAs in cancer has been discussed in several studies, and a substantial number of miRNAs, which normally act as tumor suppressors, are downregulated in cancer cells. In contrast, some miRNAs that normally act as oncogenes are expressed at higher levels in cancer cells. The consequences of these changes in miRNA levels include the altered expression of target oncogenes and tumor suppressor genes, which are undoubtedly involved in carcinogenesis [81].

In several cancers, including ovarian cancer, it has been demonstrated that the expression of a specific subset of miRNAs may potentially be used in clinical practice, for example, for screening or early diagnosis to evaluate the response to therapeutic treatments [91, 92]. It was also demonstrated that miRNA profiles can be used to distinguish between various histological ovarian cancer subtypes [93], and some profiles also appear to be closely related to early relapse in patients with advanced-stage tumors [94]. Furthermore, some miRNAs are consistently and significantly overexpressed in ovarian cancer, including miRNAs belonging to the miR-200 family (i.e., miR-200a, miR-200c, and miR-200b), whereas miRNAs of the let-7 family, miR-140, miR-145, and miR-125b1 are consistently downregulated in ovarian cancer. Altered expression has also been reported for other miRNAs, such as miR-21, miR-99a, miR-125b, and miR-199a [78, 93, 95] (Table 1). Moreover, a correlation between miRNA features and chemoresponse was also reported in other cancers, including leukemia, colorectal adenocarcinoma, and breast, pancreatic, and lung cancers, which indicates the potential use of miRNAs for diagnosis and predicting patient survival rates and risk of recurrence [78, 96–101]. It is interesting to note that miRNAs can be detected in the bloodstream; however, for stable expression, miRNAs must be protected from RNases, which are abundant in the blood and are able to degrade approximately 99% of RNA species within 15 min [102]. Thus, it is not surprising that miRNAs in serum are contained in apoptotic bodies, exosomes, and MVs [81]. The association between miRNA profiles and cancer type and stage, as well as the stability of miRNAs in the blood and other biological fluids, makes them hypothetically useful markers for early cancer diagnosis. These findings can be applied to ovarian cancer as well, as

Table 1: A list of miRNAs with altered expression in ovarian cancer.

miRNAs altered	References mentioning upregulation	References mentioning downregulation
let-7a/b/c/d/e/f		[101, 107–109]
miR-10a		[109]
miR-10b		[110]
miR-16	[110]	
miR-20a	[110]	
miR-21	[105, 109, 110]	[107]
miR-23a/b	[110]	
miR-26a		[108, 110]
miR-26b	[108]	
miR-27a	[110]	
miR-29a	[101, 105, 109]	[110]
miR-29c	[107, 109]	
miR-92	[105]	
miR-93	[105]	
miR-99a	[107, 108]	[110]
miR-103	[108, 109]	
miR-106b	[109]	[107]
miR-122		[107]
miR-125a		[110]
miR-125b	[109, 111]	[101]
miR-125b1	[93]	
miR-126	[105]	
miR-127		[105, 108]
miR-130a		[111]
miR-134		[107, 108]
miR-140		[93]
miR-141	[109, 110]	[107]
miR-143		[109]
miR-145		[93, 109, 110]
miR-146b	[109]	
miR-155		[107]
miR-182	[108, 109]	
miR-199a	[101, 107]	[93]
miR-200a/b/c	[93, 95, 101, 109, 110]	
miR-214	[101]	[110]
miR-221	[107]	
miR-222		[95, 108]
miR-296	[107]	
miR-302d	[101]	
miR-320	[101]	
miR-335		[111]
miR-346		[107]
miR-410		[108]

Table 1: Continued.

miRNAs altered	References mentioning upregulation	References mentioning downregulation
miR-422a	[109]	[107]
miR-424	[101]	
miR-432		[108]
miR-494	[107]	[101]
miR-508	[107]	[109]
miR-519a		[107]
miR-648		[107]
miR-662		[107]
miR-663	[107]	

it was demonstrated that exosome-associated miRNAs may serve as novel serum diagnostic biomarkers [103]. It was convincingly demonstrated that the miRNA signatures of exosomes released from tumors in the bloodstream were distinct from those observed in patients with benign disease and could be strongly correlated with the ovarian cancer stage of the patient. The level of detectable miRNA is significantly increased in women with invasive ovarian cancer compared to healthy patients or women with benign ovarian cancer [104, 105]. Also, the levels of tumor-derived exosomes in the bloodstream increase with increasing disease stage [105].

It should also be noted that MVs released from ovarian cancer cells may be present in biological fluids, like exosomes. Some years ago, it was demonstrated that ovarian cancer cells are able to release a large amount of MVs *in vivo* [106]. In addition, a study conducted on biological fluids obtained from patients with gynecological diseases demonstrated that benign and tumor fluids contained MVs, but that malignant tumor fluids were found to have a larger quantity of vesicles than fluids from nonmalignant pathologies (e.g., ovarian serous cysts, mucinous cystoadenomas, and fibromas). Moreover, tumor progression has been shown to correlate with an increase in MVs abundance in ascitic fluids. Importantly, increases in MVs levels appear to occur several months prior to elevation of CA 125 in serum, which further suggests that MVs have the potential to serve as early biomarkers [106]. In addition, it should be highlighted that the miRNA features of ovarian cancer-derived MVs may be useful as well, as the analysis of such MVs demonstrates distinct miRNA signatures associated with ovarian cancer (our unpublished data).

5. Conclusion

To date, very few molecules, particularly CA 125, are used as routine ovarian tumor markers. For this reason, many novel serum biomarkers are under investigation for use as diagnostic and prognostic tools to evaluate the therapeutic treatment response. Because cancer cells may release MVs into the bloodstream that contain similar miRNA characteristics as the cells from which they originated, miRNA signatures appear to be promising tools for the ovarian cancer field. It has also become evident that MVs may represent an ideal biomarker for ovarian cancer diagnosis and prognosis. However, additional ovarian cancer-derived MV characteristics should be evaluated to confirm this intriguing hypothesis. Furthermore, it is necessary to develop the ability to isolate and quantify tumor derived-MVs from the blood and other biological fluids.

Abbreviations

CEA: Carcino-embryonicantigen
CT-PET: Computertomography-positronemissiontomography
EGFR: Epidermalgrowthfactorreceptor
EMMPRIN: Extracellularmatrixmetalloproteinaseinducer
FDG-PET: Fluorodeoxyglucose-positronemissiontomography
FGF-2: Fibroblastgrowthfactor-2
HE4: Humanepididymisprotein4
HER-2: Humanepidermalgrowthfactorreceptor2
HP-α: Haptoglobin-α
HSC70: Heatshockcognate71 kDaprotein
LAMP-1: Lysosomal-associatedmembraneprotein1
LPA: Lysophosphatidicacid
miRNA: MicroRNA
MMPs: Matrixmetalloproteinases
MVs: Microvesicles
ncRNA: NoncodingRNA
TEM: Transmissionelectronmicroscopy
TSG101: Tumorsusceptibilitygene101
tTG: Tissue-transglutaminase
uPA: Urokinase-typeplasminogenactivator
VEGF: Vascularendothelialgrowthfactor
VEGFR: Vascularendothelialgrowthfactorreceptor.

Acknowledgment

The authors thank Dr. Enzo Emanuele, a holder of both the M.D. and Ph.D. degrees (Living Research s.a.s., Robbio, Pavia, Italy), for his expert editorial assistance.

References

[1] J. Rak, "Microparticles in cancer," *Seminars in Thrombosis and Hemostasis*, vol. 36, no. 8, pp. 888–906, 2010.

[2] J. A. Schifferli, "Microvesicles are messengers," *Seminars in Immunopathology*, vol. 33, no. 5, pp. 393–394, 2011.

[3] E. Shai and D. Varon, "Development, cell differentiation, angiogenesis-microparticles and their roles in angiogenesis," *Arteriosclerosis, Thrombosis, and Vascular Biology*, vol. 31, no. 1, pp. 10–14, 2011.

[4] A. K. Enjeti, L. F. Lincz, and M. Seldon, "Microparticles in health and disease," *Seminars in Thrombosis and Hemostasis*, vol. 34, no. 7, pp. 683–691, 2008.

[5] S. Mathivanan, H. Ji, and R. J. Simpson, "Exosomes: extracellular organelles important in intercellular communication," *Journal of Proteomics*, vol. 73, no. 10, pp. 1907–1920, 2010.

[6] B. Gyorgy, K. Modos, E. Pallinger et al., "Detection and isolation of cell-derived microparticles are compromised by protein complexes due to shared biophysical parameters," *Blood*, vol. 117, no. 4, pp. e39–e48, 2011.

[7] J. F. Kerr, A. H. Wyllie, and A. R. Currie, "Apoptosis: a basic biological phenomenon with wide-ranging implications in tissue kinetics," *British Journal of Cancer*, vol. 26, no. 4, pp. 239–257, 1972.

[8] E. G. Trams, C. J. Lauter, N. Salem, and U. Heine, "Exfoliation of membrane ecto-enzymes in the form of micro-vesicles," *Biochimica et Biophysica Acta*, vol. 645, no. 1, pp. 63–70, 1981.

[9] C. Théry, S. Amigorena, G. Raposo, and A. Clayton, "Isolation and characterization of exosomes from cell culture supernatants and biological fluids," *Current Protocols in Cell Biology*, vol. 3, p. 3.22, 2006.

[10] C. Théry, M. Ostrowski, and E. Segura, "Membrane vesicles as conveyors of immune responses," *Nature Reviews*, vol. 9, no. 8, pp. 581–593, 2009.

[11] K. Al-Nedawi, B. Meehan, J. Micallef et al., "Intercellular transfer of the oncogenic receptor EGFRvIII by microvesicles derived from tumour cells," *Nature Cell Biology*, vol. 10, no. 5, pp. 619–624, 2008.

[12] H. Valadi, K. Ekström, A. Bossios, M. Sjöstrand, J. J. Lee, and J. O. Lötvall, "Exosome-mediated transfer of mRNAs and microRNAs is a novel mechanism of genetic exchange between cells," *Nature Cell Biology*, vol. 9, no. 6, pp. 654–659, 2007.

[13] E. Chargaff and R. West, "The biological significance of the thromboplastic protein of blood," *Journal of Biological Chemistry*, vol. 166, no. 1, pp. 189–197, 1946.

[14] B. Hugel, F. Zobairi, and J. M. Freyssinet, "Measuring circulating cell-derived microparticles," *Journal of Thrombosis and Haemostasis*, vol. 2, pp. 1846–1847, 2004.

[15] V. Dolo, A. Ginestra, G. Ghersi, H. Nagase, and M. L. Vittorelli, "Human breast carcinoma cells cultured in the presence of serum shed membrane vesicles rich in gelatinolytic activities," *Journal of Submicroscopic Cytology and Pathology*, vol. 26, no. 2, pp. 173–180, 1994.

[16] M. A. Antonyak, B. Li, L. K. Boroughs et al., "Cancer cell-derived microvesicles induce transformation by transferring tissue transglutaminase and fibronectin to recipient cells," *Proceedings of the National Academy of Sciences of the United States of America*, vol. 108, no. 12, pp. 4852–4857, 2011.

[17] B. Hugel, M. C. Martínez, C. Kunzelmann, and J. M. Freyssinet, "Membrane microparticles: two sides of the coin," *Physiology*, vol. 20, pp. 22–27, 2005.

[18] C. D'Souza-Schorey and J. W. Clancy, "Tumor-derived microvesicles: shedding light on novel microenvironment modulators and prospective cancer biomarkers," *Genes & Development*, vol. 26, no. 12, pp. 1287–1299, 2012.

[19] J. Skog, T. Würdinger, S. van Rijn et al., "Glioblastoma microvesicles transport RNA and proteins that promote tumour growth and provide diagnostic biomarkers," *Nature Cell Biology*, vol. 10, no. 12, pp. 1470–1476, 2008.

[20] S. F. Mause and C. Weber, "Microparticles: protagonists of a novel communication network for intercellular information exchange," *Circulation Research*, vol. 107, no. 9, pp. 1047–1057, 2010.

[21] G. Taraboletti, S. D'Ascenzo, P. Borsotti, R. Giavazzi, A. Pavan, and V. Dolo, "Shedding of the matrix metalloproteinases MMP-2, MMP-9, and MT1-MMP as membrane vesicle-associated components by endothelial cells," *American Journal of Pathology*, vol. 160, no. 2, pp. 673–680, 2002.

[22] V. Dolo, S. D'Ascenzo, I. Giusti, D. Millimaggi, G. Taraboletti, and A. Pavan, "Shedding of membrane vesicles by tumor and endothelial cells," *Italian Journal of Anatomy and Embryology*, vol. 110, no. 2, pp. 127–133, 2005.

[23] A. Ginestra, M. D. la Placa, F. Saladino, D. Cassarà, H. Nagase, and M. L. Vittorelli, "The amount and proteolytic content of vesicles shed by human cancer cell lines correlates with their in vitro invasiveness," *Anticancer Research*, vol. 18, no. 5, pp. 3433–3437, 1998.

[24] J. M. Inal, E. A. Ansa-Addo, D. Stratton et al., "Microvesicles in health and disease," *Archivum Immunologiae et Therapiae Experimentalis*, vol. 60, no. 2, pp. 107–121, 2012.

[25] A. Angelucci, S. D'Ascenzo, C. Festuccia et al., "Vesicle-associated urokinase plasminogen activator promotes invasion in prostate cancer cell lines," *Clinical and Experimental Metastasis*, vol. 18, no. 2, pp. 163–170, 2000.

[26] L. E. Graves, E. V. Ariztia, J. R. Navari, H. J. Matzel, M. S. Stack, and D. A. Fishman, "Proinvasive properties of ovarian cancer ascites-derived membrane vesicles," *Cancer Research*, vol. 64, no. 19, pp. 7045–7049, 2004.

[27] F. F. van Doormaal, A. Kleinjan, M. Di Nisio, H. R. Büller, and R. Nieuwland, "Cell-derived microvesicles and cancer," *Netherlands Journal of Medicine*, vol. 67, no. 7, pp. 266–273, 2009.

[28] M. N. Abid Hussein, A. N. Böing, A. Sturk, C. M. Hau, and R. Nieuwland, "Inhibition of microparticle release triggers endothelial cell apoptosis and detachment," *Thrombosis and Haemostasis*, vol. 98, no. 5, pp. 1096–1107, 2007.

[29] K. Shedden, X. T. Xie, P. Chandaroy, Y. T. Chang, and G. R. Rosania, "Expulsion of small molecules in vesicles shed by cancer cells: association with gene expression and chemosensitivity profiles," *Cancer Research*, vol. 63, no. 15, pp. 4331–4337, 2003.

[30] V. Huber, S. Fais, M. Iero et al., "Human colorectal cancer cells induce T-cell death through release of proapoptotic microvesicles: role in immune escape," *Gastroenterology*, vol. 128, no. 7, pp. 1796–1804, 2005.

[31] W. K. Jeong, E. Wieckowski, D. D. Taylor, T. E. Reichert, S. Watkins, and T. L. Whiteside, "Fas ligand-positive membranous vesicles isolated from sera of patients with oral cancer induce apoptosis of activated T lymphocytes," *Clinical Cancer Research*, vol. 11, no. 3, pp. 1010–1020, 2005.

[32] R. Valenti, V. Huber, M. Iero, P. Filipazzi, G. Parmiani, and L. Rivoltini, "Tumor-released microvesicles as vehicles of immunosuppression," *Cancer Research*, vol. 67, no. 7, pp. 2912–2915, 2007.

[33] M. B. Whitlow and L. M. Klein, "Response of SCC-12F, a human squamous cell carcinoma cell line, to complement attack," *Journal of Investigative Dermatology*, vol. 109, no. 1, pp. 39–45, 1997.

[34] P. Carmeliet, "Angiogenesis in life, disease and medicine," *Nature*, vol. 438, no. 7070, pp. 932–936, 2005.

[35] D. G. Tang and C. J. Conti, "Endothelial cell development, vasculogenesis, angiogenesis, and tumor neovascularization: an update," *Seminars in Thrombosis and Hemostasis*, vol. 30, no. 1, pp. 109–117, 2004.

[36] K. Al-Nedawi, B. Meehan, R. S. Kerbel, A. C. Allison, and A. Rak, "Endothelial expression of autocrine VEGF upon the uptake of tumor-derived microvesicles containing oncogenic EGFR," *Proceedings of the National Academy of Sciences of the United States of America*, vol. 106, no. 10, pp. 3794–3799, 2009.

[37] D. Millimaggi, M. Mari, S. D'Ascenzo et al., "Tumor vesicle-associated CD147 modulates the angiogenic capability of endothelial cells," *Neoplasia*, vol. 9, no. 4, pp. 349–357, 2007.

[38] G. Taraboletti, S. D'Ascenzo, I. Giusti et al., "Bioavailability of VEGF in tumor-shed vesicles depends on vesicle burst induced by acidic pH 1," *Neoplasia*, vol. 8, no. 2, pp. 96–103, 2006.

[39] I. Giusti, S. D'Ascenzo, D. Millimaggi et al., "Cathepsin B mediates the pH-dependent proinvasive activity of tumor-shed microvesicles," *Neoplasia*, vol. 10, no. 5, pp. 481–488, 2008.

[40] T. H. Lee, E. D'Asti, N. Magnus, K. Al-Nedawi, B. Meehan, and J. Rak, "Microvesicles as mediators of intercellular communication in cancer-the emerging science of cellular "debris"," *Seminars in Immunopathology*, vol. 33, no. 5, pp. 455–467, 2011.

[41] G. Camussi, M. C. Deregibus, S. Bruno et al., "Exosoome/microvesicle-mediated epigenetic reprogramming of cells," *American Journal of Cancer Research*, vol. 1, no. 1, pp. 98–110, 2011.

[42] C. W. Kim, H. M. Lee, T. H. Lee et al., "Extracellular membrane vesicles from tumor cells promote angiogenesis via sphingomyelin," *Cancer Research*, vol. 62, pp. 6312–6317, 2002.

[43] M. Jayachandran, V. M. Miller, J. A. Heit, and W. G. Owen, "Methodology for isolation, identification and characterization of microvesicles in peripheral blood," *Journal of Immunological Methods*, vol. 375, no. 1-2, pp. 207–214, 2012.

[44] B. Toth, S. Liebhardt, K. Steinig et al., "Platelet-derived microparticles and coagulation activation in breast cancer patients," *Thrombosis and Haemostasis*, vol. 100, no. 4, pp. 663–669, 2008.

[45] J. I. Zwicker, H. A. Liebman, D. Neuberg et al., "Tumor-derived tissue factor-bearing microparticles are associated with venous thromboembolic events in malignancy," *Clinical Cancer Research*, vol. 15, no. 22, pp. 6830–6840, 2009.

[46] M. J. VanWijk, E. VanBavel, A. Sturk, and R. Nieuwland, "Microparticles in cardiovascular diseases," *Cardiovascular Research*, vol. 59, no. 2, pp. 277–287, 2003.

[47] R. J. Berckmans, R. Nieuwland, A. N. Böing, F. P. Romijn, C. E. Hack, and A. Sturk, "Cell-derived microparticles circulate in healthy humans and support low grade thrombin generation," *Thrombosis and Haemostasis*, vol. 85, no. 4, pp. 639–646, 2001.

[48] K. Joop, R. J. Berckmans, R. Nieuwland et al., "Microparticles from patients with multiple organ dysfunction syndrome and sepsis support coagulation through multiple mechanisms," *Thrombosis and Haemostasis*, vol. 85, no. 5, pp. 810–820, 2001.

[49] P. L. Gross, B. C. Furie, G. Merrill-Skoloff, J. Chou, and B. Furie, "Leukocyte-versus microparticle-mediated tissue factor transfer during arteriolar thrombus development," *Journal of Leukocyte Biology*, vol. 78, no. 6, pp. 1318–1326, 2005.

[50] G. M. Thomas, L. Panicot-Dubois, R. Lacroix et al., "Cancer cell-derived microparticles bearing P-selectin glycoprotein ligand 1 accelerate thrombus formation in vivo," *Journal of Experimental Medicine*, vol. 206, no. 9, pp. 1913–1927, 2009.

[51] Y. Yuana, T. H. Oosterkamp, S. Bahatyrova et al., "Atomic force microscopy: a novel approach to the detection of nanosized blood microparticles," *Journal of Thrombosis and Haemostasis*, vol. 8, no. 2, pp. 315–323, 2010.

[52] Y. Yuana, R. M. Bertina, and S. Osanto, "Pre-analytical and analytical issues in the analysis of blood microparticles," *Journal of Thrombosis and Haemostasis*, vol. 105, no. 3, pp. 396–408, 2011.

[53] A. E. Michelsen, R. Wergeland, O. Stokke, and F. Brosstad, "Development of a time-resolved immunofluorometric assay for quantifying platelet-derived microparticles in human plasma," *Thrombosis Research*, vol. 117, no. 6, pp. 705–711, 2006.

[54] W. Jy, L. L. Horstman, J. J. Jimenez et al., "Measuring circulating cell-derived microparticles," *Journal of Thrombosis and Haemostasis*, vol. 2, no. 10, pp. 1842–1851, 2004.

[55] R. Lacroix, S. Robert, P. Poncelet, R. S. Kasthuri, N. S. Key, and F. Dignat-George, "Standardization of platelet-derived microparticle enumeration by flow cytometry with calibrated beads: results of the International Society on Thrombosis and Haemostasis SSC collaborative workshop," *Journal of Thrombosis and Haemostasis*, vol. 8, no. 11, pp. 2571–2574, 2010.

[56] S. Robert, P. Poncelet, R. Lacroix et al., "Standardization of platelet-derived microparticle counting using calibrated beads and a Cytomics FC500 routine flow cytometer: a first step towards multicenter studies?" *Journal of Thrombosis and Haemostasis*, vol. 7, no. 1, pp. 190–197, 2009.

[57] D. E. Connor, T. Exner, D. D. F. Ma, and J. E. Joseph, "The majority of circulating platelet-derived microparticles fail to bind annexin V, lack phospholipid-dependent procoagulant activity and demonstrate greater expression of glycoprotein Ib," *Thrombosis and Haemostasis*, vol. 103, no. 5, pp. 1044–1052, 2010.

[58] R. Flaumenhaft, J. R. Dilks, J. Richardson et al., "Megakaryocyte-derived microparticles: direct visualization and distinction from platelet-derived microparticles," *Blood*, vol. 113, no. 5, pp. 1112–1121, 2009.

[59] C. Cerri, D. Chimenti, I. Conti, T. Neri, P. Paggiaro, and A. Celi, "Monocyte/macrophage-derived microparticles up-regulate inflammatory mediator synthesis by human airway epithelial cells," *Journal of Immunology*, vol. 177, no. 3, pp. 1975–1980, 2006.

[60] T. O. Joos and J. Bachmann, "The promise of biomarkers: research and applications," *Drug Discovery Today*, vol. 10, no. 9, pp. 615–616, 2005.

[61] T. Nozaki, S. Sugiyama, K. Sugamura et al., "Prognostic value of endothelial microparticles in patients with heart failure," *European Journal of Heart Failure*, vol. 12, no. 11, pp. 1223–1228, 2010.

[62] G. Chironi, A. Simon, B. Hugel et al., "Circulating leukocyte-derived microparticles predict subclinical atherosclerosis burden in asymptomatic subjects," *Arteriosclerosis, Thrombosis, and Vascular Biology*, vol. 26, no. 12, pp. 2775–2780, 2006.

[63] R. A. Preston, W. Jy, J. J. Jimenez et al., "Effects of severe hypertension on endothelial and platelet microparticles," *Hypertension*, vol. 41, no. 2, pp. 211–217, 2003.

[64] A. Minagar, W. Jy, J. J. Jimenez et al., "Elevated plasma endothelial microparticles in multiple sclerosis," *Neurology*, vol. 56, no. 10, pp. 1319–1324, 2001.

[65] F. Sabatier, P. Darmon, B. Hugel et al., "Type 1 and type 2 diabetic patients display different patterns of cellular microparticles," *Diabetes*, vol. 51, no. 9, pp. 2840–2845, 2002.

[66] P. A. Brogan and M. J. Dillon, "Endothelial microparticles and the diagnosis of the vasculitides," *Internal Medicine*, vol. 43, no. 12, pp. 1115–1119, 2004.

[67] E. A. J. Knijff-Dutmer, J. Koerts, R. Nieuwland, E. M. Kalsbeek-Batenburg, and M. A. van de Laar, "Elevated levels of platelet microparticles are associated with disease activity in rheumatoid arthritis," *Arthritis and Rheumatism*, vol. 46, no. 6, pp. 1498–1503, 2002.

[68] J. Simak, K. Holada, A. M. Risitano, J. H. Zivny, N. S. Young, and J. G. Vostal, "Elevated circulating endothelial membrane microparticles in paroxysmal nocturnal haemoglobinuria," *British Journal of Haematology*, vol. 125, no. 6, pp. 804–813, 2004.

[69] K. H. Jung, K. Chu, S. T. Lee et al., "Circulating endothelial microparticles as a marker of cerebrovascular disease," *Annals of Neurology*, vol. 66, no. 2, pp. 191–199, 2009.

[70] E. Colombo, B. Borgiani, C. Verderio, and R. Furlan, "Microvesicles: novel biomarkers for neurological disorders," *Frontiers in Physiology*, vol. 3, article 63, 2012.

[71] M. E. T. Tesselaar, F. P. H. T. M. Romijn, I. K. van der Linden, F. A. Prins, R. M. Bertina, and S. Osanto, "Microparticle-associated tissue factor activity: a link between cancer and thrombosis?" *Journal of Thrombosis and Haemostasis*, vol. 5, no. 3, pp. 520–527, 2007.

[72] H. K. Kim, K. S. Song, Y. S. Park et al., "Elevated levels of circulating platelet microparticles, VEGF, IL-6 and RANTES in patients with gastric cancer: possible role of a metastasis predictor," *European Journal of Cancer*, vol. 39, no. 2, pp. 184–191, 2003.

[73] D. M. Smalley, N. E. Sheman, K. Nelson, and D. Theodorescu, "Isolation and identification of potential urinary microparticle biomarkers of bladder cancer," *Journal of Proteome Research*, vol. 7, no. 5, pp. 2088–2096, 2008.

[74] H. B. Huttner, P. Janich, M. Köhrmann et al., "The stem cell marker prominin-1/CD133 on membrane particles in human cerebrospinal fluid offers novel approaches for studying central nervous system disease," *Stem Cells*, vol. 26, no. 3, pp. 698–705, 2008.

[75] D. Helley, E. Banu, A. Bouziane et al., "Platelet microparticles: a potential predictive factor of survival in hormone-refractory prostate cancer patients treated with docetaxel-based chemotherapy," *European Urology*, vol. 56, no. 3, pp. 479–485, 2009.

[76] C. L. Arteaga, M. X. Sliwkowski, C. K. Osborne, E. A. Perez, F. Puglisi, and L. Gianni, "Treatment of HER2-positive breast cancer: current status and future perspectives," *Nature Reviews*, vol. 9, no. 1, pp. 16–32, 2011.

[77] J. K. Chan, M. K. Cheung, A. Husain et al., "Patterns and progress in ovarian cancer over 14 years," *Obstetrics & Gynecology*, vol. 108, no. 3, part 1, pp. 521–528, 2006.

[78] A. Torres, K. Torres, R. Maciejewski, and W. H. Harvey, "microRNAs and their role in gynecological tumors," *Medicinal Research Reviews*, vol. 31, no. 6, pp. 895–923, 2011.

[79] A. M. Lutz, J. K. Willmann, C. W. Drescher et al., "Early diagnosis of ovarian carcinoma: is a solution in sight?" *Radiology*, vol. 259, no. 2, pp. 329–345, 2011.

[80] A. P. Heintz, F. Odicino, P. Maisonneuve et al., "Carcinoma of the ovary. FIGO 26th annual report on the results of treatment in gynecological cancer," *International Journal of Gynaecology and Obstetrics*, vol. 95, supplement 1, pp. S161–S192, 2006.

[81] E. Kobayashi, Y. Ueda, S. Matsuzaki et al., "Biomarkers for screening, diagnosis and monitoring of ovarian cancer," *Cancer Epidemiology, Biomarkers & Prevention*, vol. 21, no. 11, pp. 1902–1912, 2012.

[82] B. A. Goff, L. S. Mandel, C. W. Drescher et al., "Development of an ovarian cancer symptom index: possibilities for earlier detection," *Cancer*, vol. 109, no. 2, pp. 221–227, 2007.

[83] M. G. del Carmen, *Educational Book of the American Society of Clinical Oncology*, American Society of Clinical Oncology, Alexandria, VA, USA, 2006.

[84] R. Ozols, S. Rubin, G. Thomas, and S. Robboy, *Principles and Practice of Gynecologic Oncology*, Lippincott Williams & Wilkins, Philadelphia, Pa, USA, 4th edition, 2005.

[85] I. Díaz-Padilla, A. R. Razak, L. Minig, M. Q. Bernardini, and J. María Del Campo, "Prognostic and predictive value of CA-125 in the primary treatment of epithelial ovarian cancer: potentials and pitfalls," *Clinical & Translational Oncology*, vol. 14, no. 1, pp. 15–20, 2012.

[86] A. Sevinc, M. Adli, M. E. Kalender, and C. Camci, "Benign causes of increased serum CA-125 concentration," *Lancet Oncology*, vol. 8, no. 12, pp. 1054–1055, 2007.

[87] G. L. Anderson, "Ovarian cancer biomarker screening: still too early to tell," *Women's Health*, vol. 6, no. 4, pp. 487–490, 2010.

[88] T. P. Chendrimada, K. J. Finn, X. Ji et al., "MicroRNA silencing through RISC recruitment of eIF6," *Nature*, vol. 447, no. 7146, pp. 823–828, 2007.

[89] L. He and G. J. Hannon, "microRNAs: small RNAs with a big role in gene regulation," *Nature Reviews Genetics*, vol. 5, no. 7, pp. 522–531, 2004.

[90] X. Chen, Y. Ba, L. Ma et al., "Characterization of microRNAs in serum: a novel class of biomarkers for diagnosis of cancer and other diseases," *Cell Research*, vol. 18, no. 10, pp. 997–1006, 2008.

[91] D. C. Corney and A. Y. Nikitin, "MicroRNA and ovarian cancer," *Histology and Histopathology*, vol. 23, no. 7–9, pp. 1161–1169, 2008.

[92] N. Rosenfeld, R. Aharonov, E. Meiri et al., "microRNAs accurately identify cancer tissue origin," *Nature Biotechnology*, vol. 26, no. 4, pp. 462–469, 2008.

[93] M. V. Iorio, R. Visone, G. di Leva et al., "MicroRNA signatures in human ovarian cancer," *Ovarian Research*, vol. 67, no. 18, pp. 8699–8707, 2007.

[94] M. Bagnoli, L. de Cecco, A. Granata et al., "Identification of a chrXq27.3 microRNA cluster associated with early relapse in advanced stage ovarian cancer patients," *Oncotarget*, vol. 2, no. 12, pp. 1265–1278, 2011.

[95] S. K. Wyman, R. K. Parkin, P. S. Mitchell et al., "Repertoire of microRNAs in epithelial ovarian cancer as determined by next generation sequencing of small RNA cDNA libraries," *PLoS ONE*, vol. 4, no. 4, article e5311, 2009.

[96] N. Yanaihara, N. Caplen, E. Bowman et al., "Unique microRNA molecular profiles in lung cancer diagnosis and prognosis," *Cancer Cell*, vol. 9, no. 3, pp. 189–198, 2006.

[97] M. Bloomston, W. L. Frankel, F. Petrocca et al., "microRNA expression patterns to differentiate pancreatic adenocarcinoma from normal pancreas and chronic pancreatitis," *Journal of the American Medical Association*, vol. 297, no. 17, pp. 1901–1908, 2007.

[98] M. V. Iorio, M. Ferracin, C. G. Liu et al., "microRNA gene expression deregulation in human breast cancer," *Cancer Research*, vol. 65, pp. 7065–7070, 2005.

[99] A. J. Schetter, S. Y. Leung, J. J. Sohn et al., "microRNA expression profiles associated with prognosis and therapeutic outcome in colon adenocarcinoma," *Journal of the American Medical Association*, vol. 299, no. 4, pp. 425–436, 2008.

[100] G. A. Calin, M. Ferracin, A. Cimmino et al., "A microRNA signature associated with prognosis and progression in chronic lymphocytic leukemia," *The New England Journal of Medicine*, vol. 353, pp. 1793–1801, 2005.

[101] N. Yang, S. Kaur, S. Volinia et al., "microRNA microarray identifies Let-7i as a novel biomarker and therapeutic target in human epithelial ovarian cancer," *Cancer Research*, vol. 68, no. 24, pp. 10307–10314, 2008.

[102] I. Mikaelian, M. Scicchitano, O. Mendes, R. A. Thomas, and B. E. Leroy, "Frontiers in preclinical safety biomarkers: microRNAs and messenger RNAs," *Toxicologic Pathology*, vol. 41, no. 1, pp. 18–31, 2013.

[103] J. D. Kuhlmann, J. Rasch, P. Wimberger, and S. Kasimir-Bauer, "microRNA and the pathogenesis of ovarian cancer—a new horizon for molecular diagnostics and treatment?" *Clinical Chemistry and Laboratory Medicine*, vol. 50, no. 4, pp. 601–615, 2012.

[104] D. D. Taylor and C. Gercel-Taylor, "microRNA signatures of tumor-derived exosomes as diagnostic biomarkers of ovarian cancer," *Gynecologic Oncology*, vol. 110, no. 1, pp. 13–21, 2008.

[105] K. E. Resnick, H. Alder, J. P. Hagan, D. L. Richardson, C. M. Croce, and D. E. Cohn, "The detection of differentially expressed microRNAs from the serum of ovarian cancer patients using a novel real-time PCR platform," *Gynecologic Oncology*, vol. 112, no. 1, pp. 55–59, 2009.

[106] A. Ginestra, D. Miceli, V. Dolo, F. M. Romano, and M. L. Vittorelli, "Membrane vesicles in ovarian cancer fluids: a new potential marker," *Anticancer Research*, vol. 19, no. 4, pp. 3439–3445, 1999.

[107] N. Dahiya, C. A. Sherman-Baust, T. L. Wang et al., "microRNA expression and identification of putative miRNA targets in ovarian cancer," *PLoS ONE*, vol. 3, no. 6, article e2436, 2008.

[108] L. Zhang, S. Volinia, T. Bonome et al., "Genomic and epigenetic alterations deregulate microRNA expression in human epithelial ovarian cancer," *Proceedings of the National Academy of Sciences of the United States of America*, vol. 105, pp. 7004–7009, 2008.

[109] C. H. Lee, S. Subramanian, A. H. Beck et al., "microRNA profiling of BRCA1/2 mutation-carrying and non-mutation-carrying high-grade serous carcinomas of ovary," *PLoS ONE*, vol. 4, no. 10, article e7314, 2009.

[110] E. J. Nam, H. Yoon, S. W. Kim et al., "microRNA expression profiles in serous ovarian carcinoma," *Clinical Cancer Research*, vol. 14, pp. 2690–2695, 2008.

[111] A. Sorrentino, C. G. Liu, A. Addario, C. Peschle, G. Scambia, and C. Ferlini, "Role of microRNAs in drug-resistant ovarian cancer cells," *Gynecologic Oncology*, vol. 111, no. 3, pp. 478–486, 2008.